*Physics – Uspekhi* **49** (3) 225 – 262 (2006) 

***REVIEWS OF TOPICAL PROBLEMS*** PACS numbers: 05.70.Fh, 64.60.Cn, 74.81.Fa, 75.10.Hk, 75.50.Ee

# Phase transitions in two-dimensional systems with continuous degeneracy

S E Korshunov

DOI: 10.1070/PU2006v049n03ABEH005838

## Contents

**1. Introduction** **225**
**2. The conventional XY model** **227**
2.1 The low-temperature phase; 2.2 Vortices and the phase transition; 2.3 The Coulomb-gas representation; 2.4 Vortex pairs and the correction to the helicity modulus; 2.5 Renormalization-group analysis; 2.6 The dual representation; 2.7 The sine-Gordon model
**3. Superconducting networks and lattices and frustrated XY models** **231**
3.1 Josephson junction arrays; 3.2 Frustrated XY models; 3.3 Networks of superconducting wires; 3.4 The Coulomb-gas representation
**4. Fully frustrated XY model on a square lattice** **233**
4.1 Ground state and topological excitations; 4.2 Fractional vortices and phase transitions; 4.3 Phase transition on a domain wall and its consequences; 4.4 The sequence of phase transitions; 4.5 Structure of the phase diagram with the next-to-nearest-neighbor interaction
**5. A planar antiferromagnet with a triangular lattice** **239**
5.1 The sequence of phase transitions in the absence of a magnetic field; 5.2 Structure of the phase diagram in an external magnetic field
**6. Planar antiferromagnet with a kagome lattice** **243**
6.1 Ground states; 6.2 Zero-temperature fluctuations; 6.3 Fluctuations at a finite temperature; 6.4 Phase transition related to chirality ordering; 6.5 Structure of the phase diagram
**7. Solitons and phase-transition splitting** **250**
7.1 The XY model with modified interaction; 7.2 Classification of defects and possible phase transitions; 7.3 Dual and Coulomb representations; 7.4 Structure of the phase diagram
**8. Two-dimensional superfluid Fermi liquid with *p*-pairing** **253**
8.1 The axial phase; 8.2 The planar phase
**9. The XY model with a random phase shift** **255**
9.1 The random potential; 9.2 Disorder and the emergence of decoupled vortices; 9.3 Vortex pairs and renormalization of the helicity modulus; 9.4 Structure of the phase diagram
**10. Conclusion** **259**
**References** **260**

**Abstract. We discuss the nature and sequence of phase transitions in two-dimensional systems with continuous degeneracy, in which other factors must be taken into account in addition to the interaction of point-like topological excitations, namely, the existence of an additional discrete degeneracy (which leads to the possibility of domain wall formation), the removal of accidental degeneracy by fluctuations, the formation of solitons, and the presence of a random potential acting on vortices. Formally, we discuss various modifications of the two-dimensional XY model, while physical objects that can be described by such models are various arrays of superconducting junctions and noncollinear planar antiferromagnets.**

**S E Korshunov** Landau Institute for Theoretical Physics,
Russian Academy of Sciences,
ul. Kosygina 2, 119334 Moscow, Russian Federation
Tel. (7-495) 137 32 44. Fax (7-495) 938 20 77
E-mail: serkor@itp.ac.ru

Received 18 July 2005
*Uspekhi Fizicheskikh Nauk* **176** (3) 233 – 274 (2006)
Translated by E Yankovsky; edited by A M Semikhatov

## 1. Introduction

In the 1970s, it was found that in a broad class of two-dimensional systems with continuous degeneracy (including, in particular, planar ferromagnets [1 – 5], superfluid [6] and superconducting [7] films, thin liquid-crystal films [8], and two-dimensional crystals [9 – 11]), the phase transition into a disordered state that occurs as the temperature increases can be adequately described in terms of the dissociation of pairs of logarithmically interacting point-like topological excitations, i.e., vortices, dislocations, or disclinations (see also the review articles in Refs [12 – 15]). This raised interest in the experimental studies of various two-dimensional systems with continuous degeneracy, including systems whose thermody-

namic properties cannot be fully incorporated into the above picture. An example that first comes to mind is the artificially fabricated superconducting objects with a discrete structure, such as Josephson junction arrays [16, 17] placed in an external magnetic field. Such systems are characterized by a combination of continuous and discrete degeneracies.

The main purpose of this review is to discuss the structure of the ordered states, the nature of phase transitions, and the shape of the phase diagrams of two-dimensional systems with continuous degeneracy, whose thermodynamics can be adequately described only if, besides taking the logarithmic interaction of point-like topological defects into account, we allow for other important factors. Several situations of interest in various contexts are considered:

(1) when the classification of topological excitations in the system incorporates, besides point-like objects, linear objects such as domain walls or solitons, which in turn leads to the emergence of a new class of defects, vortices with a fractional topological charge;

(2) when the ground states have, besides a purely symmetry-related degeneracy, additional degeneracy not related to the symmetry of the Hamiltonian, and therefore establishing the nature of ordering at low temperatures requires analyzing the free energy of small fluctuations near the ground states (in the harmonic approximation or with allowance for anharmonicity); and

(3) when because of the presence of disorder in the system, the logarithmically interacting point-like defects are affected by a random potential.

Formally speaking, here we are dealing with various modifications of the two-dimensional XY model, i.e., frustrated, antiferromagnetic, with an additional minimum in the interaction, and with a random phase shift (when the differences are substantial, these modifications are analyzed using lattices with different geometries). From the physical standpoint, however, the results discussed in what follows can be used to describe arrays of Josephson, or SFS (superconductor – ferromagnet – superconductor) junctions, networks of thin superconducting wires, noncollinear planar antiferromagnets, and thin films of a superfluid Fermi liquid with *p*-pairing (in the absence of an external magnetic field or in the presence of such a field).

Section 2, which is a brief review of the well-known properties of the conventional two-dimensional XY model, introduces the necessary concepts and gives a brief description of the methods intensively used in what follows.

Section 3 discusses the possibility of using XY models to describe Josephson junction arrays and networks of superconducting wires, and also introduces the notion of frustrated XY models [18], widely used to describe similar hybrid structures in a transverse magnetic field. A sizable portion of the review (Sections 4 – 6) is devoted to the analysis of such models in the most interesting case where the magnetic field magnitude corresponds to a half-integer number of flux quanta per unit cell. These models are commonly known as fully frustrated (FF) [20].

Section 4 deals with the problem of a fully frustrated XY (FFXY) model on a square lattice, a statistical-physics model that has been studied most intensively among the models in which continuous degeneracy is combined with discrete degeneracy. In this model, discrete degeneracy is the simplest one, twofold [19]. This suggests that besides the Berezinskii – Kosterlitz – Thouless (BKT) phase transition [1 – 5], caused by vortex-pair dissociation and occurring at $T = T_v$, the system may undergo a second phase transition (of the Ising type) associated with domain-wall formation and occurring at $T = T_{dw}$ [20].

The question of the sequence in which these phase transitions occur is highly nontrivial. The problem is that the interaction of domain walls and vortices is of a nonperturbative nature and stems from the existence of a new class of topological excitations, fractional vortices [21, 22], forming on defects of the domain walls. This greatly limits the possible scenarios of events. It is important here that on a single domain wall at $T = T_k < T_v$, there occurs a phase transition related to the dissociation of pairs of logarithmically interacting kinks [23, 24]. This leads (for $T > T_k$) to the loss of coupling between phase fluctuations on both sides of the wall, which in turn ensures that the inequality $T_v < T_{dw}$ is satisfied, at least if the phase transition at $T = T_{dw}$ is continuous [24].

If the domain-wall energy were an adjustable parameter, allowing varying $T_{dw}$ independently of $T_v$ and $T_k$, a decrease of this parameter (at $T_{dw} = T_k$) would lead to a merger of the two phase transitions into one (most probably, first-order), and only after further lowering $T_{dw}$ severalfold would there be a new splitting of the phase transitions [21]. In the new mode, the loss of phase coherence would be related to the dissociation of pairs of fractional vortices and would occur as a separate phase transition at $T = T_{fv} > T_{dw}$. Unfortunately, the addition of the interaction with more distant neighbors to the Hamiltonian of the FFXY model on a square lattice does not allow varying $T_{dw}$ and $T_v$ independently [25]. Hence, in this case, too, only one of the three above-mentioned scenarios of the violation of the $U(1) \times Z_2$ ordering, in which $T_v < T_{dw}$, occurs in the system under consideration.

However, it so happens that as the interaction with the next-to-nearest neighbors increases, a phase transition of a quite different nature occurs, related to the reconstruction of the ground state, which leads to the disappearance of discrete degeneracy and the emergence of additional continuous degeneracy [26] not related to symmetry (i.e., accidental degeneracy). Therefore, establishing the complete structure of the phase diagram of the FFXY model with a square lattice and the interaction involving not only the nearest neighbors [25] becomes possible only if we take the free energy of harmonic fluctuations into account, which lifts the accidental degeneracy.

Section 5 is devoted to the analysis of the antiferromagnetic XY model on a triangular lattice [the AFXY(t) model]. In the absence of an external magnetic field, it is given by the FFXY model, whose ground state on a triangular lattice has the same $U(1) \times Z_2$ degeneracy [27] as in the case of a square lattice. Analysis of the structure of the domain walls and of the properties of the elementary defects on these walls [28] suggests that all the conclusions drawn in Section 4 regarding the properties of fluctuating domain walls and the sequence of phase transitions in the FFXY model remain valid for a triangular lattice [24].

A remarkable property of a planar antiferromagnet with a triangular lattice is that the continuous degeneracy of the ground state is preserved [29] even when an external magnetic field is applied that destroys the symmetry responsible for the existence of continuous degeneracy in the absence of the field. The difference in the free energy of spin waves lifts this accidental degeneracy [30 – 32] and results in the occurrence of three different ordered phases with a three-sublattice structure [29]. A characteristic feature

of all these phases is the existence of a real long-range order in the orientation of spins belonging to the same sublattice, while the phase transitions between them belong to the Ising universality class [32].

In Section 6, the planar antiferromagnet with a kagome lattice and the nearest-neighbor and next-to-nearest-neighbor interactions is presented as another example of a system with the combined $U(1) \times Z_2$ degeneracy. However, in contrast to the models discussed in Sections 4 and 5, the domain-wall energy is here an adjustable parameter, determined by the interaction of next-to-nearest neighbors and vanishing as the interaction disappears [33]. This encourages the discussion of an alternative sequence of phase transitions [22], when infinite domain walls appear at a temperature lower than that at which the loss of phase coherence occurs due to the dissociation of pairs of fractional vortices.

It turns out that in this situation, the domain walls are not at all of the Ising nature, because their formation leads to the mixing of six different vacua. The renormalization-group analysis based on the equivalence of the domain walls in the model under study and the steps in the $(2+2)$-dimensional analog of the crystal surface and allowing for the mutual influence of topological excitations of various types makes it possible to show that the temperature of the phase transition in which such domain walls emerge depends on the wall energy per unit length not linearly but much more slowly [34]. This leads to an extremely narrow range of parameter values at which the scenario with $T_{dw} < T_{fv}$ is realized.

When only the nearest neighbors are involved in the interaction, the domain-wall energy vanishes, which leads to the exponential degeneracy (in the number of sites in the system) of the ground state [35], not related to symmetry. This accidental degeneracy is lifted when the free energy of spin waves is taken into account. But because the Hamiltonian describing harmonic fluctuations in the given model has the same form for all ground states, this happens only when anharmonicity is taken into account. Due to the smallness of the dimensionless parameter characterizing the domain-wall free energy induced by fluctuations, the two phase transitions must occur in this situation at very different temperatures, $T_{dw} \sim 10^{-3} T_{fv}$ [34]. In the low-temperature phase (for $T < T_{dw}$), the long-range order in the discrete degrees of freedom is then characterized by macroscopically large values of the correlation radius [36], which makes observation of such an order very difficult.

As in the case of a triangular lattice, the results in Section 6 can be used to describe not only planar antiferromagnets but also Josephson junction arrays and networks of superconducting wires with a half-integer number of flux quanta per triangular cell and lattices of $\pi$-junctions in the absence of a magnetic field. In such systems, it is the magnetic interaction of currents that lifts the accidental degeneracy [37].

In contrast to Sections 4–6, where models whose ground states are characterized by a combination of continuous degeneracy and discrete degeneracy are analyzed, Sections 7–9 are devoted to effects that may manifest themselves in a system with the purely continuous $U(1)$ degeneracy. Section 7 discusses a modification of the conventional (i.e., nonfrustrated) XY model in which the ground state degeneracy is the same as in the standard version but, in addition to vortices, solitons play an important role in the thermodynamics of the system (solitons are linear defects whose existence is determined by a specific type of interaction, which exhibits an additional minimum [38–40] and is a typical feature of SFS junctions near the transition to the $\pi$-state [41–43]). In contrast to domain walls, solitons are not unremovable topological singularities and may therefore have end points (which are vortices with a half-integer topological charge; see [44–46], however).

The partition function of this model can be represented as the partition function of a Coulomb gas of half-integer charges coupled to binary variables of the Ising type. This suggests that if the soliton energy is low, the BKT transition splits into two phase transitions, one of which is of the Ising type and is related to the vanishing of the soliton free energy, and the other belongs to the BKT universality class and is related to the dissociation of pairs of vortices with an integer topological charge [44–46]. In the intermediate phase, the superfluid density remains finite. However, what is coherent is not the motion of Cooper pairs (the pair correlation function of the order parameter decays exponentially) but that of pairs of Cooper pairs [47, 48].

Section 8 demonstrates that a similar mechanism of phase-transition splitting [49] operates in both superfluid phases of a Fermi liquid with *p*-pairing, which are characterized by a much more complicated order parameter [50–52]. Here, the effective strength of the spin–orbit coupling, which determines the soliton energy and allows controlling the magnitude of splitting [49], can be reduced in an arbitrary way by placing the film in a magnetic field perpendicular to it [49, 53].

Section 9 discusses the two-dimensional XY model with a random phase shift, which in terms of vortices corresponds to a random potential with logarithmically divergent correlations [54]. Examining the effect of such disorder on the divergence of the leading correction to the interaction of vortices in powers of fugacity, Rubinstein et al. [54] concluded that such a system must have a reentrant transition into the disordered state as the temperature decreases (even if the disorder is arbitrarily weak). Analysis of higher-order corrections shows that such an approach is inadequate, because at any point of the phase diagram, a significant fraction of such corrections proves to be divergent [55–57], which, generally, could indicate instability of the ordered phase.

A more careful analysis, based on the expansions in the concentration of vortex pairs, enables constructing a phase diagram in which the ordered phase has a stability region, but there is no reentrant transition into the disordered phase [58–62]. The value of the critical disorder amplitude at low temperatures can then be found by analyzing the probability of the spontaneous formation of a single vortex [60]. The model discussed in Section 9 can be used to describe a Josephson junction array with geometric irregularities in the presence of a transverse magnetic field whose magnitude corresponds (on the average) to an integer number of flux quanta per lattice cell [63], and also planar magnets with the random Dzyaloshinsky–Moriya interaction [64, 65].

## 2. The conventional XY model

If we ignore quantum fluctuations, a two-dimensional planar ferromagnet can be described by what is known as the XY model (the model of planar rotators), which is specified by the Hamiltonian [1, 66]

$$H_{XY} = -J \sum_{(\mathbf{ij})} \cos(\varphi_{\mathbf{i}} - \varphi_{\mathbf{j}}), \tag{1}$$

where $J > 0$ is the effective coupling constant, $\varphi_{\mathbf{j}}$ is the angle of rotation (phase) of a unit spin $\mathbf{S}_{\mathbf{j}} \equiv (\cos\varphi_{\mathbf{j}}, \sin\varphi_{\mathbf{j}})$ located at the site $\mathbf{j}$ of a regular (e.g., square) lattice, and summation is performed over all pairs of nearest neighbors ($\mathbf{i}\,\mathbf{j}$) in the lattice (we always use parentheses to indicate pairs of nearest neighbors).

Hamiltonian (1) corresponds to the purely exchange-type interaction of spins. The continuous analog of (1),

$$H = \frac{1}{2} J \int \mathrm{d}^2\mathbf{r}\,(\nabla\varphi)^2\,, \tag{2}$$

where the variable $\varphi$ is also defined up to a shift by $2\pi$, can be used to describe thin films of superfluid Bose liquid [6] and superconducting films (the latter on not too great a scale [67]).

The ground state of the XY model is a state in which all the variables $\varphi_{\mathbf{j}}$ are equal. Because the Hamiltonian is symmetric with respect to a simultaneous rotation of all spins, this state is degenerate with respect to the group of two-dimensional rotations $O(2)$ [isomorphic to U(1)], while the degeneracy space is a circle, i.e., the one-dimensional sphere $\mathrm{S}^1$.

### 2.1 The low-temperature phase

At the lowest temperatures, the leading contribution to the thermodynamics of systems with continuous degeneracy is provided by small fluctuations near the ground state (spin waves). Berezinskii [1] and Wegner [66] found that the presence of such fluctuations leads to a power-law decay of the correlation function

$$C(\mathbf{r}) = \left\langle \exp\left[\mathrm{i}(\varphi_{\mathbf{j}+\mathbf{r}} - \varphi_{\mathbf{j}})\right]\right\rangle \propto |\mathbf{r}|^{-\eta}$$

at large distances. Here, $\eta = T/2\pi\Gamma$, where $\Gamma$ is the helicity modulus [68], which determines the energy of spin waves in the long-wavelength limit (the analog of superfluid density).

The value of $\Gamma$ at $T = 0$ is $J$ for model (1) with a square lattice, and $\Gamma = \sqrt{3}\,J$ for a triangular lattice. The helicity modulus $\Gamma$ decreases as the temperature grows because thermal fluctuations renormalize its magnitude. If not stated otherwise, we assume in what follows that the temperature $T$ is expressed in energy units, i.e., incorporates the Boltzmann constant $k_{\mathrm{B}}$ as a factor.

The existence of a temperature range within which $C(\mathbf{r})$ decreases in accordance with a power law means that as the temperature increases, there occurs a phase transition, because for $T \gg J$, the same correlation function must decay exponentially. Because no long-range order is possible for $T > 0$ in two-dimensional systems with continuous degeneracy of the order parameter [68–73], in what follows, for brevity, we call the low-temperature phase with a power-law decrease of $C(\mathbf{r})$ (known as the Berezinskii phase) ordered, although it would be more correct to call it 'quasiordered.'

### 2.2 Vortices and the phase transition

As the temperature increases, vortices begin to play a dominant role in the thermodynamics of two-dimensional systems with the U(1) degeneracy [2–4]. A vortex is a topological singularity going around which changes the phase by $2\pi m$, where $m$ is an integer called the topological charge of the vortex. From the energy standpoint, we can limit ourselves to vortices with a minimum topological charge, $m = \pm 1$. When a lattice system is involved, a vortex can be associated with a configuration of the $\varphi_{\mathbf{j}}$ that is a local minimum of the Hamiltonian and is centered at a certain unit cell of the lattice, going around which (along an arbitrary path) leads to a phase increment (Fig. 1).

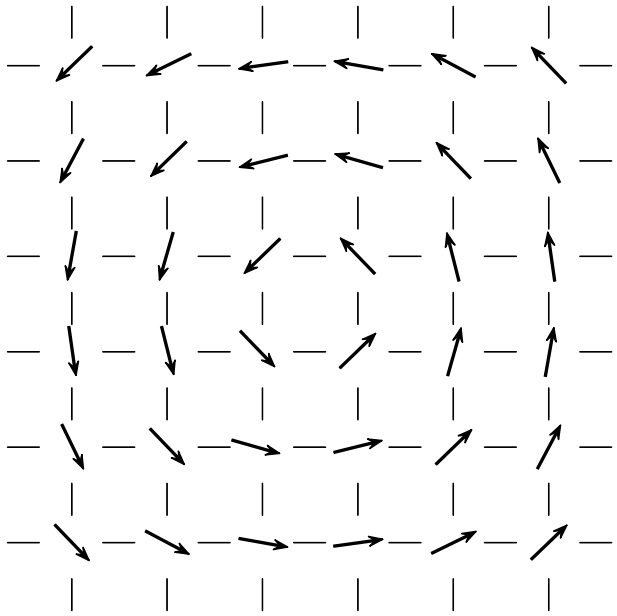

**Figure 1.** Example of a vortex with a topological charge +1 on a square lattice.

The energy of a single vortex, $E_{\mathrm{v}}$, diverges logarithmically as the system size $L$ increases:

$$E_{\mathrm{v}} \approx \pi\Gamma \ln L\,.$$

Because the entropy of a single vortex, $S_{\mathrm{v}}$, which is the logarithm of the number of possible positions of the vortex in the lattice, diverges in the same way, the free energy of the vortex

$$F_{\mathrm{v}} = E_{\mathrm{v}} - TS_{\mathrm{v}} \approx (\pi\Gamma - 2T)\ln L\,,$$

vanishes at $T = T_{\mathrm{v}} = (\pi/2)\Gamma$ [3]. At higher temperatures, one can expect the system to contain free vortices, which results in the correlation function $C(\mathbf{r})$ decaying exponentially (because each vortex leads to a strong change in $\varphi$ even far from its core). When $T < T_{\mathrm{v}}$, vortices can exist only as neutral bound pairs, whose presence has no effect on the power-law decay of $C(\mathbf{r})$. The phase transition related to the vortex-pair dissociation and the change in the behavior of the correlation function $C(\mathbf{r})$ at large distances is commonly known as the Berezinskii–Kosterlitz–Thouless (BKT) transition.

### 2.3 The Coulomb-gas representation

The partition function of the XY model can be represented as

$$Z_{\mathrm{XY}} = \prod_{\mathbf{j}} \left( \int_{-\pi}^{\pi} \frac{\mathrm{d}\varphi_{\mathbf{j}}}{2\pi} \right) \prod_{(\mathbf{i}\,\mathbf{j})} w(\varphi_{\mathbf{i}} - \varphi_{\mathbf{j}})\,, \tag{3}$$

where

$$w(\theta) = \exp\left[-\frac{V(\theta)}{T}\right]$$

is a weight factor that depends on the angle $\theta_{\mathbf{ij}} = \varphi_{\mathbf{j}} - \varphi_{\mathbf{i}}$ of relative rotation of two neighboring spins, with $V(\theta)$ being the

energy of interaction of these spins. In the conventional XY model (1), the function $V(\theta)$ is

$$V_0(\theta) = -J\cos\theta\,.$$

That the thermodynamics of the XY model can be analyzed exclusively in terms of a gas of logarithmically interacting topological excitations becomes obvious when we somewhat change the form of the function $V(\theta)$ that describes the interaction of neighboring spins, i.e., replace $V_0(\theta)$ with the Berezinskii–Villain interaction $V_{\rm BV}(\theta)$ [74, 75], defined as

$$w_{\rm BV}(\theta) \equiv \exp\left[-\frac{V_{\rm BV}(\theta)}{T}\right] = \sum_{p=-\infty}^{\infty} \exp\left[-\frac{J}{2T}(\theta+2\pi p)^2\right], \tag{4}$$

and exhibiting the same periodicity and symmetry as $V_0(\theta)$.

When $J \gg T$, the Berezinskii–Villain function $V_{\rm BV}(\theta)$ is everywhere (with the exception of a small neighborhood of $\theta = \pi$) close to a parabola:

$$V_{\rm BV}(\theta) \approx {\rm const} + \frac{J}{2}\,\theta^2\,.$$

Clearly, in this limit, the use of $V_{\rm BV}(\theta)$ instead of $V_0(\theta)$ amounts to ignoring anharmonicity. In the opposite limit, when $J \ll T$, the function

$$V_{\rm BV}(\theta) \approx {\rm const} - 2T\cos\theta\exp\left(-\frac{T}{2J}\right)$$

coincides, with exponential accuracy, with $V_0(\theta)$ but with an entirely different coupling constant,

$$J_{\rm eff} = 2T\exp\left(-\frac{T}{2J}\right) \ll J\,.$$

If we substitute (4) in partition function (3), it becomes possible to integrate over all variables $\varphi_{\mathbf{j}}$, because the integration becomes Gaussian for such a choice of $w(\theta)$. As a result, the partition function acquires the form (up to an insignificant factor) of the partition function of a Coulomb gas,

$$Z_{\rm Cg} = \prod_{\mathbf{R}}\left[\sum_{m_{\mathbf{R}}=-\infty}^{\infty} Y(m_{\mathbf{R}})\right] \exp\left[-\frac{H_{\rm Cg}\{m_{\mathbf{R}}\}}{T}\right], \tag{5}$$

with the Hamiltonian

$$H_{\rm Cg} = \frac{1}{2}\sum_{\mathbf{R}_1,\mathbf{R}_2} m_{\mathbf{R}_1} G_0(\mathbf{R}_1-\mathbf{R}_2) m_{\mathbf{R}_2}\,, \tag{6}$$

where the integer-valued variables $m_{\mathbf{R}}$ (the charges in the Coulomb gas) may be considered defined at the sites $\mathbf{R}$ of the dual lattice. Each of these variables is a sum of the integer variables $p_{\mathbf{ij}} \equiv -p_{\mathbf{ji}}$, defined on the bonds of the original lattice along the perimeter of the unit cell containing the site $\mathbf{R}$, and may be identified with the topological charge of this cell.

The interaction $G_0(\mathbf{R}_1-\mathbf{R}_2)$ in (6) is of the form

$$G_0(\mathbf{R}_1-\mathbf{R}_2) = 4\pi^2 J(-\hat{\Delta})^{-1}_{\mathbf{R}_1\mathbf{R}_2}\,, \tag{7}$$

where $\hat{\Delta}$ is the Laplace operator defined on the dual lattice, and is logarithmic for large distances:

$$G_0(0) - G_0(\mathbf{R}) \approx 2\pi\Gamma\ln|\mathbf{R}|\,. \tag{8}$$

For generality, we have also included the fugacities $Y(m)$ of the Coulomb-gas charges in (5). They become equal to unity under the formal transition from (3) to (5), but change in the renormalization process (see Section 2.5).

In the case of a square lattice, the Fourier transform of $G_0(\mathbf{R})$ is given by

$$G_0(\mathbf{q}) = \frac{4\pi^2 J}{2(1-\cos q_x)+2(1-\cos q_y)}\,, \tag{9}$$

while the difference $G_0(0) - G_0(\mathbf{R})$ for $\mathbf{R} \neq \mathbf{0}$ is very close to $2\pi J(\ln|\mathbf{R}| + \pi/2)$ [76], which allows assuming that

$$G_0(\mathbf{R}\neq\mathbf{0}) \approx G_0(0) - 2\pi J\ln|\mathbf{R}|\,,$$

$$Y(m) \approx \exp\left(-\frac{\pi^2}{2}\,\frac{J}{T}\,m^2\right).$$

In the long-wavelength limit ($|\mathbf{q}| \ll 1$), for any lattice that introduces no anisotropy,

$$G_0(\mathbf{q}) \approx \frac{4\pi^2\Gamma}{q^2}\,. \tag{10}$$

This expression can also be used for continuous model (2), but then the computation of the energy of the vortex core, whose value determines $Y$, requires going beyond the approximation that takes only phase fluctuations into account.

**2.4 Vortex pairs and the correction to the helicity modulus** The function $G_0(\mathbf{R}_1-\mathbf{R}_2)$ in (6) describes the bare interaction of the charges comprising the Coulomb gas and located at points $\mathbf{R}_1$ and $\mathbf{R}_2$. The full (i.e., renormalized) interaction may be defined as the response of the system to the addition of two infinitely small test charges (located at $\mathbf{R}_1$ and $\mathbf{R}_2$) and can be written as

$$G(\mathbf{R}_1-\mathbf{R}_2) = G_0(\mathbf{R}_1-\mathbf{R}_2) - \frac{1}{T}\sum_{\mathbf{R}_1',\mathbf{R}_2'} G_0(\mathbf{R}_1-\mathbf{R}_1')\,\Sigma(\mathbf{R}_1',\mathbf{R}_2')\,G_0(\mathbf{R}_2'-\mathbf{R}_2)\,. \tag{11}$$

The first term in the right-hand side of (11) is simply the bare interaction of the test charges, and the second term is the fluctuation correction to their interaction and involves

$$\Sigma(\mathbf{R}_1,\mathbf{R}_2) = \langle m_{\mathbf{R}_1} m_{\mathbf{R}_2}\rangle\,, \tag{12}$$

the correlation function of charges in the Coulomb gas, which in the homogeneous case depends, naturally, only on $\mathbf{R}_1-\mathbf{R}_2$.

If we assume that all the vortices are bound into neutral pairs separated by large distances, the leading contribution to $\Sigma(\mathbf{R}_1,\mathbf{R}_2)$ at $\mathbf{R}_1 \neq \mathbf{R}_2$ is related to the probability of one vortex in a pair being located at $\mathbf{R}_1$ and the other at $\mathbf{R}_2$. In the leading order in $Y \equiv Y(\pm 1)$, this contribution can be written as

$$\Sigma(\mathbf{R}_1,\mathbf{R}_2) = -2W(\mathbf{R}_1-\mathbf{R}_2)\,, \tag{13}$$

where

$$W(\mathbf{R}) = Y^2\exp\left[-\frac{E_{\rm pair}(\mathbf{R})}{T}\right] \tag{14}$$

is the weight factor for a pair of vortices with topological charges $m = \pm 1$ whose energy is $E_{\text{pair}} = G(0) - G(\mathbf{R})$, and the factor 2 occurs because there are two options for the arrangement of charges in a pair. At the same time, the neutrality of the pairs implies that

$$\Sigma(\mathbf{R}_1, \mathbf{R}_1) = -\sum_{\mathbf{R}_2 \neq \mathbf{R}_1} \Sigma(\mathbf{R}_1, \mathbf{R}_2)\,. \tag{15}$$

Substituting (8) and (12)–(15) in (11) shows that the correction to the helicity modulus caused by the presence of neutral coupled pairs is given by the formula [5, 77]

$$\delta\Gamma = -\frac{2\pi^2\Gamma^2}{T}\sum_{\mathbf{R}} R^2 W(\mathbf{R})\,. \tag{16}$$

José et al. [76] constructed a similar expression on the basis of the form of the vortex contribution to the correlation function $C(\mathbf{r})$. Substituting $E_{\text{pair}} \approx 2\pi\Gamma \ln|\mathbf{R}|$ in (16) shows that $\delta\Gamma$ diverges at the same temperature at which the divergent contribution to the free energy of a single vortex vanishes.

### 2.5 Renormalization-group analysis

A recursive procedure that allows taking the reduction of the helicity modulus into account as we move to larger and larger scales (i.e., larger and larger vortex pairs) was developed by Kosterlitz [5]. This procedure leads to renormalization equations for $\Gamma$ and $Y$ of the form

$$\begin{aligned} \frac{\mathrm{d}\Gamma}{\mathrm{d}l} &= -4\pi^3 \frac{\Gamma^2}{T}\, Y^2\,, \\ \frac{\mathrm{d}Y}{\mathrm{d}l} &= \left(2 - \frac{\pi\Gamma}{T}\right) Y, \end{aligned} \tag{17}$$

where $l$ is the logarithm of scale. Similar equations describe renormalization in a one-dimensional gas with the logarithmic interaction, provided that the signs of the charges alternate regularly [78].

The behavior of the renormalization-group flows determined by Eqns (17) is schematically depicted in Fig. 2. Clearly, in the low-temperature phase, $Y$ is renormalized to zero at large scales and $\Gamma$ tends to a finite limit, while in the high-temperature phase, the renormalized value of the helicity modulus $\Gamma(T) \equiv \Gamma(l = \infty, T)$ tends to zero. A phase transition occurs when the value of $\Gamma(T)$ satisfies the so-called universal Nelson – Kosterlitz criterion [6],

$$T_{\text{v}} = \frac{\pi}{2}\,\Gamma(T_{\text{v}})\,. \tag{18}$$

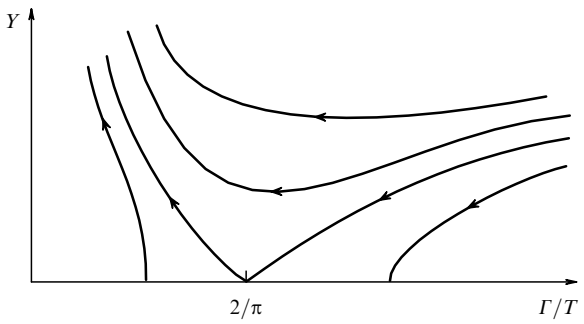


**Figure 2.** A rough picture of the behavior of the renormalization-group flows corresponding to Eqns (17).

In the case of a superfluid film, this criterion means that the ratio of the superfluid density $\rho_{\text{s}}$ to the transition temperature $T_{\text{v}}$ as $T \to T_{\text{v}} - 0$ is universal [6]:

$$\frac{\rho_{\text{s}}(T_{\text{v}})}{T_{\text{v}}} = \frac{2}{\pi}\left(\frac{m}{\hbar}\right)^2.$$

Because the value of $\Gamma$ (or $\rho_{\text{s}}$) abruptly changes from a finite value to zero at $T = T_{\text{v}}$, it is often said that the jump in $\Gamma$ (or in $\rho_{\text{s}}$) is universal.

The results of Monte Carlo simulation show that in the standard XY model with $V(\theta) = -J\cos\theta$ and a square lattice, the BKT transition occurs at $T_{\text{v}} \approx 0.89\,J$ [79–83], while on a triangular lattice, $T_{\text{v}} \approx 1.45\,J$ [84]. The high-temperature expansion on a triangular lattice yields [85, 86]

$$T_{\text{v}} \approx (1.45 - 1.47)\,J\,.$$

In both cases, the transition temperature proves to be nearly two times lower than the value that follows from the naive estimate

$$T_{\text{v}} \approx \frac{\pi}{2}\,\Gamma(T = 0)\,,$$

which ignores renormalization.

Equations (17) suggest that as $T_{\text{v}}$ is approached from below, the function $\Gamma(T)$ has a square-root singularity [6],

$$\frac{\Gamma(T)}{T} - \frac{2}{\pi} \propto \sqrt{\frac{T_{\text{v}} - T}{T_{\text{v}}}}\,,$$

while as $T_{\text{v}}$ is approached from above, the correlation radius $r_{\text{c}}$ diverges exponentially [5],

$$r_{\text{c}} \propto \exp\left[-b\left(\frac{T - T_{\text{v}}}{T_{\text{v}}}\right)^{1/2}\right].$$

The concentration of free vortices then behaves as $r_{\text{c}}^{-2}$.

### 2.6 The dual representation

With the expression for the weight factor $w(\theta)$ in terms of its Fourier transform $w_*(n)$,

$$w(\theta) = \sum_{n=-\infty}^{\infty} \exp(-\mathrm{i}\theta n)\, w_*(n)\,,$$

substituted in (3), we can integrate over all the variables $\varphi_{\mathbf{j}}$ in the partition function, after which it acquires the form (up to an unessential, i.e., nonsingular, factor) [76, 87]

$$Z_{\text{SOS}} = \prod_{\mathbf{R}}\left[\sum_{n_{\mathbf{R}}=-\infty}^{\infty}\right] \exp\left(-\frac{H_{\text{SOS}}\{n_{\mathbf{R}}\}}{T}\right), \tag{19}$$

which is the partition function of a model used to describe the crystal surface (the solid-on-solid, or SOS, model), with the Hamiltonian [88]

$$H_{\text{SOS}} = \sum_{(\mathbf{R}\mathbf{R}')} V_*(n_{\mathbf{R}} - n_{\mathbf{R}'})\,. \tag{20}$$

Here, the integer-valued variables $n_{\mathbf{R}}$ (corresponding to the height of the surface) are defined at the sites of the dual lattice, summation ranges over all bonds on this lattice, and the

interaction $V_*(n)$ is defined by the relation

$$w_*(n) = \exp\left[-\frac{V_*(n)}{T}\right].$$

In the case of the conventional XY model with $V(\theta) = -J\cos\theta$, the dual SOS model is characterized by the interaction [76, 87]

$$V_*(n) = -T\ln\left[I_{|n|}\left(\frac{J}{T}\right)\right],$$

where $I_n(z)$ is the modified Bessel function of order $n$. On the other hand, in the case of Berezinskii–Villain interaction (4), the function $V_*(n)$ is especially simple:

$$V_*(n) = \frac{J_*}{2}\,n^2,$$

where

$$J_* = \frac{T^2}{J} \tag{21}$$

is the dial coupling constant. The SOS model with this interaction is commonly known as the discrete Gaussian model.

In the ground state of the SOS model, all the variables $n_{\mathbf{R}}$ are equal. The degeneracy of this state is related to the symmetry group $Z_N$. The simplest excitations generated by thermal fluctuations in such a system are steps of unit height, or lines crossing which changes $n_{\mathbf{R}}$ by $\pm1$. In the discrete Gaussian model, the energy of such a step (per unit length) is $E_{\text{step}} = J_*/2$, with the result that for $T \ll J_*$, all steps must form closed loops, while at $T = T_{\text{R}} \sim J_*$, there occurs a roughening transition (a phase transition of the surface from the smooth phase to the rough phase [88, 89]) related to the appearance of infinite steps. In the rough phase, the surface fluctuations diverge,

$$\left\langle (n_{\mathbf{R}_1} - n_{\mathbf{R}_2})^2 \right\rangle \propto \ln|\mathbf{R}_1 - \mathbf{R}_2|,$$

in contrast to the smooth phase, where the width of the surface is constant.

It follows from (21) that the high-temperature phase of the discrete Gaussian model corresponds to the low-temperature phase of the XY model, and vice versa. This makes the dual representation (in terms of the SOS model) a convenient tool for studying the properties of the high-temperature phase of the XY model, in which fluctuations of $\varphi$ are large. In particular, van der Eerden and Knops [90] and Swendsen [91] found that the correlation radius $r_{\text{c}}$, which describes the exponential decay of $C(\mathbf{r})$, is related to the free energy $F_{\text{step}}$ of the step by the simple formula $r_{\text{c}} = T/F_{\text{step}}$ and, hence, in case of the Berezinskii–Villain interaction (4), is close to $2T/J_* = 2J/T$ when $T \gg J$.

The fact that Kosterlitz's renormalization-group analysis [5] correctly describes the critical properties of the XY model can be verified by comparing the critical behavior of the model with that of the exactly solvable SOS model proposed by van Beijeren [92] for describing fluctuations of the (001) face of a crystal with a bcc lattice. This model is isomorphic to one of the versions of the six-vertex model, commonly known as the ice model, whose exact solution was found by Lieb [94, 95].

Because the discrete Gaussian model is dual to the XY model with the Berezinskii–Villain interaction, which can be reduced to the Coulomb gas, the partition function of such a Coulomb gas can be directly derived from the partition function of the discrete Gaussian model. For this, we must replace summation over the discrete variables $n_{\mathbf{R}}$ in (19) with integration [89] via the Poisson resummation formula

$$\sum_{n=-\infty}^{\infty} f(n) = \int_{-\infty}^{\infty} \mathrm{d}n \sum_{m=-\infty}^{\infty} \exp(-2\pi i n m)\, f(n), \tag{22}$$

which gives rise to a sum over the variables $m_{\mathbf{R}}$ appearing in the partition function, but allows us to integrate over all the variables $n_{\mathbf{R}}$ because the integral is Gaussian.

The simplest way to proceed from the Coulomb-gas partition function to the partition function of the discrete Gaussian model is to decouple the variables $m_{\mathbf{R}}$ in (5) via Gaussian integration over the additional variables $n_{\mathbf{R}}$:

$$Z_{\text{Cg}} \to \prod_{\mathbf{R}}\left[\int_{-\infty}^{\infty} \mathrm{d}n_{\mathbf{R}} \sum_{m_{\mathbf{R}}=-\infty}^{\infty} Y(m_{\mathbf{R}})\right] \times \exp\left[2\pi i \sum_{\mathbf{R}} m_{\mathbf{R}} n_{\mathbf{R}} - \frac{T}{2J}\sum_{\mathbf{R}_1,\,\mathbf{R}_2} n_{\mathbf{R}_1}(-\hat{\Delta})_{\mathbf{R}_1\mathbf{R}_2} n_{\mathbf{R}_2}\right].$$

After this is done, summation over the $m_{\mathbf{R}}$ can be performed independently for each site $\mathbf{R}$. At $Y(m) \equiv 1$, as formula (21) implies, this procedure amounts to replacing the integral over $n_{\mathbf{R}}$ with a sum, which transforms $Z_{\text{Cg}}$ into the partition function of the discrete Gaussian model.

### 2.7 The sine-Gordon model

The renormalization-group analysis shows that the contributions of vortices whose topological charges exceed (in the absolute value) the minimum charge are unessential, and therefore the contributions to the partition function that correspond to such charges can be ignored from the very beginning. If we set

$$Y(m) = \begin{cases} 1, & m = 0, \\ Y \ll 1, & m = \pm 1, \\ 0, & |m| > 1 \end{cases}$$

in the Coulomb-gas partition function, the transformation described in the last paragraph of the previous section transforms it [96] into the partition function of the so-called sine-Gordon model, defined by the Hamiltonian

$$H_{\text{sG}} = \frac{J_*}{2}\sum_{(\mathbf{R}\mathbf{R}')} (n_{\mathbf{R}} - n_{\mathbf{R}'})^2 - y\sum_{\mathbf{R}} \cos(2\pi n_{\mathbf{R}}) \tag{23}$$

(where $y = 2YT$), which depends, in contrast to (20), on continuous variables $n_{\mathbf{R}}$.

The renormalization-group equations for the continuous version of Hamiltonian (23) were first written by Wiegmann [96] (see also Ref. [97]) and are equivalent to Eqns (17), as expected. The sine-Gordon representation has proved to be most convenient for systematic studies of higher-order corrections to (17) in $Y$ and $2 - \pi\Gamma/T$, and suggests that such corrections do not alter the critical behavior [98].

## 3. Superconducting networks and lattices and frustrated XY models

### 3.1 Josephson junction arrays

If we ignore the magnetic fields of currents, the XY model in (1) can be used to describe a Josephson junction array [16,

17], which is a regular pattern of superconducting islands, each of which is connected to its neighbors through Josephson junctions. Here, one can speak of tunnel junctions of the superconductor – insulator – superconductor type and of systems in which the interaction of the superconducting islands is caused by the proximity effect and occurs through a normal-metal substrate. In both cases, $\varphi_{\mathbf{j}}$ is the phase of the order parameter on the **j**th island, and

$$J = \frac{\hbar}{2e} I_{\mathrm{c}} ,$$

where $I_{\mathrm{c}}$ is the critical current of a single junction.

Generally speaking, the magnetic field of currents leads to the screening of the interaction of vortices in both continuous (superconducting films [67]) and discrete (Josephson junction arrays [17, 99]) two-dimensional superconductors. This occurs at a distance comparable to the penetration depth of the magnetic field into a two-dimensional superconductor,

$$\Lambda = \frac{\phi_0^2}{8\pi^3 \Gamma} ,$$

where

$$\phi_0 = \frac{hc}{2e}$$

is the magnetic flux quantum. In particular, for a superconducting film, formula (10) becomes

$$G(\mathbf{q}) = \frac{4\pi^2 \Gamma}{q^2 + q/\Lambda} . \tag{24}$$

However, Beasley et al. [7] found that at the temperature $T_{\mathrm{v}}$ at which vortex pairs would dissociate if there were no screening, the value of $\Lambda$ satisfies a relation that follows from (18) and (24),

$$\Lambda(T_{\mathrm{v}}) = \frac{\phi_0^2}{16\pi^2 k_{\mathrm{B}} T_{\mathrm{v}}} \approx \frac{2\ \mathrm{cm}}{T_{\mathrm{v}}} ,$$

where the temperature $T_{\mathrm{v}}$ is to be measured in degrees kelvin. Hence, at $T_{\mathrm{v}}$ of about several degrees kelvin (which is a typical transition temperature for a Josephson junction array [100, 101]), the value of $\Lambda(T_{\mathrm{v}})$ proves to be of the order of a typical array size (0.1 – 1 cm), with the result that screening can be ignored, which is what we assume from now on unless stated otherwise.

### 3.2 Frustrated XY models

With the assumptions introduced above, a regular Josephson junction array placed in an *external* magnetic field can be described by the Hamiltonian [17]

$$H_{\mathrm{fXY}} = -J \sum_{(\mathbf{ij})} \cos\left(\varphi_{\mathbf{j}} - \varphi_{\mathbf{i}} - A_{\mathbf{ij}}\right) , \tag{25}$$

where the variables $A_{\mathbf{ij}} \equiv -A_{\mathbf{ji}}$ defined on lattice bonds are expressed in terms of the integral of the vector potential $\mathbf{A}(\mathbf{r})$ of the external magnetic field along the line connecting the centers of neighboring granules,

$$A_{\mathbf{ij}} = \frac{2\pi}{\phi_0} \int_{\mathbf{r_i}}^{\mathbf{r_j}} \mathrm{d}\mathbf{r}\, \mathbf{A}(\mathbf{r}) , \tag{26}$$

and are frozen, i.e., do not fluctuate. In all cells of a regular lattice, the directed sum of the $A_{\mathbf{ij}}$ along the cell perimeter must satisfy the condition

$$\sum_{\square} A_{\mathbf{ij}} = 2\pi f , \tag{27}$$

where $f$ is the ratio of the magnetic flux $\phi$ per unit cell to the flux quantum $\phi_0$.

The model defined by Eqns (25) – (27) is commonly known as the uniformly frustrated XY model [18]. The form of Hamiltonian (25), in which each term is an even periodic function of its argument, suggests that the parameter $f$ can be assumed to belong to the interval $[0, 1/2]$, while for all the values of $f$ outside this interval, a simple change of variables allows passing to $f \in [0, 1/2]$. From now on, we assume that $f$ is reduced to the interval $[0, 1/2]$. Clearly, the value $f = 0$ corresponds to the conventional (nonfrustrated) XY model considered in the previous section. Models with the maximum irreducible value of $f$ (i.e., $f = 1/2$) are commonly known as FFXY models [20]. In the case of a triangular lattice, the XY model with the antiferromagnetic interaction can be expressed in form (25) with $A_{\mathbf{ij}} \equiv \pm\pi$, and therefore this model also belongs to the class of FFXY models.

In the last twenty years, frustrated XY models with various types of lattices and different values of $f$ have been intensively studied, which on the whole was prompted by active experimental investigations of Josephson junction arrays (the reviews in Refs [100, 101] are devoted to this subject). From the standpoint of statistical physics, the main property of uniformly frustrated XY models (with $f \neq 0$) is the combination of the continuous degeneracy of the ground state related to the simultaneous rotation of all phases and a discrete degeneracy, which is also symmetry-related. This suggests the possibility of various phase transitions occurring in the system, one of which is related to vortex-pair dissociation and is similar to the BKT transition in the conventional XY model [1 – 5], while another (or others) is (are) related to discrete degrees of freedom [20]. In its simplest form, discrete degeneracy occurs in the FFXY models on square and triangular lattices. In both cases, it is twofold [19, 27].

### 3.3 Networks of superconducting wires

In the London limit, the free energy of a thin superconducting wire can be assumed to depend solely on the gauge-invariant gradient of the phase along the wire,

$$F_{\mathrm{wire}} = \frac{J}{2} \int_0^L \mathrm{d}x \left[ \frac{\partial\varphi}{\partial x} - \frac{2\pi}{\phi_0} A_{\parallel}(x) \right]^2 , \tag{28}$$

where $A_{\parallel}(x)$ is the component of the vector potential (locally) directed along the wire. If the values of the phase at the ends of the wire are specified (e.g., $\varphi(0) = \varphi_{\mathbf{i}}$ and $\varphi(L) = \varphi_{\mathbf{j}}$), the functional in (28) attains its minima at

$$\varphi(x) = \varphi_{\mathbf{i}} + \left(\varphi_{\mathbf{j}} - \varphi_{\mathbf{i}} + 2\pi p - A_{\mathbf{ij}}\right) \frac{x}{L} + \frac{2\pi}{\phi_0} \int_0^x \mathrm{d}x'\, A_{\parallel}(x') , \tag{29}$$

where the integer-valued variable $p$ (the winding number) is the number of turns that the phase makes in the motion along the wire.

Substituting (29) in (28) shows [102, 103] that the partition function of a regular network comprised of such wires is simply the partition function of the frustrated XY model with the Berezinskii – Villain interaction:

$$Z_{\mathrm{fBV}} = \prod_{\mathbf{j}} \left( \int_{-\infty}^{\infty} \mathrm{d}\varphi_{\mathbf{j}} \right) \times \prod_{(\mathbf{ij})} \left\{ \sum_{p_{\mathbf{ij}}=-\infty}^{\infty} \exp\left[ -\frac{J}{2} (\varphi_{\mathbf{j}} - \varphi_{\mathbf{i}} + 2\pi p_{\mathbf{ij}} - A_{\mathbf{ij}})^2 \right] \right\}, \quad (30)$$

where the $\varphi_{\mathbf{j}}$ are the values of the phase at the network nodes, and the terms with different values of the variables $p_{\mathbf{ij}}$ correspond to sectors differing from each other in the number of turns that the phase makes in the motion along the network segment connecting the sites **i** and **j**. Thus, XY models with the Berezinskii – Villain interaction (both with and without frustration) are of interest not only as an approximation for studying a similar model with cosinusoidal interaction but also in describing phase fluctuations in networks comprised of thin superconducting wires.

### 3.4 The Coulomb-gas representation

Gaussian integration with respect to all the variables $\varphi_{\mathbf{j}}$ performed in (30) transforms $Z_{\mathrm{fBV}}$ into the partition function of a Coulomb gas described by Hamiltonian (6). The difference from the conventional XY model is that in the case of a uniformly frustrated model, the Coulomb-gas charges are not integers but are shifted with respect to integer values by $-f$ [104], which again emphasizes the sufficiency of considering the interval $0 \leqslant f \leqslant 1/2$.

We note that in such a situation, the term 'Coulomb gas' is strictly nominal, because by construction, all sites of the dual lattice contain finite charges in any of the possible states. In particular, the FFXY model corresponds to the filling of the dual lattice with half-integer charges. Because charges of the same sign repel each other, it is easy to see that in this case, the states with the lowest energy are those in which all charges are equal to $\pm 1/2$ and alternate in a regular pattern. In the case of a square or triangular lattice, this enables understanding the structure of the ground state without calculations.

At the same time, neither in the case of a honeycomb lattice nor in the case of a dice lattice [105 – 107] is it possible to uniquely divide the dual lattice into two equivalent sublattices, while the ground state of the FFXY model is infinitely degenerate [108 – 110], with the degeneracy originating in the possibility of the formation of domain walls with zero energy [22, 110]. In such situations, even establishing the structure of the ordered state formed at low temperatures in a Josephson junction array or a network of thin superconducting wires with a half-integer number of flux quanta per unit cell is very complicated and requires considerable effort [36, 111 – 113], due to the need to study the various mechanisms of accidental-degeneracy lifting.

The question of the sequence of phase transitions is not simple even when the structure of ordering in the low-temperature phase is clear. In the limit $f \ll 1$, the behavior of the system can be explained in terms of a transition of the vortex crystal into an incommensurate state with subsequent melting [114, 115] (which has been confirmed by numerical simulations [115 – 117]), but in the apparently much simpler case where the discrete degeneracy of the ground state is the simplest of all (i.e., twofold), establishing the number, nature, and sequence of phase transitions constitutes a highly nontrivial problem, to the discussion of which the following three sections are devoted.

## 4. Fully frustrated XY model on a square lattice

As noted in Section 3, a regular Josephson junction array placed in an external magnetic field whose magnitude corresponds to a half-integer number of flux quanta per unit cell can be described by the so-called FFXY model [20] defined by the Hamiltonian

$$H = \sum_{(\mathbf{ij})} V(\varphi_{\mathbf{j}} - \varphi_{\mathbf{i}} - A_{\mathbf{ij}}), \quad (31)$$

where $V(\theta) = -J\cos\theta$ and the variables $A_{\mathbf{ij}}$ satisfy the condition

$$\sum_{\square} A_{\mathbf{ij}} = \pi \,(\mathrm{mod}\, 2\pi) \quad (32)$$

for all unit cells of the lattice. In this section, we consider a square lattice, and discuss a similar model for a triangular lattice in Section 5.

### 4.1 Ground state and topological excitations

For an isolated lattice cell, the minimum of (31) with condition (32) satisfied is attained when all the gauge-invariant phase differences defined on the bonds (**ij**),

$$\theta_{\mathbf{ij}} = \varphi_{\mathbf{j}} - \varphi_{\mathbf{i}} - A_{\mathbf{ij}} \equiv -\theta_{\mathbf{ji}}, \quad (33)$$

are equal, which means that $\theta_{\mathbf{ij}} = \pm\pi/4$ for a square lattice. Here and in what follows, the variables $\theta_{\mathbf{ij}}$ are assumed to be reduced to the interval $(-\pi, \pi)$.

The ground state of the FFXY model on a square lattice can be constructed from the ground state for each cell and has the structure shown in Fig. 3 [19]. The form of the ground state is independent of the specific form of the interaction $V(\theta)$ and is characterized by a regular alternation (checkerboard pattern) of cells with positive and negative chiralities $\sigma_{\mathbf{R}} = \pm 1$ determined by the relation

$$\sum_{\square} \theta_{\mathbf{ij}} = \pi\sigma_{\mathbf{R}}.$$

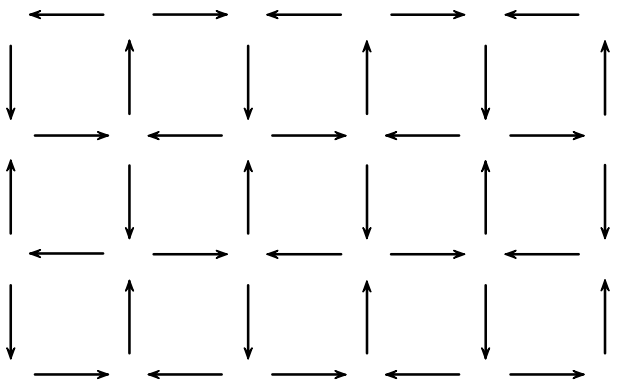

**Figure 3.** Structure of the ground state of the FFXY model on a square lattice. Each arrow corresponds to $\theta_{\mathbf{ij}} = \pm\pi/4$, with the sign of $\theta_{\mathbf{ij}}$ determined by the arrow direction.

In addition to being continuously degenerate, due to the invariance of Hamiltonian (31) under simultaneous rotation of all phases,

$$\varphi_{\mathbf{j}} \to \varphi_{\mathbf{j}} + \Delta\varphi\,,$$

the ground state of the FFXY model on a square lattice is also twofold discretely degenerate, due to the invariance of (31) under the simultaneous reversal of sign in all $\varphi_{\mathbf{j}}$ and $A_{\mathbf{ij}}$ [which does not violate condition (32)].

In accordance with the degeneracy of the ground state, the model allows the existence of two types of topological excitations: vortices and domain walls [20]. Vortices are point-like defects such that the phase rotates by $\pm 2\pi$ in going around them, and therefore have the same meaning as in the conventional XY model (without frustration); see Section 2.2.

As in the case of the conventional XY model, we can expect that vortex-pair dissociation occurs when the 'universal criterion' (18) is satisfied. For the standard interaction $V(\theta) = -J\cos\theta$, the value of the helicity modulus in the ground state of the fully frustrated XY model on a square lattice is $J/\sqrt{2}$, and therefore the simplest estimate (with the renormalization of $\Gamma$ ignored) of the vortex-pair dissociation temperature $T_{\mathrm{v}} \approx (\pi/2)\Gamma(0)$ yields $T_{\mathrm{v}} \approx 1.11\,J$ [21]. But if we assume that the renormalization of $\Gamma$ at the phase transition point is the same as in the absence of frustration, then $T_{\mathrm{v}} \approx 0.6\,J$.

In the Coulomb-gas representation, ground states are characterized by regular alternation of positive and negative changes of minimum value:

$$m_{\mathbf{R}}^{(0)} = \pm\frac{1}{2}\,(-1)^{R_x+R_y}\,, \tag{34}$$

where $R_x$ and $R_y$ (the components of $\mathbf{R}$) are integers, and the possibility of choosing the sign corresponds to the twofold discrete degeneracy of the ground state. Here, the values of the variables $m_{\mathbf{R}}$ may be associated with the chiralities of the respective cells: $\sigma_{\mathbf{R}} = 2m_{\mathbf{R}}$. On the other hand, vortices may be associated with the excessive integer charges on the background of one of states (34). To correctly reproduce the form of vortex interaction at large distances, we must replace

$$J \to J_{\mathrm{Cg}} = \frac{J}{\sqrt{2}}\,,$$

in the Coulomb-gas representation, because $\Gamma(T=0) = J/\sqrt{2}$ in the original system.

A domain wall may be defined as a topological excitation that separates two ground states that cannot be transformed into each other by rotating all phases simultaneously. It can be schematically represented by a line on the original square lattice (Fig. 4), each segment of which separates two cells with the same chirality [20].

A domain wall is characterized by a finite energy $E_{\mathrm{dw}}$ per unit length, with the result that at low temperatures ($T \ll E_{\mathrm{dw}}$), all domain walls formed as thermal fluctuations constitute closed loops. In the case of a straight wall, direct numerical calculations for the XY model with $V(\theta) = -J\cos\theta$ yielded $E_{\mathrm{dw}} \approx 0.343\,J$ [21], and the Coulomb-gas value is very close [22]:

$$E_{\mathrm{dw}} = \frac{\pi^2}{16\sqrt{3}}\,J_{\mathrm{Cg}} \approx 0.308\,J\,.$$

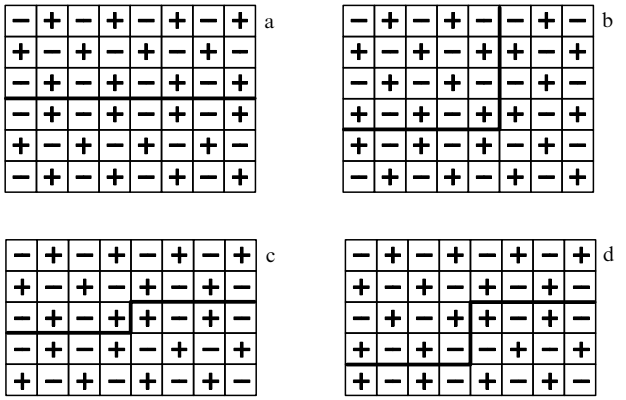


**Figure 4.** Examples of domain walls: (a) straight; (b) forming a right angle; (c) with a simple kink; and (d) with a double-height kink. The chiralities of the lattice cells are indicated by the plus and minus signs.

The Coulomb-gas representation is quite useful because it allows establishing how the interaction of domain walls depends on the distance $L$ between them: it turns out to be proportional to $c_0^L$, where $c_0 = 3 - \sqrt{8} \approx 0.172$ [22], i.e., decays exponentially, and we therefore do not take it into account in further analysis. If we ignore the part of the energy related to corners and intersections of walls, the Hamiltonian of the domain-wall subsystem is reduced to the Ising model on the dual lattice,

$$H_{\mathrm{dw}} = -\frac{E_{\mathrm{dw}}}{2}\sum_{(\mathbf{RR}')} s_{\mathbf{R}} s_{\mathbf{R}'}\,, \tag{35}$$

whose exact solution for a square lattice was found by Onsager [118] and, in a much more convenient form, by Vdovichenko [119].

The variable $s_{\mathbf{R}}$ in (35) is known as the staggered chirality:

$$s_{\mathbf{R}} = (-1)^{R_x+R_y}\sigma_{\mathbf{R}}\,.$$

The temperature $T_{\mathrm{dw}}$ at which the Ising model undergoes the phase transition related to the formation of infinite domain walls and the destruction of long-range order in $s$,

$$T_{\mathrm{dw}} = \frac{E_{\mathrm{dw}}}{\ln(1+\sqrt{2})}\,, \tag{36}$$

can be found even without knowing the exact solution, solely on the grounds of duality considerations [120]. Substituting $E_{\mathrm{dw}} \approx 0.343\,J$ in (36) yields $T_{\mathrm{dw}} \approx 0.39\,J < T_{\mathrm{v}}$ [21]. However, in the next section, we show that in the XY model under consideration, the interaction of corners and domain-wall intersections is not short-range and cannot therefore be ignored.

### 4.2 Fractional vortices and phase transitions

If we fix the ground state (the values of $\varphi_{\mathbf{j}}$) on one side of an infinite, straight domain wall, the state on the other side of the wall cannot be chosen arbitrarily and depends on both position and orientation of the wall. In particular, the equilibrium states on the other side of vertical and horizontal walls differ by rotation by $\pm\pi/2$. This means that if the domain wall forms a right angle (Fig. 4b), there is a mismatch of $\pm\pi/2$ between the states obtained by crossing the horizontal and vertical sections of the wall. The mismatch

can be removed by continuously changing the phase such that going around the corner result in a $\pm\pi/2$ increase in the phase. Thus, all corners of domain walls must behave as fractional vortices with the topological charge $\pm 1/4$, with the interaction between them being 16 times weaker than that between ordinary vortices [21, 22].

The presence of excessive vorticity at a domain-wall corner also follows from the fact that the sum of chiralities of the four cells surrounding the angle is not zero (Fig. 4b). At the same time, at all lattice sites through which the domain wall does not pass (or a straight wall passes), the similar sum vanishes.

If fractional vortices with the topological charge $\pm 1/4$ were not bound to domain walls, the dissociation of the neutral pairs they form would occur at the temperature $T = T_{\mathrm{fv}}$, where $T_{\mathrm{fv}} \ll T_{\mathrm{v}}$ is the solution of the equation

$$T_{\mathrm{fv}} = \frac{\pi}{32}\, \Gamma(T_{\mathrm{fv}})\,, \tag{37}$$

which is similar to Eqn (18). But the total topological charge of fractional vortices related to a closed domain wall is always an integer, and therefore at $T < T_{\mathrm{dw}}$, when all domain walls form closed loops, dissociation of pairs of fractional vortices is forbidden. In addition to being bound by a weak logarithmic interaction, such pairs are also bound (at large distances) by a linear interaction related to the free energy of the domain walls connecting them.

At the same time, when $T > T_{\mathrm{dw}}$, there exists a network of intersecting domain walls, with the mean distance between the walls being of the order of $\xi_{\mathrm{c}}$, the correlation radius for the variables $s$. In this case, the linear interaction of fractional vortices at distances exceeding $\xi_{\mathrm{c}}$ is screened, which indeed allows the dissociation of bound pairs of such vortices, which in turn initiates dissociation of pairs of ordinary vortices. This implies that if the naive estimates yield $T_{\mathrm{v}} \sim T_{\mathrm{dw}}$ (and, hence, $T_{\mathrm{fv}} \ll T_{\mathrm{dw}}$), the scenario with $T_{\mathrm{v}} > T_{\mathrm{dw}}$ is impossible, because the emergence of infinite domain walls at $T = T_{\mathrm{dw}}$ automatically leads to dissociation of pairs of fractional and integer vortices [21, 22].

This statement was verified in Ref. [121] by Monte Carlo simulation of a Coulomb gas with charges $m = \pm 1/2$ on a square lattice. The possibility of varying the domain-wall energy $E_{\mathrm{dw}}$ independently was ensured by adding the nearest-neighbor interaction to the standard Hamiltonian of the two-dimensional Coulomb gas in (6). The results showed that the system undergoes two phase transitions when the domain wall has a high energy and that the temperatures of these transitions satisfy the inequality $T_{\mathrm{v}} < T_{\mathrm{dw}}$ and are quite different. The temperature $T_{\mathrm{dw}}$ decreases with $E_{\mathrm{dw}}$ almost linearly, while the dependence of $T_{\mathrm{v}}$ on $E_{\mathrm{dw}}$ is much weaker. With a further decrease in $E_{\mathrm{dw}}$, the two phase-transition curves merge instead of intersecting. Similar results were obtained in Ref. [122] for the same model defined on a honeycomb lattice, which in terms of the XY models corresponds to the fully frustrated model on a triangular lattice.

Because the appearance of fractional vortices on domain-wall defects is a characteristic feature not only of fully frustrated models but also of models with smaller values of $f$ (see, e.g., Ref. [123]), we can expect that the main conclusion in this section (concerning the impossibility of a scenario with $T_{\mathrm{v}} > T_{\mathrm{dw}}$) will be valid for a broader class of uniformly frustrated models [22]. We note, however, that in the generalization of the FFXY model on a square lattice proposed in Ref. [124], in which the coupling constants are different for ferromagnetic and antiferromagnetic bonds, two types of domain walls (light and heavy [125]) emerge, and therefore the fractional vortices are bound into neutral pairs when $T > T_{\mathrm{dw}}$, which in this situation makes $T_{\mathrm{v}} > T_{\mathrm{dw}}$ possible [124, 125].

### 4.3 Phase transition on a domain wall and its consequences

We consider an infinite domain wall whose existence is ensured, for instance, by appropriate boundary conditions. At zero temperature, this wall is absolutely straight (Fig. 4a). At finite temperatures, point defects, or kinks, may appear on the wall. The simplest kink (of unit height) is shown in Fig. 4c.

If we fix the state (the values of $\varphi_{\mathbf{j}}$) on one side of the infinite straight wall, then under its shift by one lattice constant, the equilibrium state on the opposite side of the wall rotates by $\pi$ [21, 22]. Hence, the presence of a kink depicted in Fig. 4c leads to a mismatch by $\pi$ between the states obtained when the wall is crossed on the left and on the right of the kink. As in the case of a corner of a domain wall, this mismatch is to be removed by continuously changing the phase such that the necessary value be attained in going around the kink.

Accordingly, simple kinks must behave as fractional vortices with the topological charge $\pm 1/2$ [24]. The energy of such kinks diverges logarithmically, and the interaction is four times weaker than that between ordinary vortices. The double kink shown in Fig. 4d does not introduce such mismatches in the phase distribution, with the result that its energy is finite.

The existence of two dramatically different types of kinks can be easily explained on the grounds that all corners on domain walls have topological charges $\pm 1/4$. Each kink is formed by two corners; for a simple kink, their topological charges are of the same sign and therefore add up, whereas for a double kink, the charges of the corners that form the kink are of opposite signs and therefore compensate each other.

At low temperatures, a domain wall carries a finite concentration of free (i.e., not bound into pairs) double kinks, while all simple kinks are bound into neutral (in topological charge) pairs (we note that the sign of the topological charge related to a kink is determined by the kink position rather than its orientation). Therefore, although the fluctuations of a domain wall diverge (due to the presence of free double kinks) at an arbitrarily low temperature (and hence the wall is always in the rough rather than in the smooth state), the symmetry with respect to the wall displacement by an odd number of lattice constants is broken [24].

As the temperature increases, a phase transition in a one-dimensional gas of logarithmically interacting kinks leads to the neutral-pair dissociation and emergence of a finite concentration of free simple kinks [23]. Comparison of the logarithmically divergent energy of a single kink, $E_{\mathrm{k}} \approx (\pi/4)\Gamma(T)\ln L$, with the kink entropy $S_{\mathrm{k}} \approx \ln L$ suggests that this occurs at the temperature $T_{\mathrm{k}}$ satisfying the relation

$$T_{\mathrm{k}} = \frac{\pi}{4}\, \Gamma(T_{\mathrm{k}})\,. \tag{38}$$

We note that $\Gamma(T)$ is the 'bulk' value of the helicity modulus, which enters the bare interaction of the kinks and does not take wall fluctuations into account. Never-

theless, relation (38) is exact. The reason is that, according to Bulgadaev's renormalization-group analysis [126], no renormalization of the prefactor in the logarithmic interaction occurs in a one-dimensional logarithmic gas with arbitrary charge alternation (in contrast to a one-dimensional logarithmic gas with alternating charges [78] and to a two-dimensional Coulomb gas [5]), and therefore the value of the transition temperature that follows from the comparison of the charge energy with its entropy turns out to be exact.

Comparison of (38) with (18) shows that $T_k < T_v$. Kink-pair dissociation at temperatures below $T_v$ was first discovered in the numerical experiments in Ref. [127]; however, the authors took the phase transition at $T = T_k$ for the roughening transition of a domain wall.

Dissociation of simple-kink pairs restores the symmetry between predominantly even and predominantly odd positions of the domain wall and leads to a loss of the effective rigidity for phase fluctuations on the wall [24]. In the presence of free simple kinks, any attempt to create a phase gradient in the direction perpendicular to the wall fails because the shift of these kinks caused by the Magnus force (the direction of the shift is determined by the sign of the topological sign) eliminates the gradient.

The situation is similar to that occurring in the 'bulk' at $T > T_v$, when the presence of free vortices impedes formation of a phase gradient, i.e., a superfluid current. At $T < T_k$, all simple kinks are bound into neutral pairs and their relative displacement requires spending finite energy, which preserves the effective rigidity on the wall.

On the other hand, we can expect the phase gradient directed parallel to the wall not to penetrate it. Instead, there appears a difference in the concentrations of free simple kinks with topological charges of different signs that balances the difference between the phase gradients on both sides of the wall [24]. Although the creation of such a concentration difference requires spending a certain amount of energy, this amount is proportional to the wall length, while the penetration of the phase gradient to the other side of the wall requires spending an amount of energy proportional to the area of the system, which is less advantageous in the thermodynamic limit. A similar structure can be seen in grain boundaries in a crystal, where the difference in crystallite orientations at the boundary is balanced by the presence of a sequence of dislocations of the same sign.

We note that both mechanisms operate only on large scales compared to $\xi_k$, the mean distance between free simple kinks on the wall. Nevertheless, the existence of such mechanisms means that the coupling between large-scale phase fluctuations on both sides of the wall is destroyed. From now on, when speaking of domain walls, we assume that the properties of the system are analyzed on scales exceeding $\xi_k$, and therefore there can be no coupling that links the phase fluctuations on both sides of the wall. In a recent paper, Olsson and Teitel [128] concluded that at $T = T_k < T_v$, the helicity modulus is suppressed in the direction perpendicular to the domain wall and corroborated, via numerical simulations, some other conclusions drawn in this section.

### 4.4 The sequence of phase transitions

The helicity modulus $\Gamma(T)$ can be defined, e.g., as the response of the system to the introduction of a shift into the boundary conditions [68, 77] (this underlies the method of numerical calculation of $\Gamma(T)$ proposed in Ref. [20], which has now become standard). The possibility of defining the helicity modulus in such a way implies that in a situation where phase fluctuations on two sides of a domain wall become independent, the presence of at least one wall that crosses the entire system automatically results in the vanishing of $\Gamma(T)$. In the thermodynamic limit, this inevitably occurs as soon as the temperature exceeds $T_{dw}$, the temperature of the phase transition related to the loss of long-range order in the antiferromagnetic ordering of the chiralities and the formation of infinite domain walls.

If we consider the fluctuations of the discrete degrees of freedom (which amount to the formation of domains with the opposite sign of $s$) in terms of the percolation problem, then at $T < T_{dw}$, there exists an infinite cluster that crosses the entire system and is formed by cells with the same value of $s$. The introduction of a relative shift between the values of the phase on the left and right boundaries of the infinite system results in a gradient of the phase only within this infinite cluster. All other clusters are finite and hence insensitive to boundary conditions at infinity.

It is known that in two dimensions (in contrast to three dimensions), the critical point of the Ising model coincides with the percolation point in a system of spin clusters [129], and therefore, as $T_{dw}$ is approached from below, the density of an infinite cluster decreases as

$$\rho(T) \propto \xi_p^{-\Delta d},$$

where $\Delta d = 2 - \bar{d} = 5/96$ [130, 131] is the deviation of the fractal dimension $\bar{d}$ of the infinite cluster (at $T = T_{dw}$) from the Euclidean dimension $d = 2$ (in the standard problem of uncorrelated percolation, $\Delta d = 5/48$ [132]), and

$$\xi_p(T) \propto (T_{dw} - T)^{-\nu}$$

is the percolation length, whose temperature dependence in the Ising model is described by the same exponent $\nu = 1$ [133] as the temperature dependence of the correlation radius $\xi_c$.

Hence, even the bare value (i.e., not renormalized by fluctuations of $\varphi$) of the helicity modulus must decrease in accordance with a power law as $T_{dw}$ is approached,

$$\Gamma_0(T) \propto (T_{dw} - T)^t,$$

at least as fast as $\rho(T)$ (actually, much faster), which can be demonstrated by a variational calculation. Vortex-pair dissociation occurs as soon as the renormalized value of $\Gamma(T)$ becomes equal to $(2/\pi)T$, i.e., at a temperature below $T_{dw}$ [24]. If $T_{dw} \ll T_v^{(0)}$, where $T_v^{(0)} \approx (\pi/2)\Gamma(0)$ is the simplest estimate for $T_v$ that does not account for renormalizations, we can expect the dependence of $T_v$ on the ratio of $T_v^{(0)}$ to $T_{dw}$ to be

$$T_{dw} - T_v \propto \left(\frac{T_{dw}}{T_v^{(0)}}\right)^{1/t}.$$

Both transitions may occur simultaneously only as a first-order phase transition accompanied by a jump in $\Gamma(T)$ exceeding the universal value.

The conclusion that $\Gamma_0(T)$ is strongly suppressed as $T_{dw}$ is approached is corroborated by a comparison of the results of numerical simulations of the conventional and frustrated XY models [20], results that show that $\Gamma$ decreases more rapidly with increasing the temperature in the frustrated model (for

the same size of the system). The first to assert that $\Gamma(T)$ vanishes as $T \to T_{dw}$ were Dotsenko and Uimin [134, 135], who studied a similar model on a triangular lattice (with the same degeneracy of the ground state). However, they did not substantiate their assertion.

Thus, we showed that in the FFXY model on a square lattice, the presence of free simple kinks on domain walls destroys the coherency of fluctuations on different sides of a wall within a broad temperature range below $T_v$. We also showed that vortex-pair dissociation must occur at $T_v < T_{dw}$, because, as $T_{dw}$ is approached from below, the part of the system that contributes to the helicity modulus (which determines the interaction of vortices) becomes less and less dense due to that property of domain walls. This makes a merger of the two phase transitions into one phase transition with new critical behavior (as predicted in Refs [22, 136]) impossible, for $T > T_k$ at least. The next section shows that all these conclusions remain valid when the square lattice is replaced by a triangular one (which does not alter the type of the ground state degeneracy).

We note that the above conclusions are independent of a particular type of the interaction (as long as the structure of the ground state and, hence, its degeneracy remain unchanged) and can be applied, in particular, when the interaction of more distant neighbors is taken into account. The structure of the phase diagram of the FFXY model on a square lattice with the interaction that extends beyond the nearest neighbors is discussed in the next section.

At the same time, the above mechanism that forces $T_v$ to be below $T_{dw}$ operates only at $T_{dw} > T_k$. If the domain-wall energy $E_{dw}$ were an adjustable parameter, which would allow varying $T_{dw}$ independently of the vortex interaction, the lowering of $E_{dw}$ would lead to a merger of the two phase transitions (as $T_{dw}$ decreases to $T_k$). Comparison with the results of numerical simulations for $f = 2/5$ [137, 138] and other considerations (similar to those discussed in Sections 6.4 and 7.4) prompt the conclusion that this must be a first-order phase transition with a nonuniversal jump in $\Gamma(T)$ that varies along this line. The phase transitions would split again only after a further significant (severalfold) reduction in $E_{dw}$ and an increase in the ratio $\Gamma(T_c)/T_c$ to $32/\pi$ [22]. At even lower values of $E_{dw}$, the loss of phase coherence would be related to dissociation of pairs of fractional vortices, which at $T > T_{dw}$ are coupled only by logarithmic interaction and would occur at $T = T_{fv} > T_{dw}$ [22]. Section 6 shows that all the three scenarios for the destruction of the combined $U(1) \times Z_2$ order are realized in the antiferromagnetic XY model on a kagome lattice, where, in contrast to the FFXY model on a square lattice, the addition of the second-neighbor interaction to the Hamiltonian guarantees the possibility of a practically independent variation of $E_{dw}$.

In the past two decades, the FFXY model on a square lattice has been the subject of intensive numerical studies. The data obtained in earlier works either did not allow resolving $T_v$ and $T_{dw}$ [20, 124, 139] or suggested that $T_v > T_{dw}$ [140]. However, the development of numerical methods and computer facilities changed the situation dramatically. The results of more recent works using various numerical methods [141–145] yielded

$$T_v = (0.440-0.449)J, \qquad T_{dw} = (0.452-0.454)J$$

indicating that $T_v < T_{dw}$, which therefore agrees with the results of the present analysis. Numerical simulations of the model with the Berezinskii–Villain interaction in [146] and of the equivalent model of the Coulomb gas with half-integer charges in [147] and [148] also show that $T_v < T_{dw}$.

Beginning with paper [136], the main argument in favor of the idea that the temperatures of the two phase transitions are the same, suggested by many researchers, was the observation that the critical exponents differ from the Ising-model values [136, 140–142, 149–152]. However, Olsson [146] showed that the exclusion of small scales from the scaling analysis resolves this discrepancy. Boubcheur and Diep [150] drew their conclusion that the system can have only one phase transition on the grounds that the peak in the specific heat is not split. Apparently, they were unaware of the fact that a BKT transition is not accompanied by any divergences in the derivatives of the free energy.

We emphasize that for both types of interaction and for the similar model on a triangular lattice (see Section 5), the values of $T_v$ and $T_{dw}$ found by numerical simulations prove to be extremely close to each other and differ by 1–2%. It is highly probable that this is not a coincidence but a consequence of vortex-pair dissociation occurring not by itself but due to the rapid decrease in the value of the helicity modulus $\Gamma(T)$ induced by the approach to $T_{dw}$. According to the estimates in Section 4.1, in the absence of any mutual influence of the phase transitions, such a dissociation must occur at a temperature much higher than $T_{dw}$, i.e., $T_v \approx 1.5\, T_{dw}$.

The conclusion that $T_v$ is below $T_{dw}$ is also valid for the so-called XY-Ising model described by the Hamiltonian [153]

$$H = -J \sum_{(\mathbf{j}\mathbf{j}')} (1 + s_{\mathbf{j}} s_{\mathbf{j}'}) \cos(\varphi_{\mathbf{j}} - \varphi_{\mathbf{j}'}), \tag{39}$$

where $s_{\mathbf{j}} = \pm 1$ are additional variables of the Ising type. In this model, which has been thoroughly studied in Refs [154–157] as an approximant for the frustrated XY model on a square lattice, the coupling between the fluctuations of $\varphi_{\mathbf{j}}$ on the two sides of a domain wall is absent from the beginning.

Recently, Lee et al. [158] showed that a generalized version of the XY-Ising model is dual to the model proposed by den Nijs [159] for describing roughening and reconstruction transitions on the surface of a crystal with a simple cubic lattice. The expected phase diagram of this model can be found in Fig. 3 in Ref. [160]. At $\Delta = 0$ (which corresponds to XY-Ising model (39) without any coupling of the phase variables across the wall), the phase diagram has two regions: in one (with $R < 0$), both phase transitions occur simultaneously, while in the other (with $R > 0$) they occur subsequently. Both the analysis in the present section and the results of numerical simulation in Ref. [158] show that the phase transitions do not coincide in either region, i.e., for any sign of $R$.

Experimental studies of square Josephson junction arrays placed in a uniform magnetic field whose magnitude corresponds to half the magnetic flux quantum per lattice cell have been conducted by several researchers [161–167]. Unfortunately, the methods used by these researchers (in particular, in studying the temperature dependence of both components of the complex-valued frequency-dependent impedance [161, 162] and the exponent describing the behavior of the current–voltage characteristic in the small-current limit [163, 164]) allowed gathering information only about the superconducting transition but were not sensitive to the ordering of chiralities (at least when it occurred at $T = T_{dw} > T_v$).

### 4.5 Structure of the phase diagram with the next-to-nearest-neighbor interaction

We now consider the generalization of Hamiltonian (31) given by

$$H = -\sum_{\mathbf{i},\mathbf{j}} J_{\mathbf{ij}} \cos\left(\varphi_{\mathbf{j}} - \varphi_{\mathbf{i}} - A_{\mathbf{ij}}\right), \tag{40}$$

where the coupling constant $J_{\mathbf{ij}}$ is nonzero not only for the nearest neighbors on the square lattice but also for the next-to-nearest neighbors:

$$J_{\mathbf{ij}} = \begin{cases} J_1\,, & |\mathbf{i}-\mathbf{j}| = 1\,, \\ J_2\,, & |\mathbf{i}-\mathbf{j}| = \sqrt{2}\,, \end{cases} \tag{41}$$

with the values of the variables $A_{\mathbf{ij}}$ for the next-to-nearest neighbors specified in (26).

The study of such a generalization is interesting from the standpoint of finding a way to separate the temperatures of the two phase transitions farther apart (which would make their resolution more accessible in experiments or in numerical simulations) or, on the contrary, to achieve their merger in a single first-order phase transition. In studying the lattice of superconducting granules whose interaction is caused by the proximity effect and is realized through a metal substrate [168, 169], the need to include the interaction of more distant neighbors into analysis becomes stronger with decreasing the temperature, which is accompanied by an increase in the coherence length in a normal metal [170].

At $f = 1/2$, the model in (40) and (41) combines the features of the frustrated XY model and the conventional (nonfrustrated) XY model. At $J_2 = 0$, Hamiltonian (40) is reduced to (31), while at $J_1 = 0$, it transforms into the Hamiltonian of two independent conventional XY models. Because the unit cell area for each of the two $\sqrt{2} \times \sqrt{2}$ sublattices into which the square lattice separates in the absence of the nearest-neighbor interaction is twice the unit cell area of the original lattice, the next-to-nearest neighbors interaction proves to be nonfrustrated.

The structure of the ground states of model (40) depends on the ratio $x = J_2/J_1 \geqslant 0$ [26]. At $x < x_0 = 1/\sqrt{2}$, these states are of exactly the same form as at $J_2 = 0$, with their energy being independent of $J_2$. At the same time, at $x > x_0$, the ground states prove to be the same as at $J_1 = 0$, where the two $\sqrt{2} \times \sqrt{2}$ sublattices are decoupled. The energy of these states is independent of $J_1$ and the degeneracy is $\mathrm{U}(1) \times \mathrm{U}(1)$, where each of the two $\mathrm{U}(1)$ groups describes the degeneracy in one of the two independent XY models, and the relative orientation of the phase between them can be arbitrary [26].

At $x = x_0$, the energies of the two classes of ground states become equal, which, it would seem, suggests the existence of a first-order phase transition. But it turns out that at $x = x_0$, these states can be transformed into each other via a continuous transformation that does not increase the energy [25, 26]. Thus, at $x = x_0$, the degeneracy space also incorporates an additional set of 'intermediate' states, which can be obtained from the ground state for $x < x_0$ by a synchronous rotation of all the variables $\varphi_{\mathbf{j}}$ belonging to one of the two sublattices shown in Fig. 5 by an arbitrary angle $\chi$. The value $\chi = 0$ then corresponds to the form of the ground state for $x < x_0$, and $\chi = \pi$ corresponds to $x > x_0$.

Interestingly, the addition of a weak interaction with more distant neighbors does not alter this picture, with the exception of a shift in the value of $x_0$. In particular, the structure of the ground states is retained, and at $x > x_0$, the energy remains independent of the relative phase shift between the two $\sqrt{2} \times \sqrt{2}$ sublattices [25].

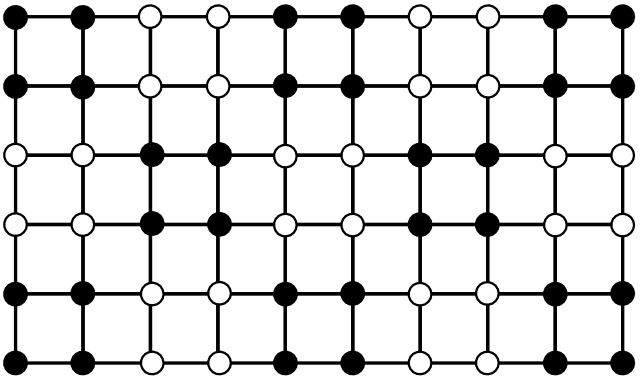

**Figure 5.** Partitioning of a square lattice into two sublattices that occurs at $x = x_0$, when an additional degeneracy of the ground state emerges, associated with the relative rotation of the variables $\varphi_{\mathbf{j}}$ that belong to the two different sublattices by an arbitrary angle $\chi$.

It turns out that at $x < x_0$, not only the structure and energy of the ground state but also the structure and energy of a straight domain wall and the helicity modulus $\Gamma$ are unaffected by the value of $J_2$. This means that an increase in $J_2$ does not change the relation between the domain-wall energy and the prefactor in the logarithmic interaction of vortices and, hence, does not allow significant changes of the ratio of $T_{\mathrm{v}}$ to $T_{\mathrm{dw}}$. The fact that $J_2$ is nonzero manifests itself only through the energies of the cores of vortices and defects on the domain walls. The results of a Monte Carlo simulation indicate that $T_{\mathrm{dw}}/J_1$ somewhat decreases with increasing $J_2$ [25], which, according to the results in the previous section, leads to a further decrease in the relative difference between $T_{\mathrm{v}}$ and $T_{\mathrm{dw}}$.

The additional degeneracy of the ground state at $x > x_0$, which amounts to the possibility of relative rotation of the phases belonging to the different $\sqrt{2} \times \sqrt{2}$ sublattices, is accidental and is not related to symmetry. Clearly, this degeneracy can be lifted for various reasons (e.g., due to the interaction with more distant neighbors). However, as discussed earlier, this mechanism of lifting the additional degeneracy does not operate in the system under consideration.

The only cause for the removal of an accidental degeneracy within the framework of a specific statistical-physics model is the difference in the free energy of fluctuations in the vicinity of different ground states [171]. For systems with continuous degeneracy, such a mechanism was first analyzed by Shender [172], who examined quantum fluctuations in the Heisenberg antiferromagnet with a square lattice and a strong ferromagnetic interaction between the next-to-nearest neighbors. Following Villain et al. [171], this mechanism of accidental degeneracy lifting is often called 'order from disorder.'

Calculations of the free energy of harmonic fluctuations as a function of the relative phase shift between the sublattices have shown that at $x > x_0$ (and at finite temperatures) the system can be regarded as two coupled XY models whose interaction is close in form to $\cos\left[p(\varphi - \varphi')\right]$ with $p = 4$. Although this perturbation is weak (its amplitude is always small compared with the temperature), it becomes relevant (increasing under renormalization) at sufficiently low tem-

peratures. This implies that at such temperatures, the system must exhibit a true long-range order with respect to the phase shift between the sublattices.

The invariance of the sublattice interaction under a shift of the relative phase by $\pi/2$ follows from the symmetry properties of the ground state, and therefore allowing for some other mechanisms of lifting the accidental degeneracy cannot lead to significant changes. One such mechanism relies on the difference of the form of the Josephson energy from $V_0(\theta) = -J\cos\theta$, with the result that in studying the lifting of accidental degeneracy in XY models, one must bear in mind that the description in terms of a Coulomb gas is exact only for a particular choice of $V(\theta)$, which does not coincide with $V_0(\theta)$.

According to the results of the renormalization-group analysis of two weakly coupled XY models in Refs [153, 173], the temperature $T_{\rm dec}$ that separates the region where the interaction of the form $y_p \cos\left[p(\varphi - \varphi')\right]$ increases under renormalization from the region where it decreases is given by

$$T_{\rm dec} = \frac{4\pi}{p^2}\, \Gamma(T_{\rm dec})\,, \tag{42}$$

where $\Gamma(T)$ is the helicity modulus in each of the two models. Comparison with (18) shows that at $p = 4$, the phase-transition temperature determined by Eqn (42) (for the phase transition related to the loss of the coupling between the sublattices) is below $T_{\rm v}$, the temperature of vortex-pair dissociation in each sublattice. Therefore, at $x > x_0$, two phase transitions must occur in the system as the temperature increases [25], the first of them being related to the $Z_4$ symmetry broken at $T < T_{\rm dec}$.

The spectrum of longwave fluctuations retains rigidity as $x \to x_0 + 0$. This means that as $x$ decreases to $x_0$, the temperature $T_{\rm v}$ of vortex-pair dissociation remains finite (this is also confirmed by the numerical simulation results in Ref. [25]). At $T < T_{\rm v}, T_{\rm dec}$ and $x \approx x_0$, there must be a transition of some sort between the phases whose structure corresponds to the two classes of ground states.

The emergence of an additional set of ground states (earlier called intermediate) at $x = x_0$ is one more example of accidental degeneracy. Numerical integration shows that the free energy of harmonic fluctuations is a convex function of the cosine of $\chi$, the angle parameterizing these additional ground states, and therefore the system must undergo a first-order phase transition as $x$ varies (at low but finite temperatures) [25]. If the free energy of fluctuations were a concave function of $\cos\chi$, the two low-temperature phases would be separated by a narrow band of a third phase in which the angle $\chi$ would vary continuously from 0 to $\pi$ with $x$.

Figure 6 schematically shows the structure of the phase diagram of the FFXY model on a square lattice with nonfrustrated interaction of the next-to-nearest neighbors that follows from the results in this section. The figure also contains the results of a Monte Carlo simulation of such a system [25], marked by squares (the Ising transition) and circles (the BKT transition), where the size of a symbol approximately corresponds to the accuracy of the result. The results of numerical studies confirm the existence of two different low-temperature phases, but their accuracy is insufficient for resolving the splitting of both lines of the phase transition into the totally disordered state. A numerical study of the nonlinear relaxation in the same model [174] confirms the presence of a second-order phase transition at $x < x_0$ and the absence of such a transition at $x > x_0$.

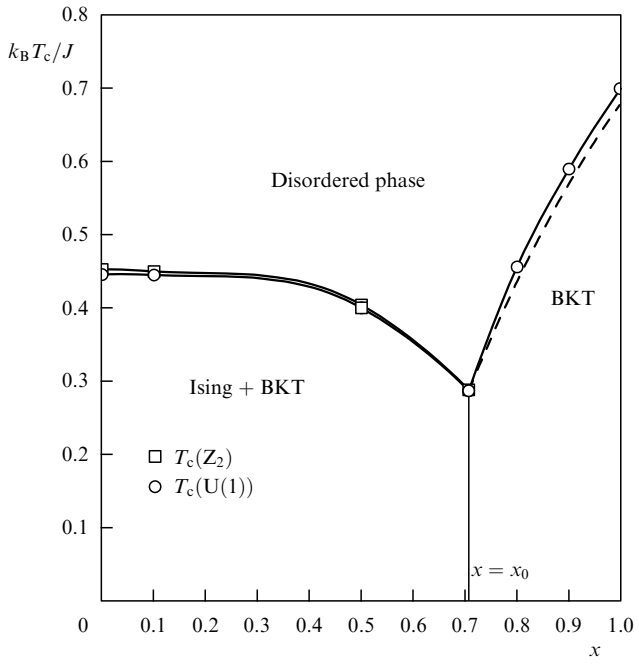


**Figure 6.** Phase diagram of the fully frustrated XY model on a square lattice with nonfrustrated interaction of the next-to-nearest neighbors.

Unfortunately, this method does not allow observing transitions of the BKT type, which are infinite-order transitions.

## 5. A planar antiferromagnet with a triangular lattice

### 5.1 The sequence of phase transitions in the absence of a magnetic field

In the absence of an external magnetic field, a planar antiferromagnet with exchange interaction can be described by the Hamiltonian

$$H_{\rm af} = J \sum_{(\mathbf{ij})} \cos\left(\varphi_{\mathbf{i}} - \varphi_{\mathbf{j}}\right), \tag{43}$$

where the coupling constant $J > 0$ and each spin is associated with a two-component unit vector $\mathbf{S_j} = (\cos\varphi_{\mathbf{j}}, \sin\varphi_{\mathbf{j}})$.

Clearly, Hamiltonian (43) of the AFXY model is equivalent to Hamiltonian (25) with $A_{\mathbf{ij}} = \pm\pi$. Summing $A_{\mathbf{ij}}$ along the perimeter of a cell shows that in the case of a square lattice, the AFXY model is not frustrated, i.e., is isomorphic to the conventional (ferromagnetic) XY model (1). But if we have a triangular lattice, such a model belongs to the class of FFXY models and therefore can also be used to describe Josephson junction arrays with a half-integer number of flux quanta per lattice cell.

The absolute minimum of (43) for three spins belonging to a triangular cell is attained when they are at the angle $2\pi/3$ to each other. This condition is satisfied simultaneously for all the cells in the lattice in a state with a three-sublattice structure [175, 176], shown in Fig. 7a. In this state, the values of the $\varphi_{\mathbf{j}}$ on the three equivalent sublattices (A, B, and C) into which the triangular lattice can be partitioned can be specified as

$$\varphi_{\rm A} = \Phi\,, \qquad \varphi_{\rm B} = \Phi \pm \frac{2\pi}{3}\,, \qquad \varphi_{\rm C} = \Phi \mp \frac{2\pi}{3}\,. \tag{44}$$

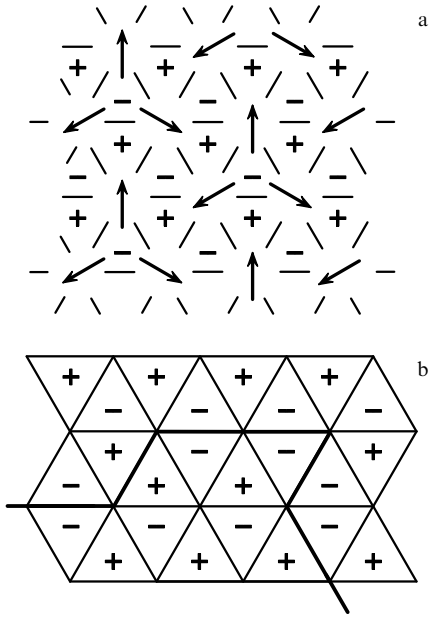


**Figure 7.** A planar antiferromagnet with a triangular lattice: (a) structure of the ground state, and (b) domain wall. The chiralities of the triangular cells are indicated by the plus and minus signs.

In terms of the gauge-invariant phase difference determined by Eqn (33), this is a state in which $\theta_{\mathbf{ij}} = \pm\pi/3$ on all bonds, while the triangular cells with positive and negative chiralities alternate in a regular way (Fig. 7a).

As in the case of a square lattice (see Section 4), the form of the ground state is not related to the specific form of the interaction and is characterized by the combined $\mathrm{U}(1) \times \mathrm{Z}_2$ degeneracy [27]. The continuous degeneracy corresponds to the choice of $\Phi$ in (44) and is related to the symmetry of Hamiltonian (43) under a simultaneous rotation of all spins:

$$\varphi_{\mathbf{j}} \to \varphi_{\mathbf{j}} + \Delta\Phi\,, \tag{45}$$

while the twofold discrete degeneracy corresponds to the choice of the upper or lower sign in (44) and is related to the symmetry of Hamiltonian (42) under simultaneous reflection of all the spins $\mathbf{S}_{\mathbf{j}}$ with respect to an arbitrary axis (e.g., the $x$ axis):

$$\varphi_{\mathbf{j}} \to -\varphi_{\mathbf{j}}\,.$$

In accordance with the degeneracy of the ground state in the model under consideration, both vortices and domain walls of the Ising type may appear in the system [29, 34]. Because the value of the helicity modulus in the ground state at $\theta_{\mathbf{ij}} = \pm\pi/3$ is twice as small as in the absence of frustration (i.e., at $\theta_{\mathbf{ij}} = 0$), a comparison with the results in Ref. [84] suggests that vortex-pair dissociation is to occur at $T_{\mathrm{v}} \approx 0.7\,J$.

A domain wall in the AFXY(t) model is a line drawn along the bonds of the triangular lattice such that it separates cells with the same chiralities (Fig. 7b). The wall carries no fractional vortices if the neighboring segments of this line form the angle $2\pi/3$ with each other [28]. The structure of such domain walls in terms of the original phase variables is shown in Fig. 8. It is interesting that in contrast to the case of the FFXY model on a square lattice, the states to the left and

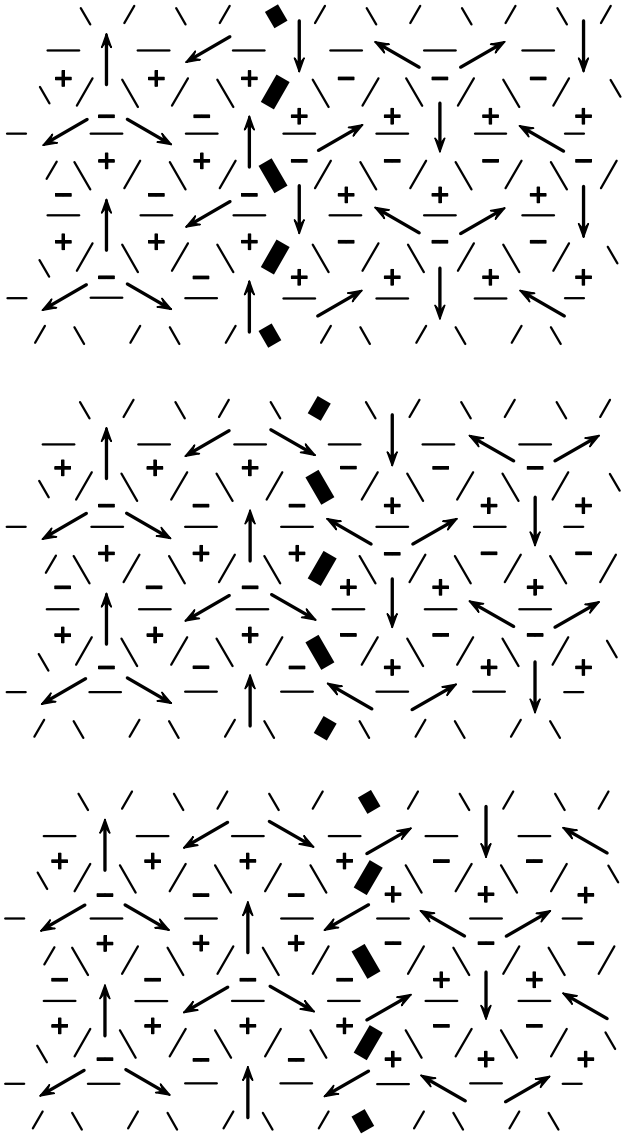

**Figure 8.** Structure of domain walls in terms of $\varphi_{\mathbf{j}}$.

to the right of the wall in the examples shown in Fig. 8 coincide with the respective ground state not only far from the wall but also very close to it. The energy (per segment) of the domain walls depicted in Fig. 8 is $E_{\mathrm{dw}} = J/2$. Substituting this value in the expression for the transition temperature in the Ising model on a honeycomb lattice (dual to the triangular lattice) [177 – 179],

$$T_{\mathrm{dw}} = \frac{E_{\mathrm{dw}}}{\ln\left(2+\sqrt{3}\right)}\,,$$

we obtain $T_{\mathrm{dw}} \approx 0.4\,J < T_{\mathrm{v}}$.

However, neither estimate (for $T_{\mathrm{dw}}$ or for $T_{\mathrm{v}}$) allows for the mutual effect of the formation of vortices and domain walls, where the dominant role is played by the fact that fractional vortices with topological charge $\pm 1/3$ are formed whenever the angle between the neighboring segments of a domain wall differs from $2\pi/3$ [28]. Figure 7b shows that in the absence of a wall or in the case where the angle between neighboring segments of the wall is $2\pi/3$, a site of the triangular lattice is surrounded by three cells with positive chiralities and three cells with negative chiralities, which is an

indication of the absence of uncompensated vorticity. At the same time, if the angle between the neighboring segments of a wall is $\pi/6$ or $\pi$, the number of cells with positive chiralities is not equal to the number of cells with negative chiralities, which indicates the presence of a fractional vortex with a nonzero topological charge. As in the case of a square lattice, the appearance of fractional vortices on domain walls leads to a situation where the scenario with $T_v > T_{dw}$ cannot be realized.

We consider a domain wall that crosses the entire system. Its energy is minimal if (1) the wall carries no fractional vortices, and (2) it is of a minimum length. If we fix the state on one side of such a wall, the equilibrium state on the other side can be obtained through permutation of the values of $\varphi$ in two of the three sublattices, followed by the rotation of all phases by $\pi$ [28]. The three different versions of the permutation correspond to the different positions of the wall and differ from each other by a global rotation of the state behind the wall by $\pm 2\pi/3$. This is illustrated by Fig. 8, where the state to the left of the wall is the same, while the states to the right can be transformed into each other via rotation by $\pm 2\pi/3$.

The defects — kinks — whose topological charges depend on their height may form on a domain wall that crosses the entire system. Triple-height kinks have a zero topological charge and, hence, a finite energy. At the same time, Fig. 8 shows that the presence of a minimum-height kink on the domain wall leads to a mismatch in the phase values by $\pm 2\pi/3$, with the result that such a kink is a fractional vortex with the topological charge equal (in absolute value) to 1/3.

The logarithmic interaction of such defects is nine times weaker than the interaction of ordinary vortices. Accordingly, the phase transition amounting to dissociation of coupled pairs of simple kinks that leads to the loss of coherence between states on both sides of the wall must occur at the temperature $T_k$ satisfying the relation [24]

$$T_k = \frac{\pi}{9}\, \Gamma(T_k)\,.$$

In the case of a triangular lattice, $T_k$ proves to be even lower (compared with $T_v$) than for a square lattice. Hence, all conclusions in the previous section concerning the properties of domain walls near $T_v$ are also valid in the AFXY(t) model. Following the argument in Section 4.4, we can conclude that a phase transition related to the vortex-pair dissociation in the AFXY(t) model must also occur at a temperature that is lower than that of the second phase transition, which is related to the destruction of the long-range order in the antiferromagnetic ordering of the chiralities $\sigma_{\mathbf{R}}$ of triangular cells [24]. In the intermediate phase, despite the presence of the long-range order in $\sigma_{\mathbf{R}}$, the correlations of $\mathbf{S_j}$ must decay (at large distances) exponentially.

Although the earlier numerical simulation results do not always allow detecting the difference between $T_v$ and $T_{dw}$ [29, 180], the results of more precise studies [175, 181, 182] confirm the conclusion that $T_v < T_{dw}$. Unfortunately, as in the case of a square lattice, experimental investigation of triangular Josephson junction arrays placed in a magnetic field with a half-integer number of flux quanta per lattice cell [162] used methods that did not allow identifying the temperature at which ordering of chiralities occurs.

### 5.2 Structure of the phase diagram in an external magnetic field

When an external magnetic field is applied, the Hamiltonian acquires an additional term that violates the symmetry under transformation (45):

$$H_{af} = J \sum_{(\mathbf{ij})} \cos(\varphi_{\mathbf{i}} - \varphi_{\mathbf{j}}) - h \sum_{\mathbf{j}} \sin \varphi_{\mathbf{j}}\,. \tag{46}$$

Here, $h$ is the field magnitude expressed in energy units, with the field assumed to be directed along the $y$ axis (i.e., vertically upward). However, such a field does not lift the continuous degeneracy of the ground state, which retains its three-sublattice structure even in the presence of the field [29].

In terms of planar unit spins $\mathbf{S}_A$, $\mathbf{S}_B$, and $\mathbf{S}_C$ belonging to the three different sublattices, the energy of an arbitrary three-sublattice state $E_3$, which we assume normalized by the number of lattice sites, depends solely on the sum of these spins,

$$E_3 = \frac{J}{2}\left[(\mathbf{S}_A + \mathbf{S}_B + \mathbf{S}_C)^2 - 3\right] - \frac{\mathbf{h}}{3}(\mathbf{S}_A + \mathbf{S}_B + \mathbf{S}_C)\,,$$

and is at its minimum at $\mathbf{S}_A + \mathbf{S}_B + \mathbf{S}_C = \mathbf{h}/3J$. This means that the minimization of $E_3$ imposes only two restrictions on $\varphi_A$, $\varphi_B$, and $\varphi_C$:

$$\sin\varphi_A + \sin\varphi_B + \sin\varphi_C = \frac{h}{3J}\,, \tag{47a}$$

$$\cos\varphi_A + \cos\varphi_B + \cos\varphi_C = 0\,, \tag{47b}$$

which leads to the preservation of the continuous degeneracy of the ground state [29]. Up to $h = 3J$, the degeneracy space is a pair of circles $Z_2 \times S^1$, which at $h = 3J$ are glued at three points. As $h$ increases further, the degeneracy space is reconnected such that it becomes isomorphic to a single circle, which at $h = 9J$ shrinks to a point [29]. At $h \geqslant 9J$, the ground state becomes trivial, $\varphi_{\mathbf{j}} = \pi/2$, and is not degenerate.

For $0 < h < 9J$, the continuous degeneracy is accidental, i.e., is not related to the symmetry of the Hamiltonian, and therefore it is lifted if we take the free energy of small fluctuations (spin waves) near the ground state into account [30–32, 183]. Computation of the free energy of spin waves in the harmonic approximation shows [32] that it is a monotonically decreasing function of

$$U(\varphi_A, \varphi_B, \varphi_C) = \cos^2(\varphi_A - \varphi_B) + \cos^2(\varphi_B - \varphi_C) + \cos^2(\varphi_C - \varphi_A)\,.$$

Therefore, taking the harmonic fluctuations into account is equivalent to adding the ferromagnetic biquadratic interaction of neighboring spins to (46).

For $0 < h < 3J$, the function $U(\varphi_A, \varphi_B, \varphi_C)$ attains its minimum in those ground states in which the spins in one of the three sublattices are antiparallel to the direction of the field [30, 31], e.g.,

$$\varphi_A = -\frac{\pi}{2}\,, \qquad \varphi_B = \Phi\left(\frac{h}{3J}\right), \qquad \varphi_C = \pi - \Phi\left(\frac{h}{3J}\right), \tag{48}$$

where

$$\Phi(\gamma) = \arcsin\frac{1+\gamma}{2}\,.$$

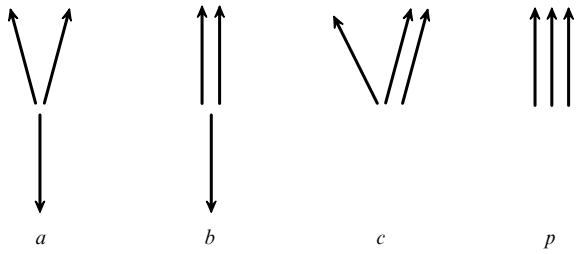


**Figure 9.** Directions of the spins in three sublattices that minimize the free energy of harmonic fluctuations: *a*, at $h < 3J$; *b*, at $h = 3J$; *c*, at $3J < h < 9J$; and *p*, at $h \geqslant 9J$.

In stronger fields ($3J < h < 9J$), the minimum is attained in the states in which two of the three sublattices are equivalent [30, 31], e.g.,

$$\varphi_A = -\pi + \Phi_1\left(\frac{h}{3J}\right), \qquad \varphi_B = \varphi_C = \Phi_2\left(\frac{h}{3J}\right), \tag{49}$$

where

$$\Phi_1(\gamma) = \arcsin\frac{3-\gamma^2}{2\gamma}, \qquad \Phi_2(\gamma) = \arcsin\frac{3+\gamma^2}{4\gamma}.$$

In both cases, the continuous degeneracy is lifted such that the total degeneracy is reduced to a sixfold one. As $h \to 3J$, both equations (48) and (49) reproduce the solution

$$\varphi_A = -\frac{\pi}{2}, \qquad \varphi_B = \varphi_C = \frac{\pi}{2}, \tag{50}$$

characterized by threefold degeneracy. The structure of the three-sublattice ground states that minimize $U(\varphi_A, \varphi_B, \varphi_C)$ at different values of $h$ is schematically shown in Fig. 9, where the magnetic field is assumed to be directed vertically upward.

Instead of seeking the structure of the ground state that minimizes $U(\varphi_1, \varphi_2, \varphi_3)$, we can minimize the free energy of the three-sublattice state that includes a fluctuation contribution in addition to $E_3$,

$$F_3 = E_3 - gJU(\varphi_A, \varphi_B, \varphi_C),$$

where $g \propto T/J$ is a small dimensionless parameter describing the relative strength of the fluctuation effects. The range of fields in which solution (50) is a minimum of the Hamiltonian then becomes finite. The width of this range proves to be proportional to $g$.

All this implies that the phase diagram of a planar antiferromagnet with a triangular lattice must have the structure [31, 32] shown schematically in Fig. 10. All three ordered phases (*a*, *b*, and *c*) that are present in the phase diagram exhibit a long-range order in spin orientation in each of the three sublattices, and the phases are denoted such that the directions of $\langle \mathbf{S} \rangle$ for the three sublattices correspond to those depicted in Fig. 9. Phases *a* and *c* are sixfold degenerate, phase *b* is threefold degenerate, and phase *p* is a disordered (paramagnetic) phase. Such a phase diagram with three ordered phases was first constructed in Ref. [29] using numerical simulations, but the mean-field analysis leads to a different, much simpler, structure of the phase diagram [176].

The phase transitions from phase *a* or phase *c* to phase *b* must be of the Ising type, because they are related to the formation of infinite domain walls, which mixes two of the six

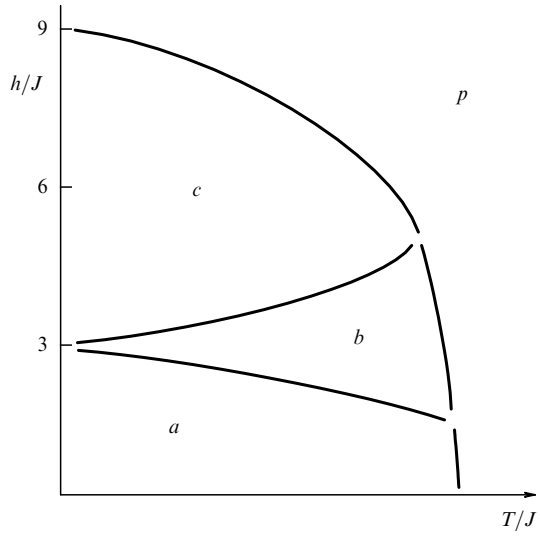


**Figure 10.** Structure of the phase diagram of a planar antiferromagnet with a triangular lattice. The figure does not show the weak splitting of the phase transition at $h = 0$ or the weak splitting of the transition from *c* to *p*, which is present at sufficiently low temperatures at least.

degenerate states [32]. Phase *b* is a $\sqrt{3} \times \sqrt{3}$ commensurate crystal of spins antiparallel to the field in the background of those parallel to the field. The results of an exact solution of the model of rigid hexagons in Ref. [184] imply that the phase transition related to the melting of such a structure as the temperature increases belongs to the universality class of the three-state Potts model.

In fields whose magnitude approaches $9J$ from below, the values of $\varphi_A$, $\varphi_B$, and $\varphi_C$ satisfying Eqn (47) can be written as [135]

$$\varphi_A \approx \frac{\pi}{2} + \Phi_0 \sin\chi,$$

$$\varphi_B \approx \frac{\pi}{2} + \Phi_0 \sin\left(\chi + \frac{2\pi}{3}\right),$$

$$\varphi_C \approx \frac{\pi}{2} + \Phi_0 \sin\left(\chi - \frac{2\pi}{3}\right),$$

where

$$\Phi_0 = 2\left(1 - \frac{h}{9J}\right)^{1/2},$$

and hence the system can be approximated by the conventional (nonfrustrated) XY model with the six-order anisotropy, related to the free energy of fluctuations [32]. The results of a renormalization-group analysis for such an XY model [76, 185] show that at least a part of the transition line from phase *c* to the disordered phase *p* must split, with both transitions then belonging to the BKT universality class. In the intermediate phase, anisotropy is irrelevant, which leads to an algebraic decay of correlations instead of the true long-range order, but the vortices of the auxiliary variable $\chi$ form bound pairs. Comparison with the structure of the phase diagram [186, 187] of a six-state cubic model [188, 189] suggest that the nonsplit part of the line of transitions from *c* to *p*, as well as the nonsplit part of the line of transitions from *a* to *p*, correspond to first-order

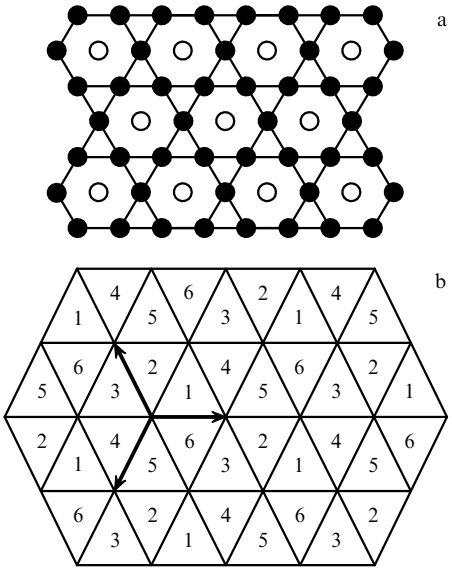


**Figure 11.** (a) The kagome lattice; (b) the triangular lattice $\mathcal{T}_a$ and the three basis vectors $\mathbf{a}_\alpha$. The sites of the dual lattice $\mathcal{H}_a$ are labeled by numbers from 1 to 6. Identical numbers correspond to physically equivalent states.

transitions similar to the phase transition in the six-state Potts model [190].

Chubukov and Golosov [191] showed that taking quantum fluctuations into account (in the approximation of large, compared to unity, spin) does not result in any unexpected changes. Quantum fluctuations play the same role as thermodynamic fluctuations, i.e., lead to stabilization of the same states. Therefore, the range of field magnitudes within which phase $b$ exists proves to be finite even at zero temperature. These conclusions are confirmed by numerical simulation of the quantum AFXY model with spin 1/2 [192].

Interestingly, in the case of a *Heisenberg* antiferromagnet with a triangular lattice placed in an external magnetic field, taking thermodynamic [193] or quantum [191, 194] fluctuations into account leads to stabilization of the ordered phases with exactly the same structure as in the case of a planar antiferromagnet. In other words, in the presence of fluctuations, the most energy-advantageous state is the one in which the spins in the three sublattices lie in the same plane (parallel to the direction of the magnetic field), with the orientations of the spins in different sublattices being as in Fig. 9. Three-sublattice phases with a similar structure are stabilized by thermodynamic fluctuations [195] and by quantum fluctuations [196] in an antiferromagnet with a kagome lattice (Fig. 11a), which has been confirmed by numerical simulation results [196, 197].

A characteristic feature of the intermediate phase $b$ is a much weaker dependence of magnetization on the magnitude of the applied magnetic field than in phases $a$ and $c$ surrounding it [191]. Such behavior of the magnetization with field variation was observed in antiferromagnets consisting of weakly coupled triangular layers, such as $EuC_6$ [198], and also in $RbFe(MoO_4)_2$ [199, 200] and $Cs_2CuBr_4$ [201], in which the anisotropy is of the easy-plane type. The phase diagram of $RbFe(MoO_4)_2$ constructed in Refs [199, 200] has the structure that is almost identical to the structure of the phase diagram in Fig. 10. The triangular lattice is typical for the adsorbed monolayer that forms a two-dimensional crystal.

## 6. Planar antiferromagnet with a kagome lattice

A kagome lattice is a triangular lattice a quarter of whose sites are removed in a regular manner (Fig. 11a). It incorporates two types of cells, triangular and hexagonal.

There is a number of layered antiferromagnets in which the magnetic ions form weakly coupled layers with the kagome lattice structure. The first to be mentioned here are jarosites [202–206], which are described by the formula $MFe_3(OH)_6(SO_4)_2$ (where $M = H_3O$, Na, K, Rb, Ag, $NH_4$, Tl, Pb, and Hg), their chromic analogs $KFe_3(OH)_6(CrO_4)_2$, and also $SrCr_{8-x}Ga_{4+x}O_{19}$ (SCGO) [207–211] and $Ba_2Sn_2ZnGa_3Cr_7O_{22}$ (QS-ferrite) [212]. Some of these substances exhibit easy-plane anisotropy. In particular, this is confirmed by data on the susceptibility of $H_3OFe_3(OH)_6(SO_4)_2$ [206].

Another object of experimental studies are networks of superconducting wires with the kagome lattice geometry [111, 213]. When the magnitude of an external magnetic field corresponds to a half-integer number of flux quanta per triangular unit cell (and hence, to an integer number of flux quanta per hexagonal cell), the phase fluctuations in such a system can also be described by an AFXY model.

### 6.1 Ground states

As in the case of a triangular lattice, the ground states of a planar antiferromagnet with a kagome lattice and with the interaction involving only the nearest neighbors can be constructed on the grounds that the minimum energy of any triangular cell is attained when the spins belonging to this cell are at the angle $2\pi/3$ to each other. Therefore, all the variables $\varphi_\mathbf{j}$ take only three different values in each of the ground states,

$$\varphi_A = \Phi\,, \qquad \varphi_B = \Phi + \frac{2\pi}{3}\,, \qquad \varphi_C = \Phi - \frac{2\pi}{3}\,,$$

and any of the triangular cells must contain a permutation of the three values, which makes it possible to put these states [35, 214] in correspondence with the ground states of a three-state antiferromagnetic Potts model on the same lattice.

The exact solution found by Baxter [215] shows that the ground state of the three-state antiferromagnetic Potts model on the kagome lattice exhibits well-developed degeneracy in which the number of ground states exponentially grows with the number of sites in the system, which corresponds to a finite value of the residual entropy per site. As in the case of the Potts model, a similar degeneracy of the ground states of the AFXY model on the kagome lattice is not related to a symmetry of the Hamiltonian. Degeneracy is retained even when the form of the nearest-neighbor interaction changes.

Discrete degeneracy of the set of ground states of the AFXY model on the kagome lattice can be described in terms of formation of zero-energy domain walls [34]. We examine the so-called $\sqrt{3} \times \sqrt{3}$ state [216] (Fig. 12a), whose structure corresponds to that of the ground state on a triangular lattice. Another state with the same energy can be formed by a permutation, e.g., of the form $\varphi_B \leftrightarrow \varphi_C$ inside any closed loop formed by sites with $\varphi_\mathbf{j} = \varphi_A$, etc. A closed loop (the simplest example of which is shown in Fig. 12c) can be considered a zero-energy domain wall separating two different $\sqrt{3} \times \sqrt{3}$ states. All such domain walls are polygonal lines in which the

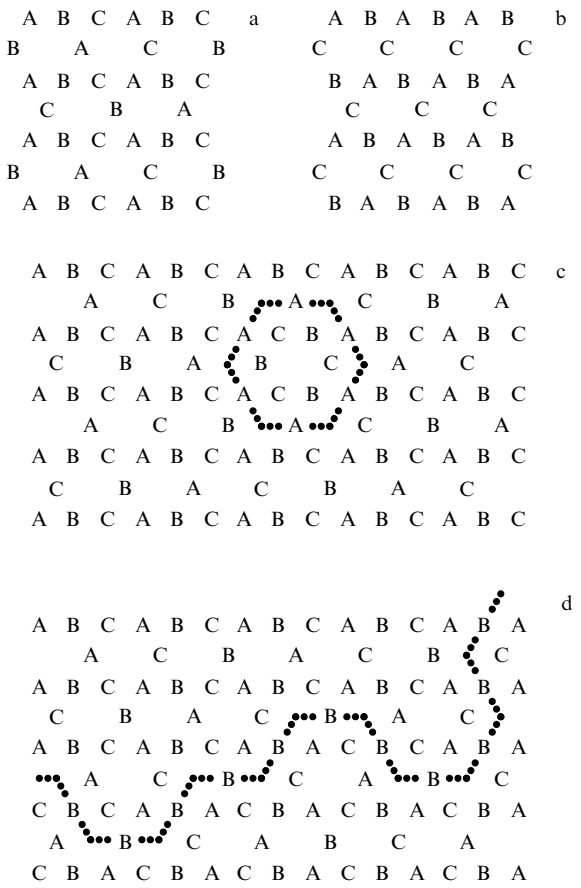


**Figure 12.** (a) The $\sqrt{3}\times\sqrt{3}$ state; (b) the $\mathbf{q}=0$ state; and (c, d) domain walls separating two different $\sqrt{3}\times\sqrt{3}$ states.

neighboring segments are at the angle $\pm 2\pi/3$ to each other (Fig. 12d). Naturally, they may be open, i.e., infinite.

Degeneracy reflecting the possibility of constructing a domain wall with zero energy is not related to a symmetry of the Hamiltonian and is lifted when the interaction of more distant neighbors is considered. To lift this accidental degeneracy, it suffices to include the interaction of the next-to-nearest neighbors, which we characterize by the coupling constant $J_2$. When the interaction involving the next-to-nearest neighbors is ferromagnetic ($J_2<0$), the ground state is a $\sqrt{3}\times\sqrt{3}$ state [216], whose structure is shown in Fig. 12a. It is characterized by the 'antiferromagnetic' ordering of the chiralities of triangular cells, with the domain-wall energy $E_{\rm dw}$ becoming positive.

In our further analysis, we restrict ourself to the limit $|J_2|\ll J_1$ (where $J_1>0$ is the coupling constant describing the interaction of neighboring spins), where $E_{\rm dw}\approx 3|J_2|$ per wall segment. Because each segment of the domain wall separates two triangular cells with the same chiralities, we can say that the interaction of next-to-nearest neighbors on the kagome lattice induces a proportional interaction of the chiralities of the neighboring triangular cells, which is of the opposite sign.

When the next-to-nearest-neighbor interaction is antiferromagnetic ($J_2>0$), the so-called $\mathbf{q}=0$ state, schematically shown in Fig. 12b, has the lowest energy [126]. This state is characterized by the 'ferromagnetic' ordering of the chiralities of triangular cells. For both signs of $J_2$, the degeneracy of the ground state is reduced to $\mathrm{U}(1)\times\mathrm{Z}_2$ [33].

### 6.2 Zero-temperature fluctuations

As noted earlier, if we take only the nearest-neighbor interaction into account, the set of ground states of the AFXY model on a kagome lattice is the same as in the three-state antiferromagnetic Potts model on the same lattice. As is known, it is possible to map this set of ground states onto the set of states of the SOS model in which the variables $\mathbf{n}_\mathbf{R}$ defined at the centers of the hexagonal cells have the meaning of 'heights' of the surface and are vectors [35]. In Fig. 11a, the sites $\mathbf{R}$ at which the variables $\mathbf{n}_\mathbf{R}$ are defined are marked by white circles. They form a triangular lattice, denoted by $\mathcal{T}$ in what follows. Each site $\mathbf{j}$ of the kagome lattice can be associated with the bond $(\mathbf{R}\mathbf{R}')$ of the lattice $\mathcal{T}$, and each variable $\varphi_\mathbf{j}=\varphi_\mathrm{A},\varphi_\mathrm{B},\varphi_\mathrm{C}$ can be associated with the Potts variable $\alpha_{\mathbf{R}\mathbf{R}'}\equiv\alpha_{\mathbf{R}'\mathbf{R}}$, which takes three values and is defined on this bond.

Because each triangular cell of the kagome lattice must contain three different variables $\varphi_\mathrm{A}$, $\varphi_\mathrm{B}$, and $\varphi_\mathrm{C}$, these variables can be associated with three basis vectors $\mathbf{a}_\alpha$ ($\mathbf{a}_1+\mathbf{a}_2+\mathbf{a}_3=0$) of a certain auxiliary lattice (Fig. 11b), to be denoted by $\mathcal{T}_a$ in what follows. The variables $\mathbf{n}_\mathbf{R}$, taking the values defined on $\mathcal{T}_a$, can be introduced by the rule

$$\mathbf{n}_{\mathbf{R}'}=\begin{cases}\mathbf{n}_\mathbf{R}+\mathbf{a}_{\alpha_{\mathbf{R}\mathbf{R}'}}\,, & \mathbf{R}'=\mathbf{R}+\mathbf{e}_\alpha\,,\\ \mathbf{n}_\mathbf{R}-\mathbf{a}_{\alpha_{\mathbf{R}\mathbf{R}'}}\,, & \mathbf{R}'=\mathbf{R}-\mathbf{e}_\alpha\,,\end{cases}\tag{51}$$

where $\mathbf{e}_\alpha$ are the three basis vectors of $\mathcal{T}$ (with $\mathbf{e}_1+\mathbf{e}_2+\mathbf{e}_3=0$). This determines the correspondence between the states of the antiferromagnetic Potts model and those of the vector SOS model in which the variables $\mathbf{n}_\mathbf{R}\in\mathcal{T}_a$, having the meaning of heights, must satisfy the condition

$$|\mathbf{n}_\mathbf{R}-\mathbf{n}_{\mathbf{R}'}|=a\tag{52}$$

on all bonds of the lattice $\mathcal{T}$. Here, $a\equiv|\mathbf{a}_\alpha|$ is the lattice constant for $\mathcal{T}_a$.

Using the known properties of the exact solution [215] of the three-state antiferromagnetic Potts model in the external field stabilizing antiferromagnetic ordering of chiralities, Huse and Rutenberg [35] demonstrated that in the vector SOS model described above (whose partition function involves all the allowed configurations with the same weight), the correlation function $\langle(\mathbf{n}_\mathbf{R}-\mathbf{n}_{\mathbf{R}'})^2\rangle$ behaves as

$$\langle(\mathbf{n}_\mathbf{R}-\mathbf{n}_{\mathbf{R}'})^2\rangle\approx\frac{3a^2}{\pi^2}\ln|\mathbf{R}-\mathbf{R}'|$$

as $|\mathbf{R}-\mathbf{R}'|\to\infty$. This means that this model is exactly at the point of a phase transition from the rough phase to the smooth phase. Hence, any additional perturbation that leads to a reduction in fluctuations can be expected to shift the system from the transition point to a smooth state where the fluctuations of $n_\mathbf{R}$ are not divergent.

According to condition (52), the values of the variables $\mathbf{n}_\mathbf{R}$ in the neighboring sites must always differ from each other, and therefore even the maximally smooth state of the 'surface' is a regular alternation of the three different values of $\mathbf{n}_\mathbf{R}$. In such a situation, the phase transition to the smooth phase is described more naturally in terms of the variables

$$\mathbf{u}_\mathbf{r}\equiv\frac{1}{3}\,(\mathbf{n}_\mathbf{R}+\mathbf{n}_{\mathbf{R}'}+\mathbf{n}_{\mathbf{R}''})\,,$$

which are the arithmetic mean of the $\mathbf{n}_\mathbf{R}$ at the three sites of $\mathcal{T}$ that belong to the same triangular cell. The variables $\mathbf{u}_\mathbf{r}$ can be

assumed to be defined at the sites $\mathbf{r}$ of the honeycomb lattice $\mathcal{H}$ dual to $\mathcal{T}$; they take values $\mathbf{u}_\mathbf{r} \in \mathcal{H}_a$, where $\mathcal{H}_a$ is the honeycomb lattice dual to $\mathcal{T}_a$ (Fig. 11b).

In terms of the original spin variables $\mathbf{S}_\mathbf{j} \equiv (\cos\varphi_\mathbf{j}, \sin\varphi_\mathbf{j})$, the smooth states of the vector SOS model (in which all the variables $\mathbf{u}_\mathbf{r}$ are equal) correspond to $\sqrt{3}\times\sqrt{3}$ states, and the zero-energy steps, whose occurrence from fluctuations leads to surface roughening, correspond to zero-energy domain walls (of the type shown in Figs 12c and d) that separate different $\sqrt{3}\times\sqrt{3}$ states. The logarithmic divergence of the correlations of $\mathbf{n}_\mathbf{R}$ (or $\mathbf{u}_\mathbf{r}$) then corresponds to a power-law decay of correlations of $\mathbf{S}_\mathbf{j}$.

It is convenient to analyze the large-scale properties of the vector SOS model (and its further generalizations) by using the multicomponent version of the sine-Gorgon model with the same symmetry [34]. The dimensionless Hamiltonian of this model can be chosen as

$$H_{\mathrm{sG}} = \int \mathrm{d}^2\mathbf{r}\left\{\frac{KQ^2}{2}\left[\nabla\mathbf{u}(\mathbf{r})\right]^2 + y\sum_{\alpha=1}^{3}\cos\left[\mathbf{Q}_\alpha\mathbf{u}(\mathbf{r})\right]\right\}. \quad (53)$$

The first term on the right-hand side of (53) describes the effective rigidity (of entropic origin) related to fluctuations of $\mathbf{u}(\mathbf{r})$, and the second term makes the values of $\mathbf{u}(\mathbf{r})$ belonging to $\mathcal{H}_a$ preferable. Here, $\mathbf{Q}_\alpha$ are the three basis vectors of the triangular lattice reciprocal to $T_a$, and therefore

$$\mathbf{Q}_\alpha^2 = \frac{16\pi^2}{3a^2}, \qquad \mathbf{Q}_1 + \mathbf{Q}_2 + \mathbf{Q}_3 = 0.$$

A similar Hamiltonian [with the opposite sign in front of the second term on the right-hand side of (53)] and the equivalent vector Coulomb gas were studied by Nelson [217] in connection with the problem of melting of a two-dimensional crystal with a triangular lattice. Although it was found later (see Refs [9–11]) that the melting problem is described by a somewhat more complicated Hamiltonian in which the contributions related to compression and shear enter separately (rather than in an invariant combination), in the present problem, the displacement occurs in an abstract space that is in no way related to real space, which actually allows introducing a single elasticity modulus, as was assumed in Eqn (53).

In our notation, the renormalization-group equations describing the evolution of $K$ and $y$ under rescaling [217] can be written as

$$\frac{\mathrm{d}K}{\mathrm{d}l} = \frac{3\pi}{8}\,y^2, \quad (54a)$$

$$\frac{\mathrm{d}y}{\mathrm{d}l} = \left(2 - \frac{1}{4\pi K}\right)y - \pi y^2, \quad (54b)$$

where $l$ is the logarithm of the scale. The corresponding renormalization-group diagram is schematically shown in Fig. 13, where $K_\mathrm{c} \equiv 1/8\pi$. The form of Eqns (54) implies that the phase transition from the smooth phase to the rough phase occurs when the renormalized value of $K$ becomes equal to $K_\mathrm{c}$. This means that the vector SOS model introduced above (which, as Huse and Rutenberg [35] found, is at a phase transition point) can be associated [34] with one of the points on the left separatrix.

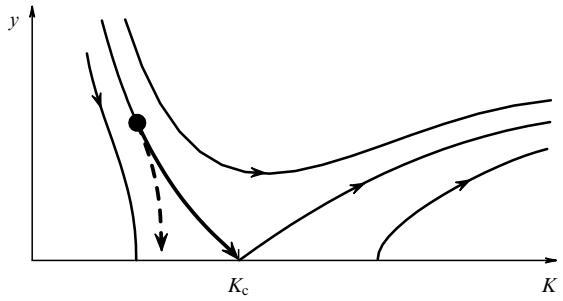


**Figure 13.** The renormalization-group diagram for Eqns (54). A system with only the nearest-neighbor interaction and zero temperature can be associated with a certain point on the left separatrix. The dashed arrow indicates the direction of flow at $T > 0$, when the negative contribution proportional to $z^2$ to the left-hand side of Eqn (54a) must be taken into account.

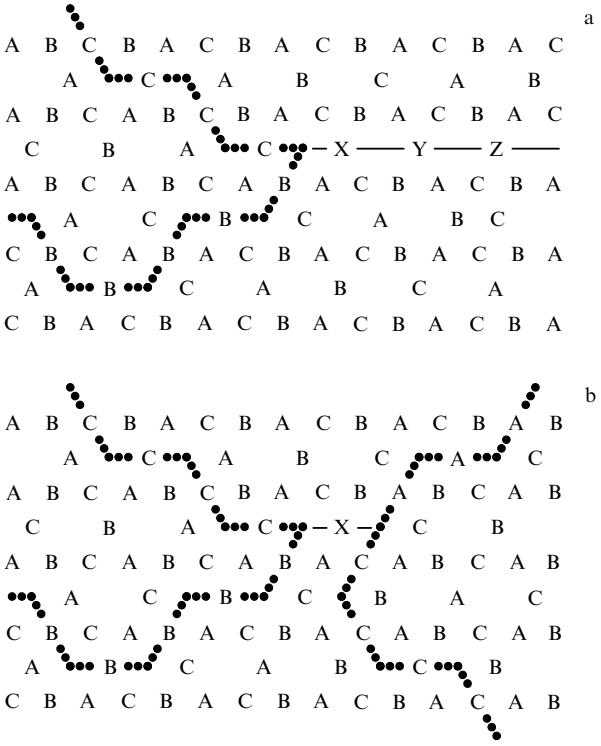


**Figure 14.** Examples of topological defects in the background of $\sqrt{3}\times\sqrt{3}$ states: (a) a fractional vortex, and (b) a dislocation that is a neutral pair of fractional vortices.

### 6.3 Fluctuations at a finite temperature

At a finite temperature, other types of fluctuations come into play. These, in contrast to the zero-temperature fluctuations discussed in the previous subsection, require an expenditure of energy. In particular, vortex formation becomes possible, with the vortices bound into small pairs at low temperatures. In addition to ordinary vortices (with integer topological charge), fractional vortices with the topological charge $\pm 1/3$ [35] may also appear, localized on domain walls at the points where the neighboring segments of the wall form an angle different from $2\pi/3$ [34] (similarly to the way this occurs for a triangular lattice; see Section 5.1).

Figure 14a shows a domain wall containing one such point. The point divides the wall into two parts: the upper part formed by sites C and the lower part formed by sites B. Clearly, as we cross the upper part of the domain wall, the state to the right of the wall must differ from the state to the left by a permutation of $\varphi_\mathrm{A}$ and $\varphi_\mathrm{B}$, while as we cross the

lower part, the state to the right of the wall differs from the state to the left by a permutation of $\varphi_A$ and $\varphi_C$. This leads to a mismatch in the values of the phase amounting to $2\pi/3$, which, for instance, may be localized along the line X–Y–Z. Naturally, the minimum energy is attained when instead of jumping by $2\pi/3$ on this line, the phase gradually changes by $2\pi/3$ as we go around the singular point, which signifies the creation of a fractional vortex with the topological charge whose absolute value is 1/3.

All fractional vortices at low temperatures are bound into neutral pairs. An example of such a pair is shown in Fig. 14b. As the temperature increases, dissociation of fractional vortex pairs must occur [35, 218, 219].

If fractional vortices were to exist independently of domain walls, the dissociation would occur at a temperature $T_{fv}$ satisfying the relation

$$T_{fv} = \frac{\pi}{18}\, \Gamma(T_{fv})\,, \tag{55}$$

similar to (37). Because $\Gamma = (\sqrt{3}/4)J_1$ in any of the degenerate states, this yields the estimate [34]

$$T_{fv} \leqslant \frac{\pi\sqrt{3}}{72}\, J_1 \approx 0.0756\, J_1\,, \tag{56}$$

which is in good agreement with the values of the phase transition temperature $T_{fv} \approx (0.070-0.076)\, J_1$ that follow from the results of numerical simulations in [220]. In Ref. [222], the same estimate for $T_{fv}$ was obtained in a much more complicated way, based on the use of the dual transformation.

Comparison of rule (51) with Fig. 14a shows that in terms of the vector SOS model introduced in the previous section, each fractional vortex corresponds to a point going around which changes the variable $\mathbf{u}$ by $\Delta\mathbf{u}$, where $|\Delta\mathbf{u}| = a$. This means that each fractional vortex is a point where a step of height $\Delta\mathbf{u}$ (or, more generally, a set of steps with the total height $\Delta\mathbf{u}$) begins or ends. Accordingly, fluctuations in the SOS model lead to an additional contribution to the interaction of fractional vortices, a contribution that stems from the difference in the entropies of states with different points at which the steps end [34]. In the entire rough phase (including the point of transition to the smooth phase), this additional interaction, which can be expressed in terms of the correlation function of some new XY model that is dual to the SOS model [90, 91], is also logarithmic. Its presence leads to a slight increase in $T_{fv}$ and a relative weakening of the mutual effect of fractional and ordinary vortices. Comparison with the results in Ref. [222] shows that such an interaction could, at least theoretically, lead to an additional phase transition related to the dissociation of pairs of ordinary vortices and occurring at $T_v > T_{fv}$. But this does not happen because the magnitude of the entropic interaction of fractional vortices is low [34].

On the other hand, for $T > 0$, the rigorous equivalence with the SOS model is lost [34]. We recall that in terms of spin variables, the infinite number of various 'smooth' states of the SOS model corresponds (for a given $\varphi_A$) to only six different $\sqrt{3} \times \sqrt{3}$ states, which can be obtained from the state shown in Fig. 12a by various permutations of A, B, and C. In Fig. 11b, the sites of the lattice $\mathcal{H}_a$ that in terms of the original phase variables $\varphi_{\mathbf{j}}$ correspond to the same states are labeled by identical numbers.

At zero temperature, the specific properties of zero-energy domain walls separating such states (in particular, two closed domain walls cannot cross) allow interpreting these states as nonequivalent states of the SOS model. A similar situation occurs when the six-vertex model of a ferroelectric (the ice model [93]) is used to construct the SOS model of the (001) face of a crystal with a bcc lattice [92].

When the temperature is finite, the set of domain walls separating two physically equivalent states acquires the capacity to merge and disappear. Such point defects are well known in the theory of transitions from a commensurate state to an incommensurate state [223]. The self-energy $E_d$ of such a defect is finite and proportional to $J_1$:

$$E_d = c_d\, J_1\,,$$

where $c_d$ is of the order of unity.

In terms of the multicomponent sine-Gordon model in (53), such defects correspond to dislocations of the field $\mathbf{u}$ whose Burgers vectors $\mathbf{b}_\alpha$ $(\alpha = 1, 2, 3)$, as follows from Fig. 11b, are given by

$$\mathbf{b}_1 = \mathbf{a}_3 - \mathbf{a}_2\,, \qquad \mathbf{b}_2 = \mathbf{a}_1 - \mathbf{a}_3\,, \qquad \mathbf{b}_3 = \mathbf{a}_2 - \mathbf{a}_1\,.$$

An example of such a dislocation is shown in Fig. 14b. It is formed by a neutral pair of fractional vortices localized at two different domain walls that are not continuations of each other. The symbol X denotes the site at which $\varphi_{\mathbf{j}} \approx (\varphi_A + \varphi_B)/2$. Near this site, the values of $\varphi_{\mathbf{j}}$ differ slightly from those at sites A, B, and C. If we consistently apply rule (51) along the perimeter of any closed contour surrounding point X, we obtain $\Delta\mathbf{n} = \mathbf{a}_2 - \mathbf{a}_1$.

Renormalization of the fugacity $z = \exp(-c_d J_1/T)$ of the dislocation under rescaling is described by the equation [9, 10]

$$\frac{dz}{dl} = \lambda_z z + 2\pi z^2\,,$$

where

$$\lambda_z = 2 - \frac{KQ^2b^2}{4\pi} \equiv 2 - 4\pi K\,.$$

In the vicinity of the roughening transition ($K \approx K_c = 1/8\pi$), the exponent $\lambda_z$ describing the renormalization of $z$ is close to $\lambda_z^0 = 3/2$, which corresponds to a rapid increase in $z$. Comparison of $\lambda_z$ with $\lambda_y = 2 - 1/(4\pi K)$ shows that $y$ and $z$ cannot be simultaneously renormalized to zero. In this respect, the situation is similar to the one that emerges in the analysis of the conventional (ferromagnetic) XY model with weak anisotropy of not too high an order [76, 185].

The presence of dislocations (or, more exactly, dislocation pairs) leads to the additional negative term proportional to $z^2$ in the right-hand side of (54a). The presence of such a term shifts the flow from the separatrix to the region corresponding to the rough phase of the SOS model [34].

On the other hand, an unlimited increase in $z$ under renormalization means that a finite concentration of free dislocations appears in the system, which transform the rough phase of the SOS model into the disordered phase of the six-state model. In this phase, the decay of correlations is characterized by a finite correlation radius $\xi_z$, which can be found as the scale on which the renormalized value of $z$ becomes of the order of unity.

The correlation radius $\xi_z$ determines the scale on which the additional (entropic) interaction of fractional vortices associated with domain-wall fluctuations is screened. The fact that $\xi_z$ is finite eliminates even the hypothetical possibility of dissociation of pairs of ordinary vortices occurring as an independent phase transition at $T_v > T_{fv}$.

### 6.4 Phase transition related to chirality ordering

As noted earlier, **the ferromagnetic interaction of next-to-nearest neighbors** leads to a situation where the energy of domain walls similar to those shown in Figs 12c and d becomes finite: $E_{dw} \approx 3|J_2|$. Usually, $T_{dw}$, the temperature of the phase transition related to the formation of infinite domain walls, can be estimated by comparing the energy and entropy contributions to the free energy of the wall [224, 225], which in the present situation would lead to $T_{dw} \propto |J_2|$. But this approach does not account for the fact that the emergence of an infinite wall leads to an additional decrease in entropy because it creates obstructions to the emergence of fluctuation-generated closed domain walls, with the result that the outcome is often incorrect.

In terms of the vector SOS model, the finite value of $E_{dw}$ (i.e., the step energy) shifts the system from the roughening transition point to the smooth phase. On the other hand, the appearance of free dislocations at a finite temperature encourages a shift in the opposite direction, i.e., into the disordered phase. The renormalization-group analysis in Ref. [34], with the competition between these two effects taken into account, allows concluding that in the limit as $|J_2|/J_1 \to 0$,

$$T_{dw} \sim J_1 \left(\frac{E_{dw}}{J_1}\right)^{3/8} \propto J_1^{5/8} |J_2|^{3/8}, \tag{57}$$

while as the ratio $|J_2|/J_1$ increases, the system goes into the regime where the value of the exponent in (57) changes from 3/8 to 1/2, which can be shown using a self-consistent approximation similar to the one introduced in Ref. [226].

The low-temperature phase existing at $T < T_{dw}$ is characterized by the presence of a true long-range order in the antiferromagnetic ordering of the chiralities of triangular cells and a power-law decay of spin correlations, i.e., of the correlation function $\langle \exp[i(\varphi_{\mathbf{j}+\mathbf{r}} - \varphi_{\mathbf{j}})] \rangle$, the decay caused primarily by the existence of spin waves.

We emphasize that Eqn (57) was derived on the assumption that all fractional vortices are bound into pairs, and therefore this equation is valid only for $T_{dw} < T_{fv}$. On the other hand, fractional-vortex pair dissociation is possible only at $T > T_{dw}$, because at $T < T_{dw}$, fractional vortices are bound, in addition to the logarithmic interaction, by the domain walls, which have a finite free energy per unit length. Hence, the scenario with $T_{dw} > T_{fv}$ does not work, and dissociation of fractional-vortex pairs occurs either at a temperature higher than that needed for the emergence of infinite domain walls or simultaneously with such emergence.

The appearance of a network of domain walls leads to a mixing of the six ground states that can be obtained from the state shown in Fig. 12a via all possible permutations of A, B, and C, and therefore the related phase transition must not belong to the Ising universality class. Construction of a six-state model with the same domain-wall statistics [28, 34] results in a model related by the duality transformation [227–229] to the six-state cubic model in which, as is known, the phase transition (provided there is a single transition) is a first-order one [186, 187]. Consequently, in the problem considered here, the phase transition at $T = T_{dw}$ must be a first-order one at $T_{dw} < T_{fv}$ at least, but probably also at larger values of $E_{dw}$, where the continuous and discrete degrees of freedom become disordered simultaneously.

Comparison of (55) with (57) shows that $T_{dw} < T_{fv}$ is possible only if $-J_{max} < J_2 < 0$, where $J_{max}$ is of the order of $10^{-3} J_1$ [34]. When $J_2 < -J_{max}$, only one phase transition can occur in the system, and the emergence of infinite domain walls in this phase transition leads to the appearance of free vortices of all possible types. In this case, dissociation of fractional-vortex pairs occurs because the linear contribution to their interaction (related to the free energy of the domain walls connecting the pairs) vanishes, while the logarithmic contribution to the interaction is too weak to hold these pairs in a bound state. Hence, we can expect that the value of the helicity modulus at the transition point is nonuniversal:

$$\frac{2}{\pi} < \frac{\Gamma(T_c)}{T_c} < \frac{18}{\pi}.$$

We emphasize that the above estimate of $J_{max}$ was made with the numerical factors that may be involved in Eqn (57) neglected, and must therefore be taken with caution.

In the intermediate phase, i.e., at $T_{dw} < T < T_{fv}$, both the correlation of spins $\mathbf{S_j}$ and the correlation of the chiralities of triangular cells decay exponentially, but the correlation function $\langle \exp[3i(\varphi_{\mathbf{j}+\mathbf{r}} - \varphi_{\mathbf{j}})] \rangle$ decays in accordance with a power law [35]. With the fractional-vortex pair dissociation, the decay of $\langle \exp[3i(\varphi_{\mathbf{j}+\mathbf{r}} - \varphi_{\mathbf{j}})] \rangle$ changes to exponential.

**When the next-to-nearest-neighbor interaction is antiferromagnetic** ($J_2 > 0$), the energy minimum is attained in one of the $\mathbf{q} = 0$ states with the ferromagnetic ordering of the chiralities of triangular cells [216] (Fig. 12b). Clearly, the discrete degeneracy of such a state is also twofold.

As in the previous case, this state allows the formation of a domain wall whose energy $E_{dw}$ (per unit segment) is proportional to the coupling constant for the next-to-nearest neighbors:

$$E_{dw} \approx 3|J_2| = 3J_2$$

(Fig. 15a). However, comparison of Fig. 15a with Fig. 15b shows that in this case, the state on the other side of the wall is uniquely determined by the orientation of the wall and is different for different orientations. The emerging mismatch of the values of $\varphi_{\mathbf{j}}$ must be balanced by the presence of fractional vortices at all corners of the domain walls, similarly to the case of the FFXY model on a square lattice (see Section 4.2).

When $J_2 \ll J_1$, the ground-state defects emerging as a result of thermal fluctuations and related to the change in the sign of chiralities have the shape of narrow stripes limited by two low-energy domain walls (Fig. 15c). As in Fig. 14, we let X denote the sites at which

$$\varphi_{\mathbf{j}} \approx \frac{\varphi_A + \varphi_B}{2}.$$

Similar in shape are structural defects that appear as the temperature increases in a uniformly frustrated XY model with $f = 1/4$ or $f = 1/3$ and a triangular lattice [230].

The energy of such a defect is close to $2E_0 + 2E_{dw}L$, where $E_0 = c_0 J_1$ ($c_0 \approx 0.55$) is the energy of each of its ends and $L$ is the length of the defect. This allows estimating the fraction $\rho$ of the area of the system occupied by such defects. When

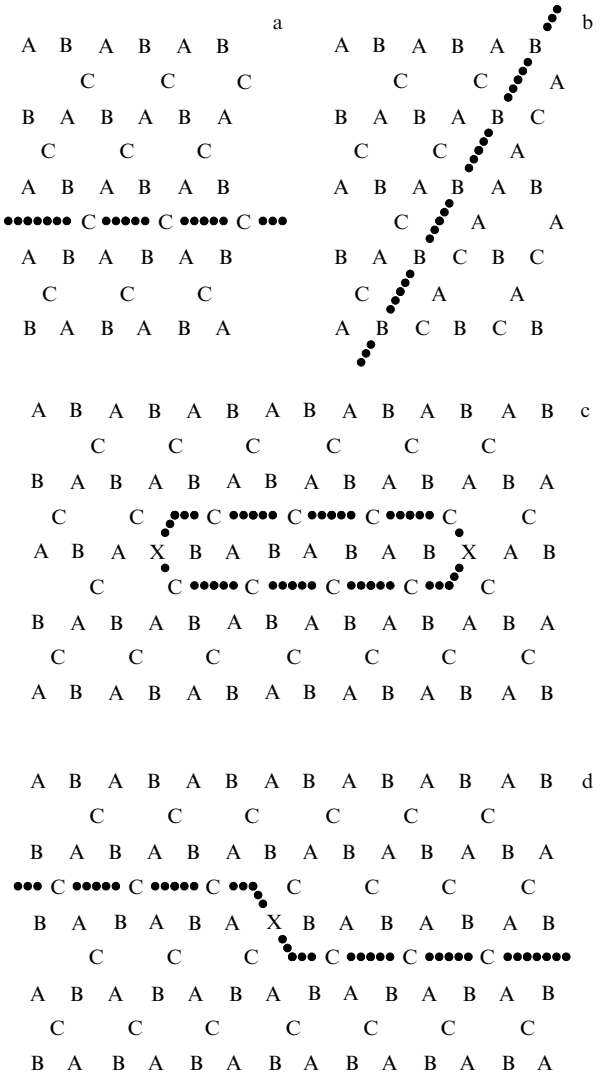


**Figure 15.** Examples of topological defects in the background of the $\mathbf{q} = 0$ state: (a, b) straight domain walls of different orientations, (c) typical finite-size defect, and (d) kink on a wall.

$E_{\rm dw} \ll T \ll J_1$, we have

$$\rho \sim \left(\frac{T}{2E_{\rm dw}}\right)^2 \exp\left(-\frac{2E_0}{T}\right).$$

The assumption that the phase transition occurs when $\rho$ becomes of the order of 1 [113] yields an equation for the transition temperature,

$$T_{\rm dw} \approx \frac{E_0}{\ln\left(T_{\rm dw}/E_{\rm dw}\right)},$$

whence [34]

$$T_{\rm dw} \sim \frac{J_1}{\ln\left(J_1/J_2\right)}.$$

A similar estimate follows from comparing the domain-wall energy $E_{\rm dw}$ with the wall entropy $S_{\rm dw} \approx 2\exp\left(-E_{\rm k}/T\right)$ related to the possibility of kinks forming on the wall. An example of such a kink is shown in Fig. 15d. Its structure is very similar to that of the endpoint of the linear defect shown in Fig. 15c, and hence $E_{\rm k} \approx E_0$.

Actually, when $J_2 \ll J_1$, the phase transition is driven by the entropy of formation of a *network* of domain walls similarly to the situation with the Ising model on a triangular lattice with the antiferromagnetic interaction between both the nearest and more distant neighbors [231]. The transition temperature then proves to be finite even at $J_1 = \infty$, when the existence of finite-size fluctuations on the background of the $\mathbf{q} = 0$ state is impossible. In this limit, the ordered phase at low temperatures is completely frozen, while its energy (per site) coincides with the energy of the $\mathbf{q} = 0$ state:

$$E_{\mathbf{q}=0} = -J_1 - J_2.$$

On the other hand, for $J_2 > 0$, the energy of the $\sqrt{3} \times \sqrt{3}$ state

$$E_{\sqrt{3}\times\sqrt{3}} = -J_1 + 2J_2$$

is the highest among the energies of all states allowed at $J_1 = \infty$, and therefore the free energy $F_{\rm d}$ of the disordered phase must satisfy the inequality

$$F_{\rm d} < F_{\rm d}^{+} = E_{\sqrt{3}\times\sqrt{3}} - TS_0,$$

where $S_0 \approx 0.1264$ [215] is the residual entropy per site (at $J_2 = 0$ and $T = 0$).

Comparison of $E_{\mathbf{q}=0}$ with $F_{\rm d}^{+}$ allows concluding that at $J_1 = \infty$, the temperature $T_{\rm dw}$ of the phase transition to the disordered phase must not exceed

$$T_{\rm dw}^{+} = \frac{E_{\sqrt{3}\times\sqrt{3}} - E_{\mathbf{q}=0}}{S_0} \approx 23.7\,J_2. \qquad (58)$$

A similar estimate was suggested in Ref. [37] based on a more general argument; in reality, the inequality $T_{\rm dw} < T_{\rm dw}^{+}$ is rigorous. Clearly, the same estimate is true for sufficiently large values of $J_1$.

As in the case of the antiferromagnetic ordering of chiralities, infinite domain walls may appear as a result of a separate phase transition (which does not cause the fractional-vortex pair dissociation) only at $T < T_{\rm fv}$. Comparison of (56) with (58) shows that the inequality $T_{\rm dw}^{+} < T_{\rm fv}$ requires that $J_2 < J_{\rm max}^{+}$, where $J_{\rm max}^{+}$ is of the order of $3 \times 10^{-3} J_1$. Because the appearance of domain walls in this case is also related to the mixing of the six (rather than two) different states, the phase transition at $T = T_{\rm dw}$ cannot be of the Ising type. The phase transition at $T = T_{\rm dw}^{+} < T_{\rm fv}$ transforms the system into the same phase with a power-law decay of the correlation function $\left\langle \exp\left[3i(\varphi_{\mathbf{j}+\mathbf{r}} - \varphi_{\mathbf{j}})\right]\right\rangle$ as the phase transition at $T = T_{\rm dw} < T_{\rm fv}$ does in the case of the opposite sign of $J_2$.

**When only the nearest-neighbor spins are involved in the interaction,** accidental degeneracy is lifted only at a finite temperature due to the difference in the free energies of small fluctuations (spin waves). A similar mechanism of accidental degeneracy lifting was examined in Sections 4.5 and 5.2. But in contrast to those two examples, the Hamiltonian describing harmonic fluctuations in the case of a planar antiferromagnet with a kagome lattice proves to be the same for all ground states. Therefore, the difference between the free energies of the fluctuations near different ground states emerges only if the anharmonicity is taken into account and must then be a quantity of the second order (at least!) in the temperature [35].

The results of calculations in Ref. [34] show that it suffices to limit oneself to anharmonic corrections of the

lowest order. The free energy of anharmonic fluctuations attains its minimum if the chiralities of neighboring triangular cells have opposite signs (i.e., in the $\sqrt{3}\times\sqrt{3}$ state), and its value is

$$E_{\rm dw}^{\rm eff} = \gamma\,\frac{T^2}{J_1}\,, \tag{59}$$

where $\gamma \approx 2\times 10^{-3} > 0$. The tendency toward ordering into the $\sqrt{3}\times\sqrt{3}$ state also manifests itself in constructing the high-temperature expansion [216], which, however, does not allow drawing any conclusions about the behavior of the system in the low-temperature limit.

As is known, both thermodynamic [232, 233] and quantum [234–236] anharmonic fluctuations in a *Heisenberg* antiferromagnet with a kagome lattice also lead to stabilization (at least local) of the planar state with the $\sqrt{3}\times\sqrt{3}$ structure. The same effect results from *harmonic* fluctuations of the magnitude of the order parameter in a kagome-geometry network of superconducting wires placed in an external magnetic field whose magnitude corresponds to a half-integer number of flux quanta per triangular cell [37].

We note that the effective domain-wall energy given by Eqn (59) is always small compared to the temperature, which, for instance, in the case of the Ising model would mean that it is not sufficiently high to stabilize the ordering of chiralities. But in the system under consideration, the situation is quite different.

Substituting (59) in (57), we see that at $J_2 = 0$, the temperature of the phase transition related to the antiferromagnetic ordering of chiralities at $J_2 = 0$ can be estimated as

$$T_{\rm dw}(J_2 = 0) \sim \gamma^{3/2} J_1\,. \tag{60}$$

With the numerically calculated value of $\gamma$ mentioned earlier substituted in (60), we have

$$T_{\rm dw}(J_2 = 0) \sim 10^{-4} J_1\,.$$

It is worth noting that in a finite system, the ordering of chiralities survives only if the free energy of a domain wall crossing the entire system is high compared to the temperature. This imposes a restriction on the system size $L$, namely, $L \gg L_{\rm c}$, where $L_{\rm c}$ is larger than or of the order of $L_{\rm c}^{\rm min} = T/E_{\rm dw}^{\rm eff} = J_1/(\gamma T)$. From Eqns (59) and (60), it follows that in the low-temperature phase with a long-range order of chiralities, $L_{\rm c}^{\rm min}$ is larger than or of the order of $10^7$ [36], which makes observation of the chirality ordering induced by anharmonic fluctuations very questionable. This agrees with the results of numerical simulations in Ref. [220], which showed that there is no ordering of chiralities at $T \geqslant 10^{-3} J_1$ and $L \leqslant 300$. The above estimates imply that the observation of such ordering requires not only much lower temperatures but also much larger systems.

Interestingly, anharmonic fluctuations must also be taken into account in analyzing FFXY models on the honeycomb [36] and dice [113] lattices. In both these models (in contrast to the antiferromagnetic model on the kagome lattice), the Hamiltonian describing harmonic fluctuations has different forms in different ground states, but the free energy of such fluctuations (as well as the energy of their zero-point oscillations) is the same for all the ground states because of a hidden gauge symmetry of such Hamiltonians [36, 113].

In both cases, the effective domain-wall energy related to anharmonic fluctuations is then also described by Eqn (59) and is extremely low because $\gamma$ is numerically small ($\gamma \sim 10^{-3}-10^{-4}$). As a result, it turns out that in both systems, the ordering of chiralities even at the optimum temperature is characterized by a correlation radius so large that its observation in numerical simulations becomes impossible [36, 113]

### 6.5 Structure of the phase diagram

The structure of the phase diagram of a planar antiferromagnet with a kagome lattice [34] is schematically shown (off scale) in Fig. 16. Phases with the ferromagnetic and antiferromagnetic ordering of chiralities are denoted by F and AF, respectively. The phase in which the ordering of chiralities is destroyed but the correlation function $\langle \exp\left[3{\rm i}(\varphi_{\mathbf{j}+\mathbf{r}} - \varphi_{\mathbf{j}})\right]\rangle$ decays in accordance with a power law (and, hence, the effective helicity is finite) is denoted by S and the completely disordered phase is denoted by D.

The phase transition from S to D is related to the dissociation of pairs of fractional vortices with topological charges $\pm 1/3$ [35, 218, 219]. In Section 6.3, it was shown that the additional interaction of fractional vortices induced by fluctuations of domain walls connecting them is short-range and, hence, unessential. The corresponding phase transition belongs to the BKT universality class, and the value of the helicity modulus at the transition point must satisfy relation (55).

However, the range of parameters where the scenario with $T_{\rm dw} < T_{\rm fv}$ develops and the fractional-vortex pair dissociation occurs as an independent phase transition turns out to be very narrow: $-J_{\rm max} < J_2 < J_{\rm max}^{+}$, where $J_{\rm max}, J_{\rm max}^{+} \sim (10^{-2}-10^{-3})J_1$. For larger values of $|J_2|$, the

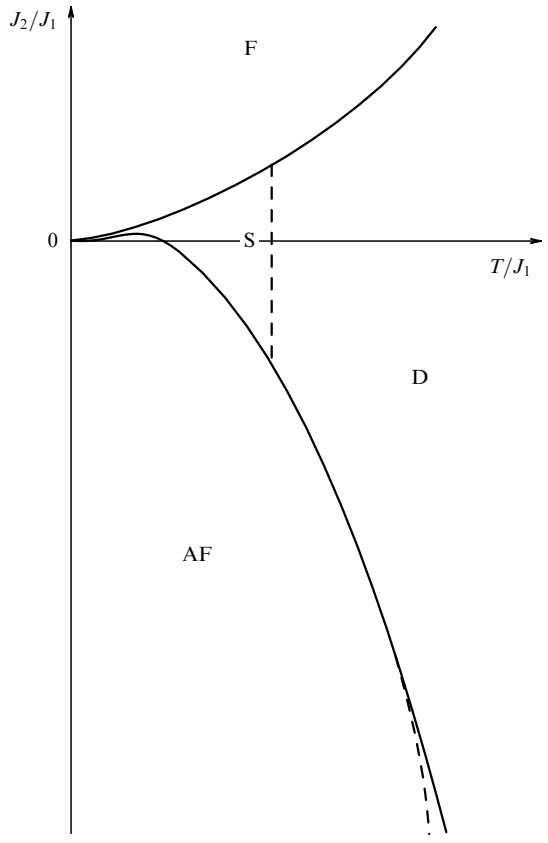


**Figure 16.** Schematic of the structure of the phase diagram of the AFXY model on a kagome lattice.

two phase transitions must merge. This is confirmed by the results of the numerical simulations done by Gekht and Bondarenko [33], who found that at $|J_2| \geqslant 0.1J_1$, the disordering in the continuous and discrete degrees of freedom occur at the same temperature and that the thermodynamic singularity is close to the Ising one.

At $J_2 < 0$ and $|J_2| \sim J_1$, a new splitting of the phase transitions into two must occur, related to the development of the scenario with $T_v < T_{dw}$ in accordance with the mechanism discussed in Section 5. This splitting is shown in the lower part of Fig. 16.

Taking anharmonic fluctuations into account leads to a slight increase in the effective magnitude of the coupling constant $J_2$, which causes the range of the existence of phase S to be bent upward, resembling a beak. As a result, for very small but positive values of $J_2$, the four phase transitions must occur in the sequence $F \to S \to AF \to S \to D$ as the temperature increases.

As in the case of a triangular lattice, the above results can be used to describe not only planar antiferromagnets but also Josephson junction arrays and networks of superconducting wires in a magnetic field with a half-integer number of flux quanta per triangular cell, and lattices of π-junctions in the absence of a field. The interaction leading to lifting the accidental degeneracy in such systems is the magnetic interaction of currents [37].

Park and Huse [37] showed that the magnetic energy of currents is at its minimum in the $\mathbf{q} = 0$ state. This implies that taking this energy into account within the scope of the analysis in this section should correspond to $J_2 > 0$. But a more systematic approach in Refs [112, 113], which accounts not only for the self-energy of the magnetic fields generated by currents but also for the effect of these fields on the change in the free energy of Josephson junctions (or superconducting wires), shows that the total variation of the free energy has the opposite sign. Therefore, taking the magnetic effects into account in frustrated superconducting systems with the kagome lattice geometry corresponds to $J_2 < 0$.

## 7. Solitons and phase-transition splitting

### 7.1 The XY model with modified interaction

We now examine a modification of the XY model described by the Hamiltonian

$$H = \sum_{(\mathbf{ij})} V(\varphi_\mathbf{i} - \varphi_\mathbf{j}) \,, \tag{61}$$

where, in contrast to the standard XY model with $V(\theta) = -J\cos\theta$ used to describe planar ferromagnets and arrays of ordinary Josephson junctions, we assume that the even periodic function $V(\theta)$ has, in addition to the main minimum at $\theta = 0$, an additional minimum at $\theta = \pi$ of an almost equal depth (Fig. 17a). The phase variables $\varphi_\mathbf{j}$, defined up to a shift by $2\pi$, are assumed to be defined at the sites of a square lattice.

As shown in Refs [38 – 40], such a dependence of the Josephson energy on the phase difference is characteristic of SFS junctions whose parameters are close to the point of transition of the junction to the so-called π-state [41 – 43], and hence the model under consideration can be used to describe a regular array fabricated from such junctions. The transition of SFS junctions into the π-state caused by temperature changes has been demonstrated experimentally in Refs [237 – 239], and by variation of the junction parameters in [240]. The first experiment that involved an SFS-junction array (albeit containing only two cells) was carried out in Ref. [241].

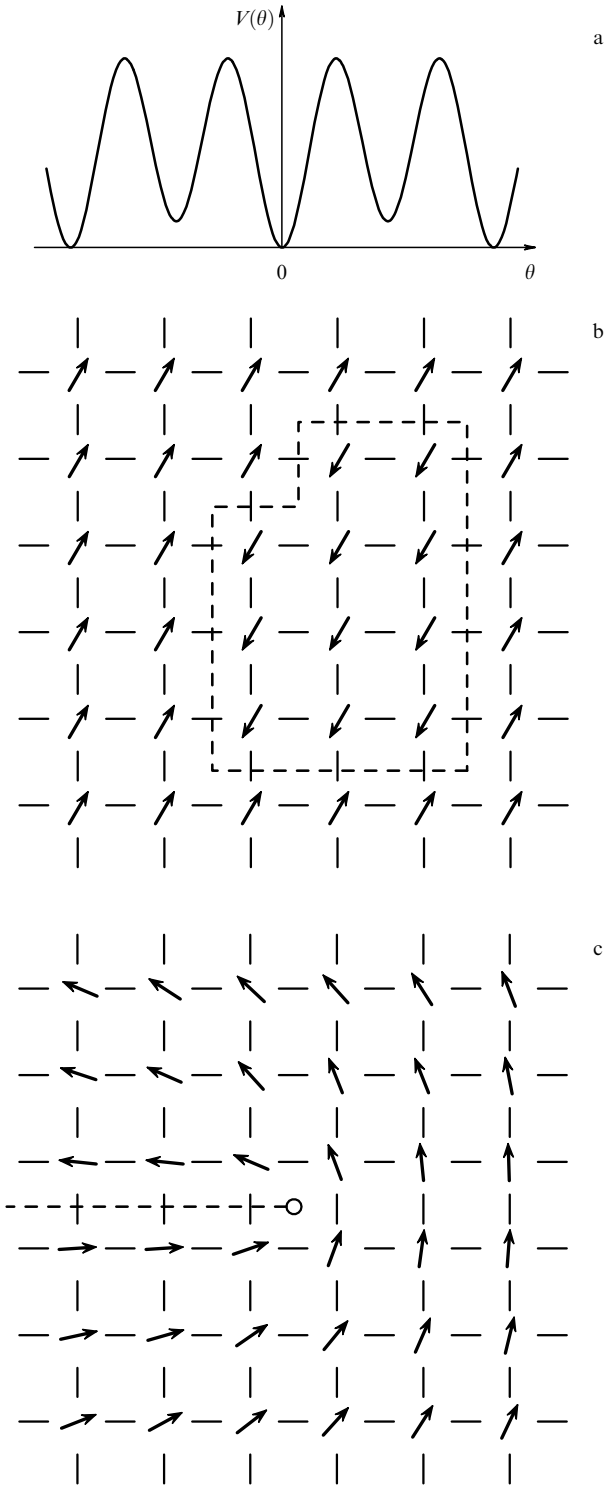


**Figure 17.** (a) The coupling $V(\theta)$ leading to the possibility of soliton formation; (b) a closed soliton; and (c) a soliton ending on a half-vortex with $m = +1/2$.

### 7.2 Classification of defects and possible phase transitions

We let $V_1 \equiv V(\pi) - V(0)$ denote the difference in energy for the nonequivalent minima of $V(\theta)$ and $V_2$ denote the curvature of this function near the minima. We assume the

curvature to be the same for both minima and to satisfy the condition $V_2 \gg V_1$. At low temperatures, the main contribution to the partition function of a system with continuous degeneracy is provided by the ground states (corresponding to the absolute minimum of the Hamiltonian), the low-lying local minima of the Hamiltonian, and small fluctuations near these minima (spin waves), which are responsible for the power-law decay of the correlation function $\langle \exp[\mathrm{i}(\varphi_{\mathbf{j}+\mathbf{r}} - \varphi_{\mathbf{j}})] \rangle$ with increasing $|\mathbf{r}|$ [1, 66].

The XY model with the modified interaction introduced above is characterized by two basic types of minima of the Hamiltonian: vortices and solitons. Vortices are point-like topological excitations with the same structure as in the conventional XY model (see Fig. 1). Because the bare value of the helicity modulus is equal to $V_2$ in this system, we can expect vortex-pair dissociation to occur at $T = T_\mathrm{v} \sim V_2$. The second type of local minima of the Hamiltonian is given by solitons, the lines on the dual lattice crossing which changes the phase by $\pi$ [44–46] (Fig. 17b). The soliton energy per unit length is $V_1$, with the result that at $T \ll V_1$, all solitons generated as thermal fluctuations must be closed and have a small length.

We emphasize that a soliton is not an unremovable topological excitation, because states on both sides of it can be transformed into each other continuously, without leaving the degeneracy space. This means that in contrast to domain walls in the Ising model, solitons may have endpoints. To balance the phase jump on a soliton, the phase must gradually change by $\pm\pi$ in going around the soliton endpoint. This means that soliton endpoints are vortices with a half-integer topological charge [44–46]. Naturally, the minimum energy corresponds to $m = \pm 1/2$. For brevity, we call such objects (Fig. 17c) half-vortices.

As in the case of integer vortices with $m = \pm 1$, the interaction of half-vortices with $m = \pm 1/2$ is logarithmic, with the coupling constant (in front of the logarithm) being four times smaller. If half-vortices were to exist independently of solitons, the dissociation of neutral pairs formed by them would occur at the temperature $T = T_\mathrm{hv}$, where $T_\mathrm{hv} \ll T_\mathrm{v}$ is the solution of the equation

$$T_\mathrm{hv} = \frac{\pi}{8} \Gamma(T_\mathrm{hv}) , \tag{62}$$

which is similar to Eqn (18). But because each half-vortex is also the endpoint of a soliton, an attempt to move two half-vortices apart to an arbitrary distance reveals the presence of a contribution to their interaction that is linear in the distance and is related to the energy of the soliton connecting the half-vortices. When $V_1$ is of the same order as $V_2$, the presence of such an interaction is an obstruction to the dissociation of pairs of half-vortices at $T = T_\mathrm{hv}$.

If $T \ll V_2/4$ and the relation between $T$ and $V_1$ is arbitrary, the logarithmic interaction of soliton endpoints leads to a situation in which they are all coupled into neutral (in the topological charge) pairs of small size. Hence, near any soliton endpoint, there is always an endpoint of another soliton, which can be considered a continuation of the first one. Thanks to this, when $T \ll V_2/4$, solitons behave as topological excitations in the Ising model (domain walls), even though they are not such excitations in essence [44, 45].

This means that at $T = T_\mathrm{S} \sim V_1$, the system undergoes a phase transition from the low-temperature phase, in which all solitons form closed loops (even if they have small openings), to a phase that contains infinite-length solitons. The behavior of the system at $T > T_\mathrm{S}$ is characterized by an exponential decay of the correlation function $\langle \exp[\mathrm{i}(\varphi_{\mathbf{j}+\mathbf{r}} - \varphi_{\mathbf{j}})] \rangle$ because as the distance between two points increases, the number of uncorrelated solitons separating these points increases also increases unlimitedly and $\varphi$ jumps by $\pi$ on each of these solitons.

At the same time, the presence of solitons has no marked effect on the behavior of the correlation function $\langle \exp[2\mathrm{i}(\varphi_{\mathbf{j}+\mathbf{r}} - \varphi_{\mathbf{j}})] \rangle$, which shows a power-law behavior at both $T > T_\mathrm{S}$ and $T < T_\mathrm{S}$ because the phase transition at $T = T_\mathrm{S}$ does not result in the vanishing of the helicity modulus. Thus, the phase transition at $T = T_\mathrm{S}$ can be interpreted as a transition to a nematic phase in which the symmetry with respect to the rotation by $\pi$ is not broken. It is interesting that although the phase transition is related to the symmetry group $Z_2$, the absence of a long-range order in $\exp(\mathrm{i}\varphi_{\mathbf{j}})$ does not allow introducing an explicit expression (in terms of $\varphi_{\mathbf{j}}$) for the order parameter related to this transition.

The vanishing of the free energy per soliton unit length at $T > T_\mathrm{S}$ means that the linear contribution to the interaction of half-vortices is screened and that the dissociation of pairs of half-vortices becomes possible. If we assume that the presence of solitons does not lead to a renormalization of the bare logarithmic coupling of half-vortices, their decoupling and the phase transition to a disordered phase, in which not only the correlation function $\langle \exp[\mathrm{i}(\varphi_{\mathbf{j}+\mathbf{r}} - \varphi_{\mathbf{j}})] \rangle$ but also the correlation function $\langle \exp[2\mathrm{i}(\varphi_{\mathbf{j}+\mathbf{r}} - \varphi_{\mathbf{j}})] \rangle$ decays exponentially, must occur at $T = T_\mathrm{hv} \sim V_2/4$. Comparison with the estimate $T_\mathrm{S} \sim V_1$ shows that as the ratio $V_1/V_2$ decreases, the phase transition must necessarily split into two [44–46].

### 7.3 Dual and Coulomb representations

To prove the possibility of the existence of an intermediate phase of a nematic nature separated from the high-temperature disordered phase by a phase transition of the BKT universality class more rigorously, we consider the interaction $V(\theta)$ such that the weight factor

$$w(\theta) = \exp\left[-\frac{V(\theta)}{T}\right]$$

has the form [45, 46]

$$w(\theta) = w_\mathrm{BV}(\theta) + \exp\left(-\frac{K}{T}\right) w_\mathrm{BV}(\theta - \pi) , \tag{63}$$

where $w_\mathrm{BV}(\theta)$ is the weight factor (4) corresponding to the Berezinskii–Villain interaction. When $K \ll T \ll J$, the parameters $V_1$ and $V_2$ defined above are close to $K$ and $J$ ($V_1 \approx K$ and $V_2 \approx J$).

Applying the duality transformation (see Section 2.6) allows transforming the partition function of the XY model defined in this way into the partition function of the SOS model defined by the Hamiltonian [44]

$$H_\mathrm{SOS} = \sum_{(\mathbf{R}\mathbf{R}')} \left[\frac{J_*}{2}(n_\mathbf{R} - n_{\mathbf{R}'})^2 - \frac{K_*}{2} s_\mathbf{R} s_{\mathbf{R}'}\right] , \tag{64}$$

where $J_* = T^2/J$, the integer variables $n_\mathbf{R}$ are defined at the sites $\mathbf{R}$ of the dual lattice,

$$s_\mathbf{R} \equiv \exp(\mathrm{i}\pi n_\mathbf{R}) = \pm 1 ,$$

and $K$ and $K_*$ are linked by the Kramers – Wannier duality relation [120]

$$\sinh\frac{K}{T}\sinh\frac{K_*}{T}=1\,,$$

and hence the condition $K\ll T\ll J$ corresponds to $K_*\gg T\gg J_*$.

It is easy to see from Hamiltonian (64) that the energy of unit-height steps $E^{(1)}_{\rm step}$ is $K_*+J_*/2$, while the energy of double-height steps $E^{(2)}_{\rm step}=2J_*$ may be lower than $E^{(1)}_{\rm step}$. As $K_*\to\infty$, the value of $E^{(1)}_{\rm step}$ tends to infinity, and therefore all the variables $n_{\mathbf{R}}$ must be either even or odd. If in addition $J_*\ll T$, the system is nevertheless in the rough state, in which the square of the surface width diverges and the double-step free energy (per unit length) is zero.

When $K_*<\infty$, formation of domain walls separating two rough 'vacua' becomes possible. Such domain walls (they are unit-height steps as well) have a high energy per unit length and, consequently, their free energy at $K_*\ll T$ must be finite (the upper bound on the entropy estimate is a value of the order of unity). This means that there are only small inclusions of one of the two vacua into the other vacuum and that the asymmetry between even and odd values of $n$, i.e., the long-range order in the variables $s$, is preserved [44].

The results in Refs [90, 91] imply that in terms of the original XY model, the finiteness of the free energy of a simple step means that the correlation function $\langle\exp\left[\mathrm{i}(\varphi_{\mathbf{j}+\mathbf{r}}-\varphi_{\mathbf{j}})\right]\rangle$ decays exponentially, while the vanishing of the free energy of a double step means that the correlation function $\langle\exp\left[2\mathrm{i}(\varphi_{\mathbf{j}+\mathbf{r}}-\varphi_{\mathbf{j}})\right]\rangle$ decays as a power-law function. Thus, we have obtained another confirmation of the fact that for $K\ll T\ll J$, the XY model with interaction (63) is in the nematic phase described above.

However, in both the original representation in terms of $\varphi_{\mathbf{j}}$ and the dual representation, the nematic phase is a phase in which fluctuations are weak only for one of the two possible types of fluctuation, while the most convincing proof of the existence of this phase would be the construction of a representation in which all fluctuations are weak when $K\ll T\ll J$.

To achieve this goal, it is convenient to pass from summation over the variables $n_{\mathbf{R}}$ in the partition function of the SOS model to integration, keeping the $s_{\mathbf{R}}$ independent variables. For this, we write $n_{\mathbf{R}}$ in the form

$$n_{\mathbf{R}}=2\tilde{n}_{\mathbf{R}}+\frac{1-s_{\mathbf{R}}}{2}\,,$$

where $\tilde{n}_{\mathbf{R}}$ is also an integer, and replace summation over $\tilde{n}_{\mathbf{R}}$ with integration via Poisson resummation formula (22). This leads to the partition function [44]

$$\begin{aligned}Z_{\rm Cg}=\prod_{\mathbf{R}}\Biggl(\sum_{m_{\mathbf{R}}=-\infty}^{\infty}\sum_{s_{\mathbf{R}}=\pm1}\Biggr)\\ \times\exp\left[-\frac{1}{2T}\sum_{\mathbf{R}_1,\mathbf{R}_2}\frac{m_{\mathbf{R}_1}}{2}\,G_0(\mathbf{R}_1-\mathbf{R}_2)\,\frac{m_{\mathbf{R}_2}}{2}\right.\\ \left.+\mathrm{i}\pi\sum_{\mathbf{R}}\frac{m_{\mathbf{R}}}{2}\,s_{\mathbf{R}}-\frac{K_*}{2T}\sum_{(\mathbf{R}\mathbf{R}')}s_{\mathbf{R}}s_{\mathbf{R}'}\right],\end{aligned}\tag{65}$$

which, together with summation over $s_{\mathbf{R}}=\pm1$, incorporates summation over the integer-valued variables $m_{\mathbf{R}}$, also defined at the dual lattice sites, with $G_0(\mathbf{R})$ having the standard form (8). Partition function (65) can be interpreted as the partition function of a Coulomb gas consisting of integer and half-integer charges $m_{\mathbf{R}}/2$ interacting with the Ising model. Clearly, at $T\ll J, K_*$, all these charges are bound into pairs and the Ising variables $s_{\mathbf{R}}$ are ordered. We now see to what consequences the coupling of $m$ and $s$ leads.

As $J\to\infty$, partition function (65) becomes the partition function of the two-dimensional Ising model, whose exact solution was first found by Onsager [118]. The phase transition in this model occurs at

$$T=T_{\rm c}=\frac{K_*}{\ln(1+\sqrt{2})}\,,$$

as can be shown from duality considerations [120].

When $J\gg T$, we can sum over $m_{\mathbf{R}}$ in (65) assuming that all charges are bound into neutral pairs separated by large distances, with the mutual effect of the pairs manifesting itself only in the renormalization of $J$. The summation gives rise to an additional ferromagnetic interaction of the variables $s_{\mathbf{R}}$ that decays as $R^{-\pi J/2T}$ at large distances. If the half-vortices are bound into pairs, then $\pi J/2T\geqslant4$ and, according to Ref. [241], this additional interaction cannot change the nature of the Ising transition.

As $K_*\to\infty$, partition function (65) becomes the partition function of a Coulomb gas consisting of charges $m_{\mathbf{R}}/2$, with the phase transition in this system related to the dissociation of the neutral pairs of charges of the minimum value $m_{\mathbf{R}}/2=\pm1/2$, i.e., half-vortices. When $K_*<\infty$, taking fluctuations of $s$ into account leads to a situation where the bare interaction of the half-vortices acquires the additional term $-T\ln\langle s_{\mathbf{R}}s_{\mathbf{R}'}\rangle$. At large values of $K_*$, when $\langle s_{\mathbf{R}}\rangle\neq0$, this leads only to a reduction of the fugacity of half-vortices, and the correction to their interaction decays exponentially. For smaller values of $K_*$, when $\langle s_{\mathbf{R}}\rangle$ vanishes, an interaction proportional to the distance between the half-vortices appears, i.e., the soliton free energy (per unit length) becomes finite.

### 7.4 Structure of the phase diagram

Figure 18 gives a rough picture of the phase diagram (in the variables $T/J$ and $K/T$) of the XY model with the modified interaction, based on the results in the present section [44 – 46]. We let D denote the disordered phase, S denote the low-temperature (superconducting) phase, and I denote the intermediate 'nematic' phase in which the superfluid density is also finite. According to Refs [47, 48], in terms of a

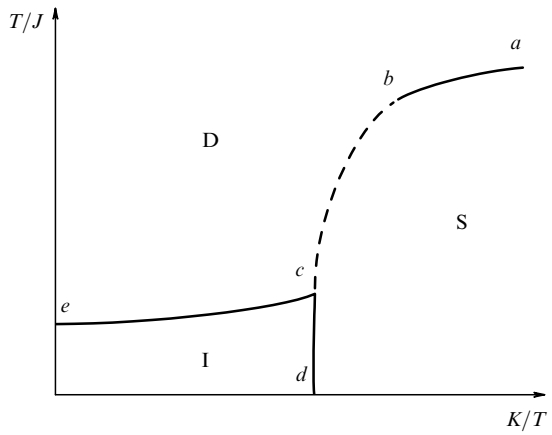


**Figure 18.** Phase diagram of the XY model with the modified interaction that leads to the possibility of soliton formation.

superconducting array, the coherency of this phase is not due to the motion of Cooper pairs (because the pair correlation function of the order parameter decays exponentially) but due to the motion of pairs of Cooper pairs.

Dissociation of pairs of ordinary vortices occurs on line *ab*, dissociation of pairs of half-vortices occurs on line *ce* (both transitions belong to the BKT universality class), and the phase transition related to solitons on line *bd*. On segment *cd*, this must be an Ising-type transition, while on segment *bc*, the soliton free energy vanishes when the logarithmic interaction of half-vortices is not strong enough to bind the half-vortices into pairs. Hence, in this case, the transition must occur directly to the disordered phase, but in a way that differs from that on line *ab*.

It can be expected that this is a first-order phase transition. The results of numerical simulations suggest that various modifications of the interaction in the XY model that increase the fugacity of vortices [243 – 246] (i.e., reduce the core energy) or a direct increase in the density of the two-dimensional Coulomb gas [247] transform the BKT transition into a first-order phase transition. The same conclusion can be drawn from attempts at a self-consistent generalization of the renormalization-group approach to the region of high fugacities [248–251].

In the model under study, a decrease in $K$ leads to the possibility of the core splitting into two half-vortices connected by a soliton, which may in turn fluctuate. Clearly, this reduces the effective free energy of the core and, accordingly, helps change the order of the transition to the first. From (18) and (62), we can expect that the value of the helicity modulus $\Gamma$ on segment *bc* in the low-temperature phase gradually changes from $(2/\pi)T$ at point *b* to $(8/\pi)T$ at point *c*.

A phase diagram with a similar topology emerges if we use a generalization of the Migdal – Kadanoff recursive procedure [252, 253] based on limiting the number of parameters that describe the interaction [45]. Such a modification of this method (whose standard version ignores the BKT transition [76]) can be used to describe systems with a U(1) degeneracy. The proposed structure of the phase diagram was also confirmed by numerical simulations [254].

The line $K = 0$ corresponds to the transition of the junctions into the $\pi$-state. When this line is crossed, the ground states change their structure. In the case of a square lattice, this transformation consists in the relative rotation of the variables $\varphi_{\mathbf{j}}$ belonging to two different $\sqrt{2} \times \sqrt{2}$ sublattices by $\pi$. A change of variables corresponding to this rotation allows verifying that the form of the partition function is independent of the sign of $K$, with the result that the complete phase diagram of the XY model with the modified interaction and a square lattice is reflection-symmetric with respect to the line $K = 0$.

## 8. Two-dimensional superfluid Fermi liquid with *p*-pairing

In the Bardeen – Cooper – Schrieffer (BCS) approximation, the minimum of the free energy of a two-dimensional superfluid Fermi liquid with *p*-pairing is attained in two different phases, axial and planar [50 – 52]. The choice between them depends on the specific features of the interaction, which manifest themselves in the next-order diagrams in $T_c/\varepsilon_F$ [49]. Experimental studies of superfluidity and phase transitions in $^3$He films whose thickness is comparable to the coherence length were carried out in Refs [255 – 260], and a transition to the superfluid state of a subatomic $^3$He film on the surface of a thin $^4$He film was observed in Ref. [261].

### 8.1 The axial phase

The order parameter in the axial phase has the form

$$A_{\alpha k} = \Delta d_\alpha (w_k^{(1)} + \mathrm{i} w_k^{(2)}) ,$$

where $\Delta$ is a real number, $d_\alpha$ is a unit vector in the spin (three-dimensional) space, and $w_k^{(1)}$ and $w_k^{(2)}$ are mutually perpendicular unit vectors in the orbital (two-dimensional) space [51]. It is convenient to parameterize the position of the vectors $w_k^{(1)}$ and $w_k^{(2)}$ by introducing a phase $\varphi$ and expressing the combination $w_k^{(1)} + \mathrm{i} w_k^{(2)}$ in terms of two fixed orthonormalized vectors $w_k'$ and $w_k''$ in the orbital space:

$$A_{\alpha k} = \Delta d_\alpha (w_k' + \mathrm{i} l w_k'') \exp \mathrm{i}\varphi , \tag{66}$$

where $l = \hat{\mathbf{z}}[\mathbf{w}^{(1)} \times \mathbf{w}^{(2)}] = \pm 1$ is the orbital number and $\hat{\mathbf{z}}$ is the unit vector normal to the surface. The degeneracy space of order parameter (66) is $((\mathrm{S}^2 \times \mathrm{S}^1)/\mathrm{Z}_2) \times \mathrm{Z}_2$, where the two-dimensional sphere $\mathrm{S}^2$ is spanned by $\mathbf{d}$, the one-dimensional sphere $\mathrm{S}^1$ is spanned by $\varphi$, and the quotient of the direct product $\mathrm{S}^2 \times \mathrm{S}^1$ over $\mathrm{Z}_2$ is taken because the pairs of variables $(\mathbf{d}, \varphi)$ and $(-\mathbf{d}, \varphi + \pi)$ correspond to the same value of $A_{\alpha k}$. If we take the spin – orbit (dipole) coupling

$$E_{\mathrm{dip}}^{\mathrm{a}} = -\frac{g_{\mathrm{dip}}^{\mathrm{a}}}{2} (\mathbf{d}\hat{\mathbf{z}})^2 \tag{67}$$

into account, the degeneracy space is reduced to $\mathrm{S}^1 \times \mathrm{Z}_2$.

Considering only the orbital part of the order parameter of the axial phase, Stein and Cross [262] concluded that two types of topological excitations exist in this phase: vortices, going around which changes $\varphi$ by $\pm 2\pi$, and domain walls separating the regions with $l = \pm 1$. Therefore, the system may undergo two phase transitions, of the BKT and Ising universality classes.

Halsey [21] demonstrated that in the axial phase, vorticity can be distributed continuously over a domain wall. In other words, fractional vortices with arbitrary topological charges may form on the domain walls without being bound into pairs. The analysis in Section 4.3 shows that this must lead to the loss of coherence between the fluctuations of the phase on both sides of the wall at arbitrarily low temperatures. As discussed in Section 4.3, the phase transition related to the vortex-pair dissociation must then occur at a temperature that is definitely lower than that of the Ising-type phase transition related to disordering in the orbital number $l$.

If we take into account that the spin part of order parameter (66) may also change, the textures that locally minimize the energy should then include, in addition to vortices and domain walls, solitons — linear objects inside which the vector $\mathbf{d}$ changes its direction (in passing through the dipole-energy maximum) but the phase $\varphi$ remains constant [49]. A soliton separates the regions with oppositely directed vectors $\mathbf{d}$, which is equivalent to the values of $\varphi$ differing by $\pi$. The soliton width is of the order of the dipole length $\xi_{\mathrm{dip}} = K_d/g_{\mathrm{dip}}^{\mathrm{a}}$, and the characteristic energy (per length equal to width) is of the order of $K_d$, where $K_d$ is one of the coefficients in the expression for the gradient energy

$$E_{\mathrm{grad}}^{\mathrm{a}} = \frac{K_d}{2} (\nabla_k d_\alpha)^2 + \frac{K_\varphi}{2} (\nabla_k \varphi)^2 .$$

We note that solitons are not unremovable topological singularities, because they separate regions of the order parameter values that can be transformed into each other by a continuous transformation. Therefore, in contrast to domain walls, solitons may have endpoints. As in the A-phase of three-dimensional $^3$He [263] and in the modified XY model examined in Section 7, a soliton may end on a vortex with a half-integer topological charge. According to the results in Section 7.2, this allows a scenario in which the phase transition related to vortex-pair dissociation splits into two separate transitions, one (at $T = T_S \sim K_d$) related to soliton formation (which at low temperatures behave as domain walls of the Ising type) and the other (at $T = T_{hv} \sim K_\varphi/4$) to the dissociation of bound pairs of half-vortices.

In the BCS approximation, $K_d = K_\varphi$, which at a first glance makes the scenario with $T_S < T_{hv}$ impossible. One must bear in mind, however, that fluctuations of the three-dimensional vector **d** may lead to a substantial renormalization of $K_d$ [264] when we proceed from scales of the order of the coherence length $\xi$ to scales of the order of $\xi_{dip}$, on which renormalization is terminated (we assume that $\xi_{dip} \gg \xi$, as is the case for superfluid $^3$He). In this case, the phase transition related to the vanishing of the soliton free energy occurs at $T_S \sim K_d/\ln(\xi_{dip}/\xi)$ (cf. Ref. [265]). The condition $\xi_{dip} \gg \xi$ suggests that this phase transition occurs at a temperature sufficiently low for the soliton endpoints to be bound (via a logarithmic interaction proportional to $K_\varphi$) into small-size pairs [45].

We emphasize that the effective strength of the spin–orbit coupling can be reduced by a magnetic field [53]. In the two-dimensional axial phase, as in its three-dimensional analog (i.e., in the A-phase of superfluid $^3$He), the part of the free energy that depends on the orientation of the order parameter and is related to the magnetic field **H** can be written as

$$E^{a}_{magn} = \frac{\chi}{2}(\mathbf{dH})^2 .$$

Comparison with (67) shows that when $\mathbf{H} \parallel \hat{\mathbf{z}}$, applying a magnetic field is equivalent to replacing $g^{a}_{dip}$ with $g^{eff}_{dip} = g^{a}_{dip} - \chi H^2$. As the magnitude of the field grows, $g^{eff}_{dip}$ decreases and vanishes at $H = g^{a}_{dip}/\chi$. The value of $\xi_{dip}$ also increases in an appropriate manner and finally becomes infinite, which makes it possible to lower $T_S$ as much as needed.

At $T > T_S$, the system is in a phase in which the pair correlation function of the order parameter $A_{\alpha k}$ decays exponentially, but the superfluid density remains finite (because fluctuations of **d** do not lead to a renormalization of $K_\varphi$). In particular, this ensures a power-law decay of the *four*-point correlation function

$$\left\langle A_{\alpha k}(\mathbf{r}_1)\, A_{\alpha k'}(\mathbf{r}_1)\, A^*_{\beta k}(\mathbf{r}_2)\, A^*_{\beta k'}(\mathbf{r}_2)\right\rangle \propto \left\langle \exp\left\{2i\left[\varphi(\mathbf{r}_1) - \varphi(\mathbf{r}_2)\right]\right\}\right\rangle .$$

In the absence of a spin–orbit coupling, such a phase can exist at an arbitrarily low temperature. Due to fluctuations in the spin part of the order parameter, the symmetry with respect to rotation of the phase by $\pi$ is restored, and therefore further disordering proceeds via dissociation of pairs of half-vortices rather than vortices. As a result, the ratio of the superfluid density to the temperature in the phase transition into the completely disordered state is four times larger [49],

$$\frac{\rho_s(T_{hv})}{T_{hv}} = \frac{8}{\pi}\left(\frac{2m_3}{\hbar}\right)^2 , \tag{68}$$

than in the case where the transition is related to the dissociation of pairs of ordinary vortices, as was assumed in Ref. [262].

If we recall that the above-mentioned disordering in $l$ occurs at even higher temperatures, we can conclude that in the presence of a weak spin–orbit coupling, the transition from the axial phase to the completely disordered phase consists of three subsequent phase transitions (two Ising transitions and a BKT transition between them [49]). If the condition needed for the weak-coupling approximation to be applicable is satisfied ($T_c \ll \varepsilon_F$), all these transitions occur in a narrow neighborhood of $T_c$ (the transition temperature in the BCS approximation), because only at

$$\frac{T_c - T}{T_c} \sim \frac{T_c}{\varepsilon_F}$$

do the constants in the expression for the gradient energy become comparable with $T$.

A Monte Carlo simulation of the lattice model of the axial phase that ignored the dipole interaction confirmed (see Ref. [266]) the presence of two phase transitions. As the temperature decreases, first comes the transition of the Ising type, which can be detected by the divergence of specific heat, and then comes the BKT transition related to the emergence of quasiordering in $\exp(2i\varphi)$.

### 8.2 The planar phase

The order parameter of the planar phase can be written as

$$A_{\alpha k} = \Delta R_{\alpha k'}(\delta_{k'k} - \hat{z}_{k'}\hat{z}_k)\exp(i\varphi) , \tag{69}$$

where $R_{\alpha k}$ is a matrix of three-dimensional rotations. Because of the presence of the projecting factor $(\delta_{k'k} - \hat{z}_{k'}\hat{z}_k)$, the index $k$ takes only two values. Such a projection leads to a situation in which the same value of $A_{\alpha k}$ can be represented in form (69) in two different ways, with different matrices $R_{\alpha k}$ and with phases $\varphi$ that differ by $\pi$. Therefore, the degeneracy space of order parameter (69) has the $(SO(3) \times S^1)/Z_2$ structure, where SO(3) is spanned by $R_{\alpha k}$, the circle $S^1$ is spanned by $\varphi$, and the quotient over $Z_2$ reflects the ambiguity mentioned above.

The situation with the planar phase is totally similar to the situation with the axial phase described in Section 8.1 (if we ignore the presence of an additional discrete degree of freedom in the axial phase). The gradient energy separates into terms related to $R_{\alpha k}$ and $\varphi$. In the absence of a spin–orbit coupling, only the rigidity related to $\varphi$ (superfluid density) is not renormalized to zero. The pair correlation function of the order parameter then decays exponentially, but the superfluid density $\rho_s$ remains finite. As $\rho_s$ decreases to the value determined by (68), a transition to the completely disordered states occurs (this transition is related to the dissociation of half-vortex pairs).

The dipole energy in the planar phase depends on the matrix $R_{\alpha k}$ of a three-dimensional rotation, which can be conveniently parameterized in the standard way [267, 268], i.e., using a vector **n** that specifies the direction of rotation and an angle $\theta$ of that rotation. Then, the expression for the dipole

energy that follows from Leggett's general formula [269] becomes [49]

$$E_{\rm dip}^{\rm pl} = g_{\rm dip}^{\rm pl}\left\{\frac{1}{3}\cos^2\theta + \frac{3}{8}\left[(1-\cos\theta)n_\parallel^2 + \frac{4}{3}\cos\theta\right]^2\right\}, \quad (70)$$

where $\mathbf{n}_\parallel = \mathbf{n} - (\mathbf{n}\hat{\mathbf{z}})\hat{\mathbf{z}}$ is the projection of $\mathbf{n}$ on the plane. The minimum of (70) is attained at $\cos\theta = 0$ and $\mathbf{n} = \pm\hat{\mathbf{z}}$. All the values of $A_{\alpha k}$ that minimize (70) can be specified by the same matrix $R_{\alpha k}$ (the rotation by $\pi/2$ around $\hat{\mathbf{z}}$) and various values of the phase. This means that the degeneracy space reduces to $S^1$.

In the planar phase, as in the axial one, the fact that the dipole interaction is finite leads to the existence of solitons [49]. In this case, the vector $\mathbf{n}$ reverses its direction inside a soliton (which is again equivalent to the rotation of the phase by $\pi$). If $\xi_{\rm dip} \gg \xi$, then, due to the non-Abelian nature of the SO(3) group, the constant in the gradient energy that is responsible for fluctuations in $R_{\alpha k}$ (and, eventually, for the characteristic soliton energy) is strongly renormalized by the fluctuations, just as it is in the axial phase. The corresponding renormalization-group equations can be found in the work by Azaria et al. [270, 271], devoted to the study of noncollinear antiferromagnets.

In view of all this, in the planar phase, too, there emerges a situation in which the first transition to occur as the temperature increases is related to the vanishing of the soliton free energy and is of the Ising type. This is the transition to a phase with an exponential decay of the correlation functions of $A_{\alpha k}$ but with a finite superfluid density (at $g_{\rm dip}^{\rm pl} = 0$, the existence range of this phase extends to absolute zero). As the temperature increases further, a second phase transition, related to vortex-pair dissociation, emerges. The value of the discontinuity in the superfluid density in this transition is given by the same formula (68). For the same reasons as in the case of the axial phase, both phase transitions must occur at temperatures that are fairly close to the transition temperature in the BCS approximation.

In the case of the planar phase, the anisotropic part of the magnetic energy can be written as

$$E_{\rm magn}^{\rm pl} = -\frac{\chi}{2}(H_\alpha R_{\alpha j}\hat{z}_j)^2,$$

which for $\mathbf{H} \parallel \hat{\mathbf{z}}$ is reduced to

$$E_{\rm magn}^{\rm pl} = -\frac{\chi}{2}H^2\left[\cos\theta - (1-\cos\theta)n_\parallel^2)\right]^2,$$

implying that in this case, the soliton energy also decreases when a magnetic field is applied to the system, and this assists the splitting of the phase transition even if there is no splitting in the absence of a field.

## 9. The XY model with a random phase shift

As already noted in Section 3.1, if the number of flux quanta per unit cell is an integer, a Josephson junction array can be described by the nonfrustrated XY model. This means that all the $A_{\mathbf{ij}}$ variables in the Hamiltonian

$$H = \sum_{(\mathbf{ij})} V(\varphi_{\mathbf{j}} - \varphi_{\mathbf{i}} - A_{\mathbf{ij}}) \quad (71)$$

can then be simultaneously set equal to zero by a gauge transformation. However, such simplification is possible only if the geometric structure of the array is ideally regular. But if the areas of the different cells differ from each other randomly, all the $A_{\mathbf{ij}}$ cannot vanish simultaneously even if the mean number of flux quanta per cell is an integer. In such a situation, the $A_{\mathbf{ij}}$ can be considered frozen (i.e., not fluctuating) random variables with a zero mean:

$$\overline{A_{\mathbf{ij}}} = 0. \quad (72)$$

In this case, the model in (71) is commonly called the XY model with positional disorder [63] or with a random phase shift [58]. In (72) and below, averaging over frozen disorder (i.e., over the distribution of $A_{\mathbf{ij}}$) is denoted by an overline.

If the variation of the areas of the array cells is caused by displacements in the positions of the Josephson junctions, while the positions of the lattice sites remain unchanged (as shown in Fig. 19), the random variables $A_{\mathbf{ij}}$ can be considered independent of each other. But if the positions of the array sites fluctuate [63, 272–274], the variables $A_{\mathbf{ij}}$ are characterized by short-range correlations, which, however, does not lead to any drastic changes. Therefore, to simplify matters in what follows, we assume that the variables $A_{\mathbf{ij}}$ are independent. Analytic calculations are usually done under the assumption that the distribution of the $A_{\mathbf{ij}}$ is Gaussian and can be characterized by a single parameter $\sigma$ that determines the distribution width:

$$\overline{A_{\mathbf{ij}}^2} = \sigma. \quad (73)$$

The limit $\sigma \to \infty$ corresponds to a uniform distribution of $A_{\mathbf{ij}}$. This version of model (71) is known as gauge glass [275].

Model (71)–(73) with $V(\theta) = -J\cos\theta$ was first proposed by Rubinstein, Shraiman, and Nelson [54]. They used it to describe planar magnets in which the interaction of magnetic impurities is mediated by nonmagnetic impurities (the random Dzyaloshinsky–Moriya interaction [64, 65]). Only later was it found (by Granato and Kosterlitz [63]) that this model could also be used to describe Josephson junction arrays with positional disorder in the presence of an external magnetic field. According to Nelson [276], a similar model

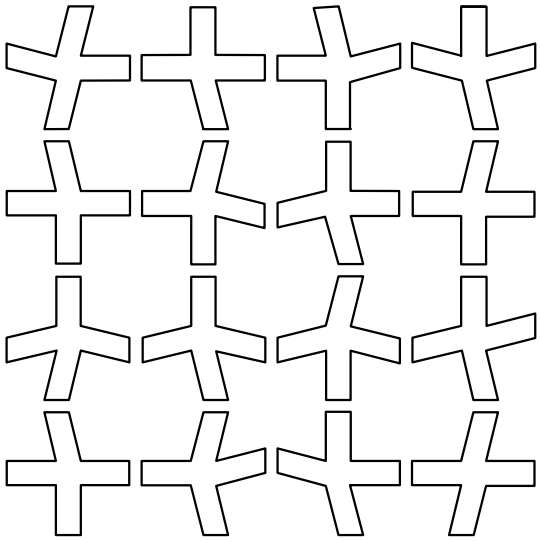

**Figure 19.** A square array formed by randomly displaced Josephson junctions.

can be used to describe dislocation-mediated melting of two-dimensional crystals with frozen density inhomogeneities (i.e., impurity atoms).

In contrast to the frozen fluctuations of the coupling constant, which are certainly irrelevant for weak disorder [54] but may change the order of transition to the first for strong disorder [277, 278], strong positional disorder leads to the total destruction of the low-temperature ordered phase.

### 9.1 The random potential

In terms of vortices, the presence of randomly distributed phase shifts $A_{\mathbf{ij}}$ manifests itself through the generation of a random potential $v_{\mathbf{R}}$ dependent on $A_{\mathbf{ij}}$. Each variable $A_{\mathbf{ij}}$ can then be assigned a frozen vortex dipole, and $v_{\mathbf{R}}$ is the sum of the potentials of all such dipoles, which may be considered uncorrelated. Because the dipole potential falls off as $1/R$ in the two-dimensional world, the square of $v_{\mathbf{R}}$ averaged over the disorder is found to diverge logarithmically as the system size increases [54].

If the interaction in (71) is chosen in the Berezinskii–Villain form (see Section 2.3), $v_{\mathbf{R}}$ can be found exactly for any values of $A_{\mathbf{ij}}$. The partition function corresponding to Hamiltonian (71) then becomes the partition function of a two-dimensional Coulomb gas described by the Hamiltonian

$$H_{\mathrm{Cg}} = \frac{1}{2}\sum_{\mathbf{R}_1,\,\mathbf{R}_2} m_{\mathbf{R}_1} G_0(\mathbf{R}_1 - \mathbf{R}_2) m_{\mathbf{R}_2} - \sum_{\mathbf{R}} v_{\mathbf{R}} m_{\mathbf{R}}\,, \tag{74}$$

where the potential $v_{\mathbf{R}}$ is a Gaussian random quantity with zero mean, and the correlations of this quantity at different sites of the dual lattice depend on the distance between the sites in the same way as the bare interaction of vortices [59]:

$$\overline{v_{\mathbf{R}}} = 0\,, \qquad \overline{v_{\mathbf{R}_1} v_{\mathbf{R}_2}} = \sigma J G_0(\mathbf{R}_1 - \mathbf{R}_2)\,, \tag{75}$$

which implies that the correlation function

$$U(\mathbf{R}_1 - \mathbf{R}_2) \equiv \overline{(v_{\mathbf{R}_1} - v_{\mathbf{R}_2})^2} \tag{76}$$

diverges logarithmically as $|\mathbf{R}_1 - \mathbf{R}_2| \to \infty$. For instance, in the case of a square lattice [56],

$$U(\mathbf{R}) \approx 4\pi\sigma J^2 \ln|\mathbf{R}|\,. \tag{77}$$

The same relation holds for the continuous version of the model, obtained when a random vector potential $A_\alpha(\mathbf{r})$ with

$$\overline{A_\alpha(\mathbf{r})\, A_\beta(\mathbf{r}')} = \sigma\delta_{\alpha\beta}\,\delta(\mathbf{r} - \mathbf{r}')$$

is included in (2). The difference $v_{\mathbf{R}_1} - v_{\mathbf{R}_2}$ on the right-hand side of Eqn (76) is simply the disorder-induced contribution to the energy of the vortex pair that consists of a positive vortex located at $\mathbf{R}_1$ and a negative vortex located at $\mathbf{R}_2$. We note that the presence of disorder does not change the form of the function $G_0(\mathbf{R})$ describing the vortex interaction.

### 9.2 Disorder and the emergence of decoupled vortices

A phase transition in the conventional XY model is related to the emergence of free vortices (i.e., vortices not bound into pairs) caused by thermal fluctuations. We now consider whether a Gaussian-distributed random potential whose parameters are determined by (75) can also generate single vortices even if there are no thermal fluctuations.

To consistently take the logarithmic divergence of various quantities into account, we assume that the system has a finite linear size $L$. This makes both the part of the vortex energy not related to disorder,

$$E_{\mathrm{v}}(L) \approx \pi J \ln L\,, \tag{78}$$

and the width of the distribution

$$\varepsilon(L) \approx J(2\pi\sigma \ln L)^{1/2} \tag{79}$$

of the random contribution to this energy $v_{\mathbf{R}}$ (which depends on the position $\mathbf{R}$ of the vortex core) finite.

Comparison of (78) with (79) shows that in the limit as $L \to \infty$, the typical value of $v_{\mathbf{R}}$ becomes negligible compared to $E_{\mathrm{v}}(L)$. But this does not mean that spontaneous vortex formation is impossible. To see whether creation of a vortex is energy-advantageous, we must compare the self-energy $E_{\mathrm{v}}(L)$ of the vortex not with the typical value of $v_{\mathbf{R}}$ for the given $L$ but with the maximum value of $v_{\mathbf{R}}$ for the given realization of the random potential, i.e., the maximum gain in the energy, $v_{\max} \equiv \max\{v_{\mathbf{R}}\}$, to which the vortex formation can lead.

The simplest estimate for this quantity can be obtained by ignoring the correlations of $v_{\mathbf{R}}$ at the different sites of the dual lattice, i.e., assuming that the $N = L^2$ variables $v_{\mathbf{R}}$ are independent random quantities characterized by the same Gaussian distribution,

$$p(v) = \frac{1}{\sqrt{2\pi}\,\varepsilon}\exp\left[-\frac{v^2}{2\varepsilon^2}\right],$$

whose width is determined by (79) and, hence, depends on the number of variables. In this approximation, the system under consideration is equivalent to the so-called random energy model [279] and the distribution of $v_{\max}$ can be found exactly:

$$P(v_{\max}) = N p(v_{\max})\left[\int_{-\infty}^{v_{\max}} \mathrm{d}V\, p(V)\right]^{N-1}. \tag{80}$$

By finding the derivative of $\ln P(v_{\max})$, we can establish (see Ref. [60]) that for $N \gg 1$, the peak of distribution (80) is at

$$v_{\max} = v_{\max}^{(0)} \approx \sqrt{2\ln N}\,\varepsilon \tag{81}$$

and is relatively narrow:

$$\frac{1}{v_{\max}^{(0)}}\left(\overline{[v_{\max} - v_{\max}^{(0)}]^2}\right)^{1/2} \sim \frac{1}{2\ln N}\,,$$

and hence the mean value of $v_{\max}$ is close to $v_{\max}^{(0)}$.

Substituting (79) in (81) shows that $\overline{v_{\max}}$ logarithmically diverges as the system becomes larger [60]:

$$\overline{v_{\max}}\,(L) \approx J(8\pi\sigma)^{1/2}\ln L\,,$$

and therefore the mean energy of a vortex that appears at a lattice position that is most favorable for this is given by

$$E_{\min}(L) \equiv E_{\mathrm{v}}(L) - \overline{v_{\max}}\,(L) \approx \pi J\left[1 - \left(\frac{\sigma}{\sigma_0}\right)^{1/2}\right]\ln L\,,$$

where $\sigma_0 = \pi/8$. When $\sigma < \sigma_0$, the proper energy of the vortex is dominant, and formation of a vortex (in the limit as $L \to \infty$) requires infinite energy. On the other hand, when

$\sigma > \sigma_0$, the creation of a vortex at the optimal position reduces the system energy, with the result that spontaneous vortex formation [58, 60, 61] is guaranteed to occur. A similar approach was used in Ref. [280] to analyze the creation of dislocations in a two-dimensional crystal interacting with a random potential.

Taking the correlations between the values of the random potential at different sites into account reduces the relative spread of the variables $v_{\mathbf{R}}$, and therefore the above estimate for $\overline{v_{\max}}(L)$ should be interpreted as an upper bound. This means that at $\sigma < \sigma_0$ at least, the system is stable under the disorder-induced spontaneous formation of vortices at zero temperature. To verify that such an instability does arise at large values of $\sigma$, we must find a lower bound for $v_{\max}$, which is also logarithmic.

One way to do this is to separate the contributions to $v_{\mathbf{R}}$ from different scales [60]. We partition our system consisting of $N = L^2$ sites into $M \gg 1$ equal parts and examine the contribution to the random potential generated inside each part by all the other subsystems. To estimate this contribution to the random potential, we replace each of the $M - 1$ subsystems (surrounding the given subsystem) with a random dipole.

The width of the distribution of these random dipoles is $(N/M)^{1/2}$ times larger than $\sigma^{1/2}$, i.e., that of the distribution of 'elementary' random dipoles associated with the variables $A_{\mathbf{ij}}$. Because the linear size of each subsystem exceeds the lattice constant by the same factor and the dipole potential falls off as $1/R$, the two factors $(N/M)^{1/2}$ in the expression for the potential cancel and we return to the same problem, but with the number of sites $N$ replaced by the number of subsystems $M$.

Hence, if we select a subsystem inside which the value of the random potential generated by the other subsystems is at its maximum, the mean value of this potential is determined by the same function $\overline{v_{\max}}(l)$ (where $l = M^{1/2}$), which, generally speaking, we seek. However, in this approach, we still have the possibility to further optimize the position of the vortex, now inside the subsystem selected at the earlier stage. This optimization can be carried out by the same procedure, which leads to one more term, equal to $\overline{v_{\max}}(l)$, being added to the potential. Clearly, if the complete system consists of $N \gg M$ sites, the procedure can be repeated $\ln N/\ln M = \ln L/\ln l$ times, which leads to the choice of the site with

$$v_{\mathbf{R}} \approx v_{\max}^{(1)}(L) = \frac{\ln L}{\ln l}\,\overline{v_{\max}}(l)\,.$$

As a result, we have constructed an explicit algorithm for selecting the site with a sufficiently large value of the random potential, which proved to be logarithmically dependent on the size of the system. Because this algorithm does not allow determining the site with the truly largest value of $v_{\mathbf{R}}$, the function $v_{\max}^{(1)}(L)$ constructed in this manner is a lower bound for $\overline{v_{\max}}$. The logarithmic dependence of this estimate on $L$ proves that as $L \to \infty$, we indeed have $\overline{v_{\max}} \propto \ln L$, and hence there exists a critical value of $\sigma$, exceeding which allows the formation of vortices not bound into pairs to occur [60].

The argument based on comparing the different contributions to the vortex energy does not take thermal fluctuations into account and can be used directly only in the zero-temperature limit. At finite temperatures, we must also account for the entropy contribution to the free energy of the vortex, which in the case of a homogeneous system is logarithmic (see Section 2.2). For an inhomogeneous system, the entropy of a single vortex is

$$S_{\mathrm{v}}(L) = -\ln\left[\sum_{\mathbf{R}} \exp\left(-\frac{v_{\max} - v_{\mathbf{R}}}{T}\right)\right]. \tag{82}$$

Because the difference between the values of the random potential at different points increases with the distance between the points, we can expect that the result of summation in Eqn (82) is determined only by a certain neighborhood of the point at which the value of $v(\mathbf{R})$ is maximum, i.e., equal to $v_{\max}$, and therefore $S_{\mathrm{v}}(L)$ does not contain a contribution that increases as $\ln L$. This would mean that the critical value of $\sigma$ at low temperatures must remain the same as at $T = 0$.

### 9.3 Vortex pairs and renormalization of the helicity modulus

As shown in Section 2.4, the presence of bound pairs of vortices reduces the effective rigidity and, hence, narrows the existence range of the phase in which all vortices are bound into pairs. We now see how this mechanism operates in the presence of a random potential.

From the physical interpretation of expression (14) for the weight factor for a pair of vortices, it follows that in the presence of a random potential, this expression can be replaced with

$$W(\mathbf{R}_1, \mathbf{R}_2) = Y^2 \exp\left\{-\frac{1}{T}\left[G(0) - G(\mathbf{R}_1 - \mathbf{R}_2) - v_{\mathbf{R}_1} + v_{\mathbf{R}_2}\right]\right\}, \tag{83}$$

where to the self-energy of a vortex pair we have added the energy of its interaction with the potential. Averaging (83) over fluctuations of the random potential and substituting the result in (16) shows (see Ref. [54]) that in this case, the correction to the helicity modulus related to vortex pairs converges only if

$$\frac{2\pi J}{T} - \frac{2\pi\sigma J^2}{T^2} > 4\,, \tag{84}$$

i.e., in the temperature range

$$T_-(J,\sigma) < T < T_+(J,\sigma)\,, \tag{85}$$

where

$$T_\pm(J,\sigma) = 2J\sigma_0\left[1 \pm \left(1 - \frac{\sigma}{\sigma_0}\right)^{1/2}\right], \tag{86}$$

and diverges as

$$T \to T_\pm(J,\sigma) \mp 0\,.$$

The same divergence manifests itself when we use the replica formalism, which consists in averaging the partition function of $n$ identical replicas of the system over the disorder, which in the limit $n \to 0$ is equivalent to averaging the free energy [281–283]. In the replica representation, the interaction of the charges comprising a Coulomb gas, $G_0^{ab}(\mathbf{R})$, depends not only on the distance $\mathbf{R}$ between the charges but also on the numbers $a$ and $b$ of the replicas to which the charges belong [54]:

$$G_0^{ab}(\mathbf{R}) = G_0(\mathbf{R})\left(\delta^{ab} - \frac{\sigma J}{T}\right).$$

Clearly, the combination on the left-hand side of (84) is simply the prelogarithmic factor in the expression for the energy of a neutral pair of charges belonging to the same replica.

It follows from (85) and (86) that not only a rise but also a drop in temperature suppresses the helicity modulus, even if the disorder is weak. The discovery of this fact, together with a modification of the Kosterlitz renormalization group based on it, led Rubinstein, Shraiman, and Nelson [54] to the conclusion that even when the disorder is very weak, there must be a reentrant transition into the disordered state in the system. However, this statement has not been confirmed by later experimental studies of Josephson junction arrays with positional disorder [272] or by the results of numerical simulation of the respective XY model [272–274]. Moreover, it contradicts a theorem proved by Ozeki and Nishimori [284] (see Section 9.4).

An attempt to account for the corrections to $\Gamma$ of higher orders in $Y$ than the one studied in Ref. [54] demonstrated the presence of a new divergence [56] in each next order in the expansion in $Y^2$, which, it would seem, should be applicable in the region where the ordered phase exists. The occurrence of these divergences becomes especially evident when we use the replica approach, within which this phenomenon is due to the existence not only of neutral pairs consisting of single charges (belonging to the same replica) but also of more complicated objects, or neutral pairs formed by many-particle complexes consisting of $k > 1$ bound charges of the same sign belonging to different replicas. The prelogarithmic factor in the expression for the energy of a pair of such complexes is given by [55,56]

$$2\pi\left(\frac{J}{T}\,k - \frac{\sigma J^2}{T^2}\,k^2\right),$$

which implies that for any values of the parameters, the corrections to $\Gamma$ corresponding to large values of $k$ are divergent.

The presence of such a set of divergences means (see Ref. [56]) that either there is no ordered phase at all (and its observations in [272–274] should be interpreted as a finite-size effect) or such a phase cannot be found by the method proposed in [54] and developed in [55–57]. It turns out that the problems are rooted in the use of the formal expansion in powers of the fugacity $Y$, whereas a more adequate approach is to use the expansion in the vortex-pair concentration [59].

From the physical standpoint, it is understandable that the simplest correction to the interaction of vortices in the ordered phase (if such a phase exists at all) is a correction from bound vortex pairs, which is proportional to their density. The contributions of different pairs to this correction can then be considered uncorrelated.

In the presence of a random potential, the function $\Sigma(\mathbf{R}_1, \mathbf{R}_2)$, which according to (11) determines the magnitude of the fluctuation-induced correction to the interaction of the Coulomb-gas charges, is given by the irreducible part of the correlation function of the charges of this gas [54, 59]:

$$\Sigma(\mathbf{R}_1, \mathbf{R}_2) = \langle m_{\mathbf{R}_1} m_{\mathbf{R}_2}\rangle - \langle m_{\mathbf{R}_1}\rangle\langle m_{\mathbf{R}_2}\rangle\,. \tag{87}$$

In the absence of disorder, we have $\langle m_{\mathbf{R}}\rangle = 0$, and the second term on the right-hand side of (87) vanishes. Expression (87) can also be represented in the form of the second derivative of the free energy [59]:

$$\Sigma(\mathbf{R}_1, \mathbf{R}_2) = -T\,\frac{\partial^2 F}{\partial v_{\mathbf{R}_1}\,\partial v_{\mathbf{R}_2}}\,. \tag{88}$$

We note that both (87) and (88) are exact expressions. Deriving them involves no approximations or averaging over the disorder.

In the lowest order in the concentration of vortex pairs, the contributions to the right-hand side of Eqn (88) provided by different pairs can be assumed to be independent. Hence, in calculating $\Sigma(\mathbf{R}_1, \mathbf{R}_2)$, we can ignore the interaction between charges belonging to different pairs. In this approximation, the partition function of the Coulomb gas in the phase where all charges form bound pairs can be approximated by the expression [59]

$$Z_{\mathrm{Cg}} = \prod_{(\mathbf{R}_1, \mathbf{R}_2)} \left[1 + W(\mathbf{R}_1, \mathbf{R}_2) + W(\mathbf{R}_2, \mathbf{R}_1)\right], \tag{89}$$

where $W(\mathbf{R}_1, \mathbf{R}_2)$ has form (83), and the product is over all pairs of the dual lattice sites.

The structure of (89) assumes that three possibilities are considered for each pair of sites $(\mathbf{R}_1, \mathbf{R}_2)$: the absence of a vortex pair, the presence of a vortex with the topological charge $+1$ at $\mathbf{R}_1$ and a vortex with the opposite charge at $\mathbf{R}_2$, and the presence of a vortex pair with the opposite polarization. Partition function (89) accounts for the interaction of all vortices with a random potential and for the interaction of the vortices belonging to the same pair. It does not account only for the interaction of vortices belonging to different pairs.

Substituting $F_{\mathrm{Cg}} = -T \ln Z_{\mathrm{Cg}}$ in (88) and finding the derivatives with respect to $v_{\mathbf{R}_1}$ and $v_{\mathbf{R}_2}$, we can represent $\Sigma(\mathbf{R}_1, \mathbf{R}_2)$ (for $\mathbf{R}_1 \neq \mathbf{R}_2$) as

$$\Sigma(\mathbf{R}_1, \mathbf{R}_2) = -2W_*(\mathbf{R}, v)\,, \tag{90}$$

where $\mathbf{R} = \mathbf{R}_1 - \mathbf{R}_2$, $v = v_{\mathbf{R}_1} - v_{\mathbf{R}_2}$, and

$$W_*(\mathbf{R}, v) = -\frac{T}{2}\,\frac{\partial}{\partial v}\left[\frac{W(\mathbf{R}, v) - W(\mathbf{R}, -v)}{1 + W(\mathbf{R}, v) + W(\mathbf{R}, -v)}\right], \tag{91}$$

with $W(\mathbf{R}, v)$ given by (83). At the same time, the form of $\Sigma(\mathbf{R}_1, \mathbf{R}_2)$ at $\mathbf{R}_1 = \mathbf{R}_2$ follows from the relation

$$\sum_{\mathbf{R}_2} \Sigma(\mathbf{R}_1, \mathbf{R}_2) = 0\,,$$

reflecting the fact that all vortices are bound into neutral pairs. The random variable $v \equiv v_{\mathbf{R}_1} - v_{\mathbf{R}_2}$ that enters (90) and (91) is characterized by a Gaussian distribution whose width is determined by (77) and depends only on the difference $\mathbf{R} = \mathbf{R}_1 - \mathbf{R}_2$ but not on $\mathbf{R}_1$ and $\mathbf{R}_2$ separately.

Substituting (90) in (11), we find that in the presence of a random potential, we must replace $W(\mathbf{R})$ with $\overline{W_*(\mathbf{R}, v)}$ in expression (16) for the correction to the helicity modulus:

$$\delta\Gamma = -\frac{2\pi^2\Gamma^2}{T}\sum_{\mathbf{R}} R^2\,\overline{W_*(\mathbf{R}, v)}\,. \tag{92}$$

In the limit as $R \to \infty$, the result of averaging $W_*(\mathbf{R}, v)$ over the disorder is characterized by a power-law behavior [59]:

$$\overline{W_*(\mathbf{R}, v)} \approx B(T) R^{-K(T)}\,, \tag{93}$$

but the temperature dependence of the parameters in (93) proves to be essentially different. For $T > T_*(J,\sigma) \equiv 2J\sigma$,

$$B(T) = \frac{2}{T}, \qquad K(T) = 2\pi\left(\frac{J}{T} - \frac{\sigma J^2}{T^2}\right), \tag{94}$$

while for $T < T_*(J,\sigma)$,

$$B(T) = \frac{\pi T/T_*}{\sin(\pi T/T_*)}\,\frac{1}{\pi J\sqrt{2\sigma \ln R}}, \qquad K(T) = \frac{\pi}{2\sigma}. \tag{95}$$

The temperature dependences described by Eqns (94) coincide with those found by Rubinstein et al. [54]. In terms of the above approach, the approximation used in Ref. [54] amounts to replacing the denominator on the right-hand side of (91) with unity. A more consistent analysis shows that such an approach is justified only at $T > T_*$, while at $T < T_*$, the complete denominator must be taken into account. Interestingly, an attempt to expand

$$\frac{1}{1 + W(\mathbf{R}, v) + W(\mathbf{R}, -v)}$$

in a power series in $W(\mathbf{R}, v) + W(\mathbf{R}, -v)$, i.e., in powers of $Y^2$, leads to the reproduction of the entire set of divergences discovered in Refs [55, 56]. Thus, the use of the expansion in the concentration of vortex pairs is simply an effective way of summing this set of divergences.

### 9.4 Structure of the phase diagram

Substituting (93)–(95) in (91) shows that at $T > T_*(J,\sigma)$, the correction to the helicity modulus becomes divergent at $T = T_+(J,\sigma) = 2J\sigma_0(1 + \sqrt{1 - \sigma/\sigma_0})$ (i.e., on line $CD$ in Fig. 20), while at lower temperatures $[T < T_*(J,\sigma)]$, the convergence domain is limited by the line $\sigma = \sigma_0 = \pi/8$ (line $AC$ in Fig. 20) parallel to the temperature axis [58, 59].

This determines the stability range of the ordered phase in the limit of zero fugacity (which corresponds to a high core energy). But if the core energy is not very high (or is zero), we must take the renormalization effects into account, which narrows the range of stability of the ordered phase. Because only the helicity modulus is renormalized in this approximation, while the parameter $\sigma$ characterizing the disorder remain unchanged [59], the position of the low-temperature part of the phase transition line ($\sigma = \sigma_0$) must remain the same, while the curved part of this line ($CD$) is shifted toward lower temperatures ($BE$). The structure of the phase diagram shown in Fig. 20 agrees with the results of both numerical simulations [272–274, 285] and experimental studies [272].

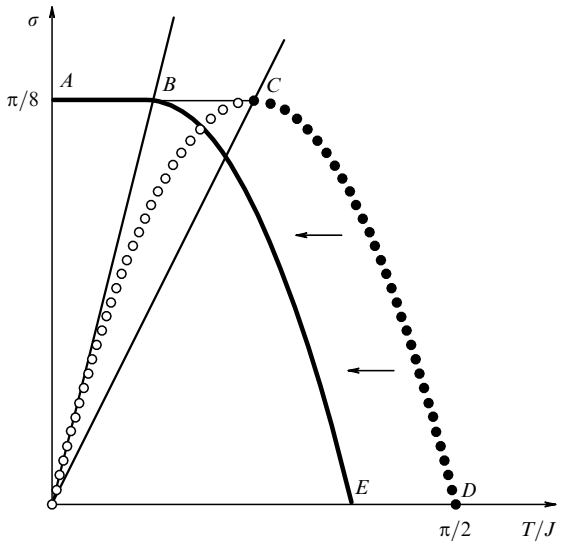


**Figure 20.** In the limit of zero fugacity, the stability region of the ordered phase is located below the line $ABCD$. Renormalization effects lead to a shift of the curved part of the phase transition line into the region of lower temperatures.

We recall that in examining the possibility of a single vortex creation (see Section 9.2), we also arrived at the conclusion that the critical value of $\sigma$ at low temperatures, i.e., $\sigma_c$, is independent of the temperature. Furthermore, the values of $\sigma_c$ obtained by two methods coincide. At the same time, taking additional terms in the renormalization-group equations into account leads to the conclusion (see Refs [61, 62]) that at $T < T_*$, the value of $\sigma$ can be renormalized, which in turn leads to a temperature dependence of $\sigma_c$ in the low-temperature region. But this conclusion contradicts a theorem proved by Ozeki and Nishimori [284]. According to this theorem, the phase transition line (if it exists) for $T < J\sigma$ must be parallel to the temperature axis, and it is therefore assumed in Fig. 20 that the renormalization effects shift the singular point separating the phase transition line into two parts from point $C$ to point $B$ where the line $\sigma = \sigma_0$ intersects the line $T = J\sigma$.

The right-hand part of the phase transition line (segment $BE$ in Fig. 20) corresponds to values of the parameters at which the denominator in (91) is irrelevant, and hence the renormalization-group equations derived in Ref. [54] can be used to describe the critical behavior on this line (see Refs [58, 61, 62]). They do not change the critical behavior compared to the pure case ($\sigma = 0$), but the magnitude of the jump in $\Gamma$ at the transition point becomes nonuniversal.

Carpentier and Le Doussal [286, 287] showed that the description of the phase transition on the line $AB$ in terms of the renormalization of a finite number of parameters (e.g, $\sigma$ and $\Gamma$) is not truly meaningful because it does not embrace the highly nontrivial renormalization of the distribution function of the energy of the vortex core, which turns out to be non-Gaussian. Explicitly taking such renormalization into account has allowed these two researchers to demonstrate [287] that at $T = 0$, the phase transition occurs at $\sigma = \sigma_0 = \pi/8$, the value also following from simple estimates that do not involve renormalization (see Section 9.2), but a generalization of this result to $T > 0$ remains a subject of future studies. The data of the numerical simulations done by Maucourt and Grempel [285] show that in a broad temperature range, $0.392 < \sigma_c(T) < 0.393$; in other words, if there is a shift of $\sigma_c$ in relation to $\sigma_0 = \pi/8 \approx 0.3927$, it is extremely small.

Interestingly, if the average number of flux quanta per cell is *half-integer*, then even a very weak positional disorder destroys the ordering of chiralities [288]. The effect of such disorder is similar to that of a random field in the two-dimensional Ising model, which, as is known [289–292], destroys the order, no matter how weak the disorder is.

## 10. Conclusion

The main goal of the present review was to give the reader an idea about the wide scope of problems encountered in studies of the nature and sequence of phase transitions in two-

dimensional systems with continuous degeneracy in situations where knowing the symmetry of the system is not enough to determine the number and type of the phase transitions occurring in the system, and also about the methods used to solve these problems.

The most adequate approach to the analysis of such problems is to classify the topological excitations and to study the mutual effect of the various classes of such excitations. This allows establishing that even in systems with the same symmetry-related degeneracy, various sequences of phase transitions are possible, and that the correct choice between them depends on the relations between the coupling parameters and on the type of the lattice. It often happens that the structure of ordering in the low-temperature phase is related to lifting the accidental degeneracy of the ground state by small fluctuations of the continuous degrees of freedom. The review also discusses the role of the interaction of point-like topological excitations (vortices) with a random potential caused by geometric inhomogeneities.

Without a doubt, the study of two-dimensional systems with continuous degeneracy will be actively continued. Today, we know the sequence of phase transitions only for a very limited number of uniformly frustrated XY models (some of which have been discussed in detail in the review), and therefore it would very important to understand how general the classification of possible scenarios [28] discussed in Section 4.4 is. In particular, we still do not know how the properties of the model with $f = 1/3$ and a square lattice established by numerical simulations [138] fit into this classification.

No less interesting is the study of systems characterized by glassy behavior at low temperatures [293 – 295], occurring despite the absence of any inhomogeneities. On the other hand, studies on the effect of inhomogeneities on the properties of systems with combined degeneracy have so far been focused on the fully frustrated XY model on a square lattice [288, 296 – 300]. However, it remains to be established whether the results in these works are universal to some degree or can be applied only to a specific model.

Thus, the spectrum of the problems requiring further research is extremely broad.

## References


1. Berezinskii V L *Zh. Eksp. Teor. Fiz.* **59** 907 (1970) [*Sov. Phys. JETP* **32** 493 (1971)]
2. Berezinskii V L *Zh. Eksp. Teor. Fiz.* **61** 1144 (1971) [*Sov. Phys. JETP* **34** 610 (1972)]
3. Kosterlitz J M, Thouless D J *J. Phys. C: Solid State Phys.* **5** L124 (1972)
4. Kosterlitz J M, Thouless D J *J. Phys. C: Solid State Phys.* **6** 1181 (1973)
5. Kosterlitz J M *J. Phys. C: Solid State Phys.* **7** 1046 (1974)
6. Nelson D R, Kosterlitz J M *Phys. Rev. Lett.* **39** 1201 (1977)
7. Beasley M R, Mooij J E, Orlando T P *Phys. Rev. Lett.* **42** 1165 (1979)
8. Nelson D R, Pelcovits R A *Phys. Rev. B* **16** 2191 (1977)
9. Halperin B I, Nelson D R *Phys. Rev. Lett.* **41** 121, 519 (1978)
10. Nelson D R, Halperin B I *Phys. Rev. B* **19** 2457 (1979)
11. Young A P *Phys. Rev. B* **19** 1855 (1979)
12. Kosterlitz J M, Thouless D J, in *Progress in Low Temperature Physics* Vol. VIIB (Ed. D F Brewer) (Amsterdam: North-Holland, 1978) p. 371
13. Nelson D R, in *Fundamental Problems in Statistical Mechanics V: Proc. of the 5th Intern. Summer School, Enschede, The Netherlands, June 23 – July 5, 1980* (Ed. E G D Cohen) (Amsterdam: North-Holland, 1980) p. 53
14. Nelson D R, in *Phase Transitions and Critical Phenomena* Vol. 7 (Eds C Domb, J L Lebowitz) (London: Academic Press, 1983) p. 1
15. Minnhagen P *Rev. Mod. Phys.* **59** 1001 (1987)
16. Efetov K B *Zh. Eksp. Teor. Fiz.* **78** 2017 (1980) [*Sov. Phys. JETP* **51** 1015 (1980)]
17. Lozovik Yu E, Akopov S G *J. Phys. C: Solid State Phys.* **14** L31 (1981)
18. Teitel S, Jayaprakash C *Phys. Rev. Lett.* **51** 1999 (1983)
19. Villain J *J. Phys. C: Solid State Phys.* **10** 1717 (1977)
20. Teitel S, Jayaprakash C *Phys. Rev. B* **27** 598 (1983)
21. Halsey T C *J. Phys. C: Solid State Phys.* **18** 2437 (1985)
22. Korshunov S E *J. Stat. Phys.* **43** 17 (1986)
23. Lee J-R et al. *Phys. Rev. Lett.* **79** 2172 (1997)
24. Korshunov S E *Phys. Rev. Lett.* **88** 167007 (2002)
25. Franzese G, Cataudella V, Korshunov S E, Fazio R *Phys. Rev. B* **62** R9287 (2000)
26. Cataudella V, Franzese G, Korshunov S E, Fazio R *Physica B* **284 – 288** 431 (2000)
27. Alexander S, Pincus P *J. Phys. A: Math. Gen.* **13** 263 (1980)
28. Korshunov S E, Uimin G V *J. Stat. Phys.* **43** 1 (1986)
29. Lee D H et al. *Phys. Rev. Lett.* **52** 433 (1984); *Phys. Rev. B* **33** 450 (1986)
30. Kawamura H *J. Phys. Soc. Jpn.* **53** 2452 (1984)
31. Korshunov S E *Pis'ma Zh. Eksp. Teor. Fiz.* **41** 525 (1985) [*JETP Lett.* **41** 641 (1985)]
32. Korshunov S E *J. Phys. C: Solid State Phys.* **19** 5927 (1986)
33. Gekht R S, Bondarenko I N *Zh. Eksp. Teor. Fiz.* **113** 2209 (1998) [*JETP* **86** 1209 (1998)]
34. Korshunov S E *Phys. Rev. B* **65** 054416 (2002)
35. Huse D A, Rutenberg A D *Phys. Rev. B* **45** 7536 (1992)
36. Korshunov S E, Douçot B *Phys. Rev. Lett.* **93** 097003 (2004)
37. Park K, Huse D A *Phys. Rev. B* **64** 134522 (2001)
38. Chtchelkatchev N M et al. *Pis'ma Zh. Eksp. Teor. Fiz.* **74** 357 (2001) [*JETP Lett.* **74** 323 (2001)]
39. Barash Yu S, Bobkova I V *Phys. Rev. B* **65** 144502 (2002)
40. Golubov A A, Kupriyanov M Yu, Fominov Ya V *Pis'ma Zh. Eksp. Teor. Fiz.* **75** 709 (2002) [*JETP Lett.* **75** 588 (2002)]
41. Bulaevskii L N, Kuzii V V, Sobyanin A A *Pis'ma Zh. Eksp. Teor. Fiz.* **25** 314 (1977) [*JETP Lett.* **25** 289 (1977)]
42. Buzdin A I, Bulaevskii L N, Panyukov S V *Pis'ma Zh. Eksp. Teor. Fiz.* **35** 147 (1982) [*JETP Lett.* **35** 178 (1982)]
43. Buzdin A I, Vujicic B, Kupriyanov M Yu *Zh. Eksp. Teor. Fiz.* **101** 231 (1992) [*Sov. Phys. JETP* **74** 124 (1992)]
44. Korshunov S E *Pis'ma Zh. Eksp. Teor. Fiz.* **41** 216 (1985) [*JETP Lett.* **41** 263 (1985)]
45. Korshunov S E *J. Phys. C: Solid State Phys.* **19** 4427 (1986)
46. Lee D H, Grinstein G *Phys. Rev. Lett.* **55** 541 (1985)
47. Ioffe L B, Feigel'man M V *Phys. Rev. B* **66** 224503 (2002)
48. Douçot B, Feigel'man M V, Ioffe L B *Phys. Rev. Lett.* **90** 107003 (2003)
49. Korshunov S E *Zh. Eksp. Teor. Fiz.* **89** 531 (1985) [*Sov. Phys. JETP* **62** 301 (1985)]
50. Fujita T et al. *Prog. Theor. Phys.* **64** 396 (1980)
51. Brusov P N, Popov V N *Zh. Eksp. Teor. Fiz.* **80** 1564 (1981) [*Sov. Phys. JETP* **53** 804 (1981)]
52. Brusov P N, Popov V N *Phys. Lett. A* **87** 472 (1982)
53. Tešanović Z *Phys. Lett. A* **100** 158 (1984)
54. Rubinstein M, Shraiman B, Nelson D R *Phys. Rev. B* **27** 1800 (1983)
55. Korshunov S E *Helv. Phys. Acta* **65** 492 (1992)
56. Korshunov S E *Phys. Rev. B* **48** 1124 (1993)
57. Mudry C, Wen X-G *Nucl. Phys. B* **549** 613 (1999)
58. Nattermann T, Scheidl S, Korshunov S E, Li M S *J. Phys. I* (France) **5** 565 (1995)
59. Korshunov S E, Nattermann T *Phys. Rev. B* **53** 2746 (1996)
60. Korshunov S E, Nattermann T *Physica B* **222** 280 (1996)
61. Tang L-H *Phys. Rev. B* **54** 3350 (1996)
62. Scheidl S *Phys. Rev. B* **55** 457 (1997)
63. Granato E, Kosterlitz J M *Phys. Rev. B* **33** 6533 (1986)
64. Dzyaloshinsky I *J. Phys. Chem. Solids* **4** 241 (1958)
65. Moriya T *Phys. Rev. Lett.* **4** 228 (1960); *Phys. Rev.* **120** 91 (1960)
66. Wegner F *Z. Phys. B* **206** 465 (1967)

67. Pearl J, in *Proc. of the Ninth Intern. Conf. on Low Temperature Physics, 1964* (*LT-9*) (Eds J G Daunt et al.) (New York: Plenum Press, 1965) p. 566
68. Fisher M E, Barber M N, Jasnow D *Phys. Rev. A* **8** 1111 (1973)
69. Landau L D *Zh. Eksp. Teor. Fiz.* **7** 627 (1937); *Phys. Z. Sowjetunion* **11** 545 (1937); in *Sobranie Trudov* (Collected Papers of L D Landau) Vol. 1 (Moscow: Nauka, 1969) Article 29 [Translated into English (Oxford: Pergamon Press, 1965)]
70. Peierls R E *Ann. Inst. Henri Poincaré* **5** 177 (1937)
71. Mermin N D, Wagner H *Phys. Rev. Lett.* **17** 1133 (1966)
72. Mermin N D *Phys. Rev.* **176** 250 (1968)
73. Hohenberg P C *Phys. Rev.* **158** 383 (1967)
74. Berezinskii V L, Ph.D Thesis in Physics and Mathematics (Moscow: L D Landau Institute for Theoretical Physics, 1971)
75. Villain J *J. Phys.* (Paris) **36** 581 (1975)
76. José J V et al. *Phys. Rev. B* **16** 1217 (1977)
77. Ohta T, Jasnow D *Phys. Rev. B* **20** 139 (1979)
78. Anderson P W, Yuval G, Hammann D R *Phys. Rev. B* **1** 4464 (1970)
79. Tobochnik J, Chester G V *Phys. Rev. B* **20** 3761 (1979)
80. Fernández J F, Ferreira M F, Stankiewicz J *Phys. Rev. B* **34** 292 (1986)
81. Weber H, Minnhagen P *Phys. Rev. B* **37** 5986 (1988)
82. Gupta R et al. *Phys. Rev. Lett.* **61** 1996 (1988)
83. Olsson P *Phys. Rev. B* **52** 4526 (1995)
84. Shih W Y, Stroud D *Phys. Rev. B* **30** 6774 (1984)
85. Ferer M, Velgakis M J *Phys. Rev. B* **27** 314 (1983)
86. Butera P, Comi M *Phys. Rev. B* **50** 3052 (1994)
87. Knops H J F *Phys. Rev. Lett.* **39** 766 (1977)
88. Weeks J D, in *Ordering in Strongly Fluctuating Condensed Matter Systems* (Ed. T Riste) (New York: Plenum Press, 1980) p. 293
89. Chui S T, Weeks J D *Phys. Rev. B* **14** 4978 (1976)
90. van der Eerden J P, Knops H J F *Phys. Lett. A* **66** 334 (1978)
91. Swendsen R H *Phys. Rev. B* **17** 3710 (1978)
92. van Beijeren H *Phys. Rev. Lett.* **38** 993 (1977)
93. Rys F *Helv. Phys. Acta* **36** 537 (1963)
94. Lieb E H *Phys. Rev. Lett.* **18** 1046 (1967)
95. Lieb E H, Wu F Y, in *Phase Transitions and Critical Phenomena* Vol. 1 (Eds C Domb, M S Green) (London: Academic Press, 1972) p. 331
96. Wiegmann P B *J. Phys. C*: *Solid State Phys.* **11** 1583 (1978)
97. Ohta T *Prog. Theor. Phys.* **60** 968 (1978)
98. Amit D J, Goldschmidt Y Y, Grinstein S *J. Phys. A*: *Math. Gen.* **13** 585 (1980)
99. Stroud D, Kivelson S *Phys. Rev. B* **35** 3478 (1987)
100. Newrock R S et al., in *Solid State Physics* Vol. 54 (Eds H Ehrenreich, F Spaepen) (San Diego: Academic Press, 2000) p. 263
101. Martinoli P, Leemann C *J. Low Temp. Phys.* **118** 699 (2000)
102. Vallat A, Korshunov S E, Beck H *Phys. Rev. B* **43** 8482 (1991)
103. Vallat A, Beck H *Phys. Rev. B* **50** 4015 (1994)
104. Fradkin E, Huberman B, Shenker S H *Phys. Rev. B* **18** 4789 (1978)
105. Kanô K, Naya S *Prog. Theor. Phys.* **10** 158 (1953)
106. Horiguchi T, Chen C C *J. Math. Phys.* **15** 659 (1974)
107. Sutherland B *Phys. Rev. B* **34** 5208 (1986)
108. Shih W Y, Stroud D *Phys. Rev. B* **32** 158 (1985)
109. Teitel S, Jayaprakash C *J. Phys. Lett.* (Paris) **46** L33 (1985)
110. Korshunov S E *Phys. Rev. B* **63** 134503 (2001)
111. Xiao Y et al. *Phys. Rev. B* **65** 214503 (2002)
112. Korshunov S E, Douçot B *Phys. Rev. B* **70** 134507 (2004)
113. Korshunov S E *Phys. Rev. B* **71** 174501 (2005)
114. Straley J P, Morozov A Y, Kolomeisky E B *Phys. Rev. Lett.* **79** 2534 (1997)
115. Franz M, Teitel S *Phys. Rev. Lett.* **73** 480 (1994); *Phys. Rev. B* **51** 6551 (1995)
116. Hattel S, Wheatley J *Phys. Rev. B* **50** 16590 (1994)
117. Hattel S A, Wheatley J M *Phys. Rev. B* **51** 11951 (1995)
118. Onsager L *Phys. Rev.* **65** 117 (1944)
119. Vdovichenko N V *Zh. Eksp. Teor. Fiz.* **47** 715 (1964) [*Sov. Phys. JETP* **20** 477 (1965)]
120. Kramers H A, Wannier G H *Phys. Rev.* **60** 252 (1941)
121. Thijssen J M, Knops H J F *Phys. Rev. B* **37** 7738 (1988)
122. Thijssen J M *Phys. Rev. B* **40** 5211 (1989)
123. Korshunov S E *Phys. Rev. Lett.* **94** 087001 (2005)
124. Berge B et al. *Phys. Rev. B* **34** 3177 (1986)
125. Eikmans H et al. *Phys. Rev. B* **39** 11759 (1989)
126. Bulgadaev S A *Phys. Lett. A* **86** 213 (1981); *Teor. Mat. Fiz.* **51** 424 (1982) [*Theor. Mat. Phys.* **51** 593 (1982)]
127. Lee S J, Lee J-R, Kim B *Phys. Rev. E* **51** R4 (1995)
128. Olsson P, Teitel S *Phys. Rev. B* **71** 104423 (2005)
129. Coniglio A et al. *J. Phys. A*: *Math. Gen.* **10** 205 (1977)
130. Stella A L, Vanderzande C *Phys. Rev. Lett.* **62** 1067 (1989)
131. Vanderzande C, Stella A L *J. Phys. A*: *Mat. Gen.* **22** L445 (1989)
132. Stauffer D *Phys. Rep.* **54** 1 (1979)
133. Klein W et al. *Phys. Rev. Lett.* **41** 1145 (1978)
134. Dotsenko Vik. S, Uimin G V *Pis'ma Zh. Eksp. Teor. Fiz.* **40** 236 (1984) [*JETP Lett.* **40** 1009 (1984)]
135. Dotsenko V S, Uimin G V *J. Phys. C*: *Solid State Phys.* **18** 5019 (1985)
136. Lee J, Kosterlitz J M, Granato E *Phys. Rev. B* **43** 11531 (1991)
137. Lee Y-H, Teitel S *Phys. Rev. Lett.* **65** 2595 (1990)
138. Denniston C, Tang C *Phys. Rev. Lett.* **79** 451 (1997); *Phys. Rev. B* **58** 6591 (1998)
139. Nicolaides D B *J. Phys. A*: *Math. Gen.* **24** L231 (1991)
140. Ramirez-Santiago G, José J V *Phys. Rev. Lett.* **68** 1224 (1992); *Phys. Rev. B* **49** 9567 (1994)
141. Lee S, Lee K-C *Phys. Rev. B* **49** 15184 (1994)
142. Ozeki Y, Ito N *Phys. Rev. B* **68** 054414 (2003)
143. Olsson P *Phys. Rev. Lett.* **75** 2758 (1995)
144. Olsson P *Phys. Rev. Lett.* **77** 4850 (1996)
145. Cataudella V, Nicodemi M *Physica A* **233** 293 (1996)
146. Olsson P *Phys. Rev. B* **55** 3585 (1997)
147. Grest G S *Phys. Rev. B* **39** 9267 (1989)
148. Lee J-R *Phys. Rev. B* **49** 3317 (1994)
149. Granato E, Nightingale M P *Phys. Rev. B* **48** 7438 (1993)
150. Boubcheur E H, Diep H T *Phys. Rev. B* **58** 5163 (1998)
151. Luo H J, Schülke L, Zheng B *Phys. Rev. Lett.* **81** 180 (1998); *Phys. Rev. E* **57** 1327 (1998)
152. Lee S et al. *Phys. Rev. B* **60** 9256 (1999)
153. Yosefin M, Domany E *Phys. Rev. B* **32** 1778 (1985)
154. Granato E *J. Phys. C*: *Solid State Phys.* **20** L215 (1987)
155. Granato E et al. *Phys. Rev. Lett.* **66** 1090 (1991)
156. Lee J, Granato E, Kosterlitz J M *Phys. Rev. B* **44** 4819 (1991)
157. Nightingale M P, Granato E, Kosterlitz J M *Phys. Rev. B* **52** 7402 (1995)
158. Lee S, Lee K-C, Kosterlitz J M *Phys. Rev. B* **56** 340 (1997)
159. den Nijs M *Phys. Rev. B* **46** 10386 (1992)
160. Davidson D, den Nijs M *Phys. Rev. E* **55** 1331 (1997)
161. Lerch Ph et al. *Phys. Rev. B* **41** 11579 (1990)
162. Martinoli P et al. *Phys. Scripta* **T49** 176 (1993)
163. van Wees B J, van der Zant H S J, Mooij J E *Phys. Rev. B* **35** 7291 (1987)
164. van der Zant H S J, Rijken H A, Mooij J E *J. Low Temp. Phys.* **82** 67 (1991)
165. van der Zant H S J, Geerligs L J, Mooij J E *Europhys. Lett.* **19** 541 (1992)
166. van der Zant H S J et al. *Phys. Rev. Lett.* **69** 2971 (1992)
167. van der Zant H S J et al. *Phys. Rev. B* **54** 10081 (1996)
168. Feigel'man M V, Larkin A I *Chem. Phys.* **235** 107 (1998)
169. Feigel'man M V, Larkin A I, Skvortsov M A *Phys. Rev. Lett.* **86** 1869 (2001); in *Mesoscopic and Strongly Correlated Electron Systems* "*Chernogolovka 2000*": *Proc. of the Intern. Conf., Chernogolovka, Moscow Region, Russian Federation, 9 – 16 July 2000*; *Usp. Fiz. Nauk* (Suppl.) 99 (2001)
170. Deutscher G, de Gennes P G, in *Superconductivity* Vol. 2 (Ed. R D Parks) (New York: M. Dekker, 1969) p. 1005
171. Villain J et al. *J. Phys.* (Paris) **41** 1263 (1980)
172. Shender E F *Zh. Eksp. Teor. Fiz.* **83** 326 (1982) [*Sov. Phys. JETP* **56** 178 (1982)]
173. Choi M Y, Stroud D *Phys. Rev. B* **32** 5773 (1985)
174. Chen Q-H, Luo M-B, Jiao Z-K *Phys. Rev. B* **64** 212403 (2001)
175. Miyashita S, Shiba J *J. Phys. Soc. Jpn.* **53** 1145 (1984)
176. Lee D H et al. *Phys. Rev. B* **29** 2680 (1984)
177. Wannier G H *Rev. Mod. Phys.* **17** 50 (1945)
178. Wannier G H *Phys. Rev.* **79** 357 (1950); *Phys. Rev. B* **7** 5017 (1973)
179. Husimi K, Syôzi I *Prog. Theor. Phys.* **5** 177, 341 (1950)
180. Van Himbergen J E *Phys. Rev. B* **33** 7857 (1986)
181. Xu H-J, Southern B W *J. Phys. A*: *Math. Gen.* **29** L133 (1996)

182. Lee S, Lee K-C *Phys. Rev. B* **57** 8472 (1998)
183. Rastelli E et al. *Phys. Rev. B* **45** 7936 (1992)
184. Baxter R J *J. Phys. A*: *Math. Gen.* **13** L61 (1980)
185. Pokrovsky V L, Uimin G V *Phys. Lett. A* **45** 467 (1973); *Zh. Eksp. Teor. Fiz.* **65** 1691 (1973) [*Sov. Phys. JETP* **38** 847 (1974)]
186. Riedel E K *Physica A* **106** 110 (1981)
187. Nienhuis B, Riedel E K, Schick M *Phys. Rev. B* **27** 5625 (1983)
188. Kim D, Levy P M, Uffer L F *Phys. Rev. B* **12** 989 (1975)
189. Aharony A *J. Phys. A*: *Math. Gen.* **10** 389 (1977)
190. Baxter R J *J. Phys. C*: *Solid State Phys.* **6** L445 (1973)
191. Chubukov A V, Golosov D I *J. Phys.*: *Condens. Matt.* **3** 69 (1991)
192. Suzuki N, Matsubara F *Phys. Rev. B* **55** 12331 (1997)
193. Kawamura H, Miyashita S *J. Phys. Soc. Jpn.* **54** 4530 (1985)
194. Golosov D I, Chubukov A V *Pis'ma Zh. Eksp. Teor. Fiz.* **50** 416 (1989) [*JETP Lett.* **50** 451 (1989)]
195. Zhitomirsky M E *Phys. Rev. Lett.* **88** 057204 (2002)
196. Cabra D C et al. *Phys. Rev. B* **65** 094418 (2002)
197. Hida K *J. Phys. Soc. Jpn.* **70** 3673 (2001)
198. Suematsu H et al. *Solid State Commun.* **40** 241 (1981)
199. Svistov L E et al. *Phys. Rev. B* **67** 094434 (2003)
200. Svistov L E et al. *Pis'ma Zh. Eksp. Teor. Fiz.* **81** 133 (2005) [*JETP Lett.* **81** 102 (2005)]
201. Ono T et al. *Phys. Rev. B* **67** 104431 (2003)
202. Wang R, Bradley W F, Steinfink H *Acta Crystallogr.* **18** 249 (1965)
203. Bonnin A, Lecerf A *C.R. Acad. Sci.* (Paris) **262** 1782 (1966)
204. Townsend M G, Longworth G, Roudaut E *Phys. Rev. B* **33** 4919 (1986)
205. Wills A S et al. *Phys. Rev. B* **61** 6156 (2000)
206. Wills A S et al. *Phys. Rev. B* **62** R9264 (2000)
207. Obradors X et al. *Solid State Commun.* **65** 189 (1988)
208. Ramirez A P, Espinosa G P, Cooper A S *Phys. Rev. Lett.* **64** 2070 (1990)
209. Broholm C et al. *Phys. Rev. Lett.* **65** 3173 (1990)
210. Uemura Y J et al. *Phys. Rev. Lett.* **73** 3306 (1994)
211. Ramirez A P, Hessen B, Winklemann M *Phys. Rev. Lett.* **84** 2957 (2000)
212. Hagemann I S et al. *Phys. Rev. Lett.* **86** 894 (2001)
213. Higgins M J et al. *Phys. Rev. B* **61** R894 (2000)
214. Elser V *Phys. Rev. Lett.* **62** 2405 (1989)
215. Baxter R J *J. Math. Phys.* **11** 784 (1970)
216. Harris A B, Kallin C, Berlinsky A J *Phys. Rev. B* **45** 2899 (1992)
217. Nelson D R *Phys. Rev. B* **18** 2318 (1978)
218. Ritchey I, Chandra P, Coleman P *Phys. Rev. B* **47** 15342 (1993)
219. Chandra P, Coleman P, Ritchey I *J. Phys. I* (Paris) **3** 591 (1993)
220. Rzchowski M S *Phys. Rev. B* **55** 11745 (1997)
221. Cherepanov V B, Kolokolov I V, Podivilov E V *Pis'ma Zh. Eksp. Teor. Fiz.* **74** 674 (2001) [*JETP Lett.* **74** 596 (2001)]
222. Lee D H, Grinstein G, Toner J *Phys. Rev. Lett.* **56** 2318 (1986)
223. Coppersmith S N et al. *Phys. Rev. Lett.* **46** 549 (1981); *Phys. Rev. B* **25** 349 (1982)
224. Peierls R E *Proc. Cambr. Philos. Soc.* **32** 477 (1936)
225. Domb C, in *Phase Transitions and Critical Phenomena* Vol. 3 (Eds C Domb, M S Green) (New York: Academic Press, 1974)
226. Saito Y *Z. Phys. B* **32** 75 (1978)
227. Wu F Y, Wang Y K *J. Math. Phys.* **17** 439 (1976)
228. Zamolodchikov A B *Zh. Eksp. Teor. Fiz.* **75** 341 (1978) [*Sov. Phys. JETP* **48** 168 (1978)]
229. Dotsenko V S *Zh. Eksp. Teor. Fiz.* **75** 1083 (1978) [*Sov. Phys. JETP* **48** 546 (1978)]
230. Korshunov S E, Vallat A, Beck H *Phys. Rev. B* **51** 3071 (1995)
231. Korshunov S E *Phys. Rev. B* **72** 144417 (2005)
232. Chalker J T, Holdsworth P C W, Shender E F *Phys. Rev. Lett.* **68** 855 (1992)
233. Reimers J N, Berlinsky A J *Phys. Rev. B* **48** 9539 (1993)
234. Sachdev S *Phys. Rev. B* **45** 12377 (1992)
235. Chubukov A *Phys. Rev. Lett.* **69** 832 (1992)
236. Chubukov A *J. Appl. Phys.* **73** 5639 (1993)
237. Veretennikov A V et al. *Physica B* **284 – 288** 495 (2000)
238. Ryazanov V V et al. *Phys. Rev. Lett.* **86** 2427 (2001)
239. Frolov S M et al. *Phys. Rev. B* **70** 144505 (2004)
240. Kontos T et al. *Phys. Rev. Lett.* **89** 137007 (2002)
241. Ryazanov V V et al. *Phys. Rev. B* **65** 020501 (2002)
242. Fisher M E, Ma S, Nickel B G *Phys. Rev. Lett.* **29** 917 (1972)
243. Swendsen R H *Phys. Rev. Lett.* **49** 1302 (1982)
244. Domany E, Schick M, Swendsen R H *Phys. Rev. Lett.* **52** 1535 (1984)
245. Van Himbergen J E *Phys. Rev. Lett.* **53** 5 (1984)
246. Jonsson A, Minnhagen P, Nylén M *Phys. Rev. Lett.* **70** 1327 (1993)
247. Caillol J M, Levesque D *Phys. Rev. B* **33** 499 (1986)
248. Minnhagen P *Phys. Rev. Lett.* **54** 2351 (1985); *Phys. Rev. B* **32** 3088 (1985)
249. Minnhagen P, Wallin M *Phys. Rev. B* **36** 5620 (1987); **40** 5109 (1989)
250. Thijssen J M, Knops H J F *Phys. Rev. B* **38** 9080 (1988)
251. Levin Y, Li X, Fisher M E *Phys. Rev. Lett.* **73** 2716 (1994)
252. Migdal A A *Zh. Eksp. Teor. Fiz.* **69** 1457 (1975) [*Sov. Phys. JETP* **42** 743 (1975)]
253. Kadanoff L P *Ann. Phys.* (New York) **100** 359 (1976)
254. Askew C R et al. *Comput. Phys. Commun.* **42** 21 (1986)
255. Sachrajda A et al. *Phys. Rev. Lett.* **55** 1602 (1985)
256. Daunt J G et al. *J. Low Temp. Phys.* **70** 547 (1988)
257. Davis J C et al. *Phys. Rev. Lett.* **60** 302 (1988)
258. Freeman M R et al. *Phys. Rev. Lett.* **60** 596 (1988)
259. Freeman M R, Richardson R C *Phys. Rev. B* **41** 11011 (1990)
260. Xu J, Crooker B C *Phys. Rev. Lett.* **65** 3005 (1990)
261. Wang X W, Gasparini F M *Phys. Rev. B* **34** 4916 (1986)
262. Stein D L, Cross M C *Phys. Rev. Lett.* **42** 504 (1979)
263. Volovik G E, Mineev V P *Zh. Eksp. Teor. Fiz.* **72** 2256 (1977) [*Sov. Phys. JETP* **45** 1186 (1977)]
264. Polyakov A M *Phys. Lett. B* **59** 79 (1975)
265. Khokhlachev S B *Zh. Eksp. Teor. Fiz.* **70** 265 (1976) [*Sov. Phys. JETP* **43** 137 (1976)]
266. Kawamura H *Phys. Rev. Lett.* **82** 964 (1999)
267. Leggett A J *Rev. Mod. Phys.* **47** 331 (1975)
268. Mineev V P *Usp. Fiz. Nauk* **139** 303 (1983) [*Sov. Phys. Usp.* **26** 160 (1983)]
269. Leggett A J *Ann. Phys.* (New York) **85** 11 (1974)
270. Azaria P, Delamotte B, Mouhanna D *Phys. Rev. Lett.* **68** 1762 (1992)
271. Azaria P et al. *Phys. Rev. B* **45** 12612 (1992)
272. Forrester M G et al. *Phys. Rev. B* **37** 5966 (1988)
273. Forrester M G, Benz S P, Lobb C J *Phys. Rev. B* **41** 8749 (1990)
274. Chakrabarti A, Dasgupta C *Phys. Rev. B* **37** 7557 (1988)
275. Fisher M P A, Tokuyasu T A, Young A P *Phys. Rev. Lett.* **66** 2931 (1991)
276. Nelson D R *Phys. Rev. B* **27** 2902 (1983)
277. Korshunov S E *Phys. Rev. B* **46** 6615 (1992)
278. Li M S, Cieplak M *Phys. Lett. A* **184** 223 (1994)
279. Derrida B *Phys. Rev. Lett.* **45** 79 (1980); *Phys. Rev. B* **24** 2613 (1981)
280. Cha M-C, Fertig H A *Phys. Rev. Lett.* **74** 4867 (1995)
281. Sherrington D, Kirkpatrick S *Phys. Rev. Lett.* **35** 1792 (1975)
282. Edwards S F, Anderson P W *J. Phys. F*: *Met. Phys.* **5** 965 (1975)
283. Mézard M, Parisi G, Virasoro M A *Spin Glass Theory and Beyond* (Singapore: World Scientific, 1987)
284. Ozeki Y, Nishimori H *J. Phys. A*: *Math. Gen.* **26** 3399 (1993)
285. Maucourt J, Grempel D R *Phys. Rev. B* **56** 2572 (1997)
286. Carpentier D, Le Doussal P *Phys. Rev. Lett.* **81** 2558 (1998)
287. Carpentier D, Le Doussal P *Nucl. Phys. B* **588** 565 (2000)
288. Gupta P, Teitel S *Phys. Rev. Lett.* **82** 5313 (1999)
289. Imry Y, Ma S *Phys. Rev. Lett.* **35** 1399 (1975)
290. Binder K *Z. Phys. B* **50** 343 (1983)
291. Aizenman M, Wehr J *Phys. Rev. Lett.* **62** 2503 (1989)
292. Hui K, Berker A N *Phys. Rev. Lett.* **62** 2507 (1989)
293. Lee S J, Kim B, Lee J *Physica A* **315** 314 (2002)
294. Ko M K et al. *Phys. Rev. E* **67** 046120 (2003)
295. Cataudella V, Fazio R *Europhys. Lett.* **61** 341 (2003)
296. Choi M Y, Chung J S, Stroud D *Phys. Rev. B* **35** 1669 (1987)
297. Benedict K A, Moore M A *Phys. Rev. B* **39** 4592 (1989)
298. Granato E, Kosterlitz J M *Phys. Rev. Lett.* **62** 823 (1989)
299. Cataudella V *Europhys. Lett.* **44** 478 (1998)
300. Granato E, Domínguez D *Phys. Rev. B* **63** 094507 (2001)